1-1-2011

An Integrated Platform to Increase the Range/Endurance of Unmanned Helicopters

Roy Godzdanker
University of Denver

AN INTEGRATED PLATFORM TO INCREASE THE RANGE/ENDURANCE OF UNMANNED HELICOPTERS

_____

A Dissertation

Presented to

The Faculty of Engineering and Computer Science

University of Denver

_____

In Partial Fulfillment

of the Requirements for the Degree

Doctor of Philosophy

_____

by

Roy Godzdanker

November 2011

Advisor: Kimon P. Valavanis
&
Matthew J. Rutherford

Author: Roy Godzdanker
Title: AN INTEGRATED PLATFORM TO INCREASE THE RANGE/ENDURANCE OF UNMANNED HELICOPTERS
Advisor: Kimon P. Valavanis and Matthew J. Rutherford
Degree Date: November 2011

ABSTRACT

Class I (<150 kg) autonomous helicopters are becoming increasingly popular for a wide range of non-military applications such as, surveillance, reconnaissance, traffic monitoring, emergency response, agricultural spraying, and many other "eye in the sky" missions. However, an efficient landing/takeoff platform with refueling/recharging capabilities has not yet been developed to increase the endurance and decrease the cost for Class I helicopters.

This dissertation presents a three-prong approach for increasing the range and endurance of Class I autonomous helicopters, which will then spur demand by non-military organizations wanting to take advantage of such capabilities and, therefore, drop their price. The proposed Intelligent Self-Leveling and Nodal Docking System (ISLANDS) is developed as a mobile refueling/recharging station, which is one part of a three-pronged approach. ISLANDS is an electro-mechanical system that provides a safe landing surface for helicopters on gradients of up to 60%. ISLANDS operates "off the grid" and, therefore, must provide its own energy sources for the refueling/recharging tasks it performs. A method for determining ISLANDS' energy needs for refueling/recharging of gas and/or electric helicopters for an arbitrary number of days is provided as the second part of the three-pronged approach. The final step for increasing autonomous helicopter endurance is a method for determining placement of ISLANDS

nodes in the area to be serviced ensuring that the helicopters can achieve their mission goal.

In this dissertation all aspects of the three-pronged approach are presented and explained in detail, providing experimental results that validate the proposed methods to solve each of the three problems. A case study using Commercially Off The Shelf (COTS) components that shows how all the parts of the proposed three-pronged solution work together for increasing the endurance of Class I helicopters is provided as a conclusion to the dissertation.

ACKNOWLEDGMENTS

I have benefited from the advice, friendship, and support of quite a number of people throughout my PhD journey at the University of Denver and will surely continue keeping in touch with those people wherever my life will take me. I would specifically like to thank my two advisors Dr. Kimon P. Valavanis and Dr. Matthew J. Rutherford for challenging and supporting me throughout. Additionally I would like to thank my entire family that was always there to cheer me and providing their unwavering support. Finally I would like to thank my beautiful fiancé for dealing with me during the final months of this process, I love you.

TABLE OF CONTENTS

LIST OF FIGURES

LIST OF TABLES

CHAPTER 1: INTRODUCTION

Three important steps must occur for new inventions to successfully integrate into society. First, there must be a market for the invention – a desire or need for the public to purchase the product. Second, the product must be affordable for its potential consumers. Third, an infrastructure must be established to support the new product. A classic example is the automobile; the first non-human powered car was invented in 1769 [1]. Prior to the invention of the automobile, people needed weeks, months, or even years to travel from one location to another either by foot, train, or horse – clearly indicating the need for a more efficient means of transportation. However, due to the inefficient means of production, cars were not affordable for the middle and lower class consumers. In 1914, Henry Ford made cars affordable by implementing the assembly line [2]. Next, gas stations were built around the country to provide infrastructure for this new invention. Today, about 90% of Americans own a car and there are about 115,000 gas stations in the United States [3]. Without the infrastructure gas stations provide, the automobile would not have become such an integral part of society. The automobile is one example in which the price of the invention decreased due to increased demand and a supporting infrastructure allowing the invention to successfully integrate into society.

Airplanes and helicopters are other inventions that took many years to become an integral part of society. From the Wright Brothers' experimental airplane flights in 1905

[4], to the military planes used in World War I, to commercial jet airliners' appearance in 1949, to autonomous planes that are constantly made smaller and used today in various applications. Helicopters saw a similar development cycle to that of planes, from the first helicopter flown in 1907 [5], to the first commercial helicopter available in 1950s [5], to the development of autonomous helicopter systems of various sizes. The next step is unmanned aviation, and as part of this, autonomous helicopters could be made smaller and more reliable. However, an infrastructure must also be established to provide the appropriate resources and support the autonomous helicopters need to complete resource-exhausting tasks. With an infrastructure provided, autonomous helicopters will be granted the ability, for the first time ever, to increase their range and endurance, which can be used for a wide spectrum of applications

1.1 Background and Motivation

There are two main categories of aerial vehicles, the most common being fixed wing or airplanes, and rotorcraft or helicopters as shown in Figure 1.

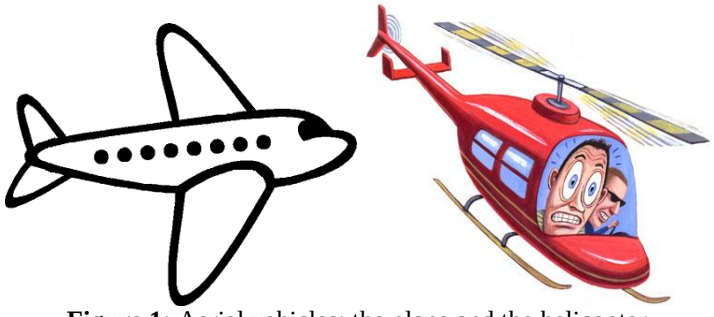

Figure 1: Aerial vehicles: the plane and the helicopter

The primary difference between these two aerial vehicles is their method of flight. Planes have a motor that propels them through the air, and their specific wing shape creates regions of low pressure under the wing and high pressure over the wing, which results in lift. Helicopters use a rotor driven by a motor to produce the necessary lift. The different methods of flight between helicopters and planes lend each system for use in specific applications.

Planes are more fuel-efficient than helicopters, allowing them to transport people and goods over long distances. Conversely, helicopters are used for applications requiring short-range transportation to remote regions, or those requiring the ability to hover due to the lack of a landing site. The helicopter capability of Vertical Takeoff and Landing (VTOL) is what makes them versatile and an important asset for many governmental and non-governmental agencies. The major drawback of helicopters is that they require more fuel than a plane for a mission of equal distance.

The armed forces were one of the first groups that saw potential in the concept of an airplane. This caused these systems to be developed quickly from proof of concepts in 1901 to combat use in World War I. With the quick development and use in the harsh and dangerous conditions of war it is not surprising that developing planes to operate autonomously was also done quickly for the sake of saving lives. The first Unmanned Aerial Vehicle (UAV) was developed by Lawrence and Elmer Sperry 1916 [6] depicted in Figure 2.

Figure 2: First UAV from 1916 [6]

This first UAV was equipped with a gyroscope to mechanically stabilize the plane allowing it to fly autonomously. These first UAVs were to be used as "Torpedo Bombers" similar to the piloted kamikaze bombers Japan used in World War II. The first attempt at developing a UAV turned out to be an exercise in engineering, providing technically immature proofs-of-concept never to be implemented. The Firebee [7] was the first UAV system deployed in combat by the United States, being used in the Vietnam War in 1960 as shown in Figure 3. The long gap between initial proofs–of-concept and actual implementation of an unmanned plane was followed by rapid growth in the UAV industry led by the United States and Israel.

Figure 3: The Firebee UAV, 1960 [8]

While Israel developed small, lower-priced UAV systems, it was the United States that developed large, long endurance systems, such as the Predator Drone [9] (shown in Figure 4) and the Global Hawk [10]. The Predator system has an endurance of 24 hours while the Global Hawk system has an endurance of 40 hours and can fly at altitudes up to 65,000 feet (20,000 meters). These new systems developed by the United States and Israel are called Unmanned Ariel Systems (UAS) as they include both the aerial vehicle and the extensive ground station associated with controlling the vehicle.

Figure 4: The Predator UAV [11]

Helicopters or rotor-based vehicles were invented several years after fixed-wing aircraft. As with planes, the military first saw the potential capabilities of the helicopter, and accelerated their development process. The primary developmental difference between helicopters and planes was that the progression from manned to unmanned aerial vehicles took longer for helicopters. Although the first helicopter prototype was built in 1907 [5], the first autonomous helicopter was not built until 1960. The first autonomous helicopter was designed as an anti-submarine bomber, as depicted in Figure 5. The goal of this system was to fly an unmanned helicopter over a shipyard and drop torpedoes in the water to disable enemy submarines.

Figure 5: First unmanned helicopter [12]

Similar to the first autonomous plane, the first autonomous helicopter proved to be unreliable. However, it was useful as a target practice drone for the United State Air Force. The initial failure opened the door for development of other unmanned helicopters, such as the Firescout from Northrop Grumman [13], which is depicted in Figure 6. Only now, 50 years after the development of the first autonomous helicopter, are these vehicles seeing use in combat applications. The primary reason for the roughly 50 year gap

between the first unmanned helicopter and first unmanned plane is the complexity of the flight dynamics associated with helicopters.

Figure 6: Modern Unmanned Helicopter- QH-50 and Firescout by Northrop Grumman [13]

As stated previously, helicopters are agile but not fuel efficient. For this reason, more capacity needs to be set aside for fuel to increase mission length and endurance. Along with the development of larger autonomous helicopters for military applications, over the past 50 years a niche for smaller helicopters (<150kg or 330lb) has begun to develop. The need for smaller autonomous helicopters has been driven by civilian applications such as surveillance, traffic monitoring, forest fire hot-spot detection, port monitoring, border patrol, oil/gas pipeline inspection, search and rescue, along with other missions that require an “eye in the sky" capability. Some companies, such as Rotomotion, have begun developing and selling small autonomous helicopter systems, as shown in Figure 7, to be used in such applications as those previously stated.

Figure 7: Small autonomous helicopters by Rotomotion LLC [14 ,15, 16, 17]

The applications listed previously are mainly for civilian customers with smaller budgets than the military. However, price remains as a significant drawback of systems such as Rotomotions' because they are still not mass-produced. The other disadvantage of these smaller helicopters is their limited endurance, requiring frequent refueling/recharging, and in turn leading to a smaller effective radius of operation.

Short flight times, and thus short periods of autonomy, is one reason why small helicopters are not currently being used widely. To take greater advantage of these smaller and cheaper helicopters, supporting infrastructure must be developed. If refueling stations were available in the area in which these small autonomous helicopters are operating, longer autonomy and increased mission endurance would be possible. The refueling/recharging stations must also be placed to maximize the autonomous operations of the helicopters. The work presented in this dissertation is on developing a refueling/recharging station for small autonomous helicopters in order to make them

more usable for civilian applications, which, in a virtuous cycle, will also help bring down their price making them more affordable to more civilian groups.

1.2 Problem Statement

Class I unmanned helicopters suffer from limited range/endurance capabilities. As such, it is essential to 'design' a system that indirectly overcomes these limitations. This design must not drastically modify exciting Class I helicopters as their current design and capabilities are well suited for the applications they serve. The problem may be solved by designing supporting infrastructure and new methods for helicopter deployment.

1.3 Proposed Solution

A three-pronged approach is presented to solve this problem. An electromechanical refueling/recharging station is designed and built to provide a safe landing surface for a helicopter weighing up to 150 kg. For the purpose of this work, 'safe' is defined as a level surface for landing relative to the environment, on slopes of up to 25^{o}, to within 1^{o} of level. To act as a refueling station, it is shown that the proposed Intelligent Self Leveling and Nodal Docking System (ISLANDS) design is capable of latching onto a helicopter in a predefined reference frame, which in a future design will allow for efficient refueling or recharging. To allow for longer endurance of the ISLANDS nodes, a hybrid gas electric system is proposed. This system will determine

the number of batteries to the volume of fuel needed on board ISLANDS based on the available solar array used and the mission endurance required. A placement algorithm based on maximal area coverage problems is also developed to take full advantage of the system. The work done on these three problems will serve as the foundation of an infrastructure to integrate small autonomous helicopters into everyday use by civilian organizations.

1.4 Objectives and Aims

One of the main goals of this dissertation is to develop a physical prototype of a landing platform that can be shown to have capabilities of refueling or recharging. To achieve successful refueling and recharging, mechanical and electrical modification of an existing helicopter fuel system is required. These modifications were deemed out of the scope of this work, and for this reason, only a centering and latching mechanism is introduced. Once the reference frame of the helicopter is in line with the reference frame of the landing platform, refueling/recharging of a stationary helicopter is straightforward. Additionally, as the goal is to produce a working prototype, extensive mathematical modeling of individual components and systems is bypassed in favor of less extensive calculations with padded safety factors, and a working prototype. The power analysis performed on ISLANDS was done on the basis of fundamental fluids and mechanical equations with efficiency calculations based on existing datasheets. No physical testing was performed because the components integrated into the ISLANDS power systems

have been thoroughly designed and understood, and the information from the data sheets was deemed acceptable for the calculations performed.

1.5 Contributions

The contributions of this dissertation are summarized as follows:

1) A functional electro-mechanical system is designed, which is capable of leveling to the environment via the actuation of two degrees of freedom (DOF) with the ability of centering and latching an autonomous helicopter to a predefined reference frame for the purpose refueling/recharging and possible data exchange.
2) A method for determining the total energy needs of ISLANDS is presented based on the duration of mission deployment and the type of helicopters ISLANDS is to service. Based on the total energy needs of ISLANDS a way of determining the battery capacity and fuel needs to sustain ISLANDS for prolonged missions is calculated.
3) An algorithm is designed for strategically placing ISLANDS nodes in the work arena in order for autonomous helicopters to increase their mission endurance is developed.
4) A case study of ISLANDS deployment is presented using the algorithm proposed in 3 and the power system from 2 using available off-the-shelf components easily sourced by civilian personal is performed.

1.6 Comprehensive Outline

The remaining chapters of this dissertation are aimed at addressing each of the contributions mentioned in Section 1.5. Chapter 2 will present the ISLANDS electro-mechanical system, Chapter 3 will present the analysis of the hybrid solar gas fuel power system and the parameter identification tool developed. Chapter 4 presents work on the placement algorithms of ISLANDS. Chapter 5 presents the case study for the deployment strategy presented in Chapter Four. Finally, Chapter 6 summarizes the entire dissertation and proposes the future direction of this work.

CHAPTER 2: INTELLIGENT SELF LEVELING AND NODAL DOCKING SYSTEM (ISLANDS)

The initial stage in developing a way of increasing the endurance of Class I unmanned helicopter is the building of an electro-mechanical system capable of providing a safe landing deck for refueling and/or recharging such helicopters weighing less than 150kg (320lbs). A safe landing deck, according to the Federal Aviation Administration (FAA), means a landing surface that levels to within five degrees of the environment [5]. A level landing surface is needed due to the aerodynamics phenomenon known as *ground effect*, associated with the main rotor of the helicopter. Ground effect is experienced by a helicopter when it reaches an altitude which is equal to or less than two times the main rotor diameter from the ground. The level landing surface is needed so the ground effect loads the main rotor disc equally. To achieve a level landing surface independent of the environment, a mechanism with two Degrees Of Freedom (DOF) is needed: one to align the landing surface major axis with the primary gradient, and the other to level the landing surface to the gradient. To accommodate refueling/recharging capabilities, ISLANDS incorporates a centering mechanism to move the helicopter to a known location and orientation relative to the landing deck. This alignment mechanism is necessary to compensate for a vision based attitude controller on-board the autonomous helicopter, which cannot guarantee precise landing.

This chapter first presents work on existing landing platforms in development explaining how ISLANDS differs from them and how it improves upon those systems' capabilities. Additional background on pneumatic systems is presented, as their use in robotic systems has increased over the past 10-15 years as an effective alternative to traditional Direct Current (DC) motors. Following the literature review, a detailed explanation of all of ISLANDS subsystems is presented. The chapter concludes with results from the pneumatic system proposed for use on ISLANDS.

2.1 Previous Work

2.1.1 Other Landing Platforms

Currently in the literature, there are references to two systems similar to the one described in this dissertation. These systems have drawbacks and limitations that are overcome by ISLANDS. The first system, from the Space and Naval Warfare Systems Command (SPAWAR), is part of a larger marsupial deployment project. Marsupial deployment is characterized by having a large vehicle or system carrying a smaller vehicle or system for deployment and subsequent retrieval. The larger vehicle, usually called the *parent*, is capable of carrying additional mechanical and computational resources for the mission that the smaller vehicle, referred to as the *child*, can use to increase mission endurance. In the SPAWAR system [18], the parent is an autonomous modified All Terrain Vehicle (ATV) called Mobile Detection Assessment and Response

System (MDARS), to which a launch and recovery system tailored to the iSTAR vertical takeoff and landing (VTOL) vehicle is mounted, as shown in Figure 8.

Figure 8: The system from SPAWAR with MDARS and iSTAR [18]

The iSTAR VTOL system used by SPAWAR is a ducted-fan design, which has a specific and greatly differing form factor from conventional tail and main rotor helicopters shown in Figure 7. Figure 9 shows the general schematic of a ducted fan where exit air comes out at a much higher velocity than the intake air, hence providing thrust. The ducted fan schematic of Figure 9 has an electric motor, while the motor for the iSTAR ducted fan is gas fueled. Both styles are acceptable in building a ducted fan VTOL.

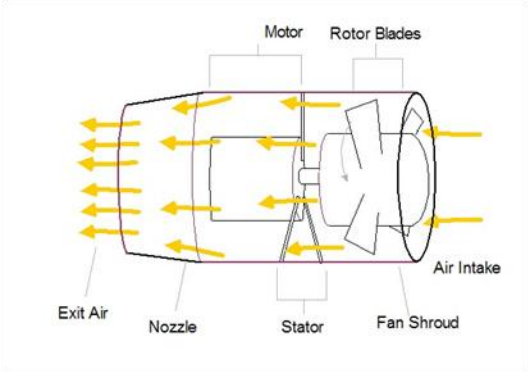

Figure 9: General mechanical structure of a ducted fan [19]

Besides the form factor dependency associated with the SPAWAR system, it does not have the capability of leveling to the environment. Therefore, this system will only work on level ground. Additionally, the system is designed to only fit on the MDARS base platform and therefore cannot work as a standalone system or attach to any other

platform, such as a ship, without a re-design. Finally, the SPAWAR system does not claim to have recharging or refueling capabilities, but the system's form factor dependency would lend itself to easily incorporate this capability.

The second reference to a system similar to the ISLANDS platform is the system described in patent number 7,299,762 [20] shown in Figure 10.

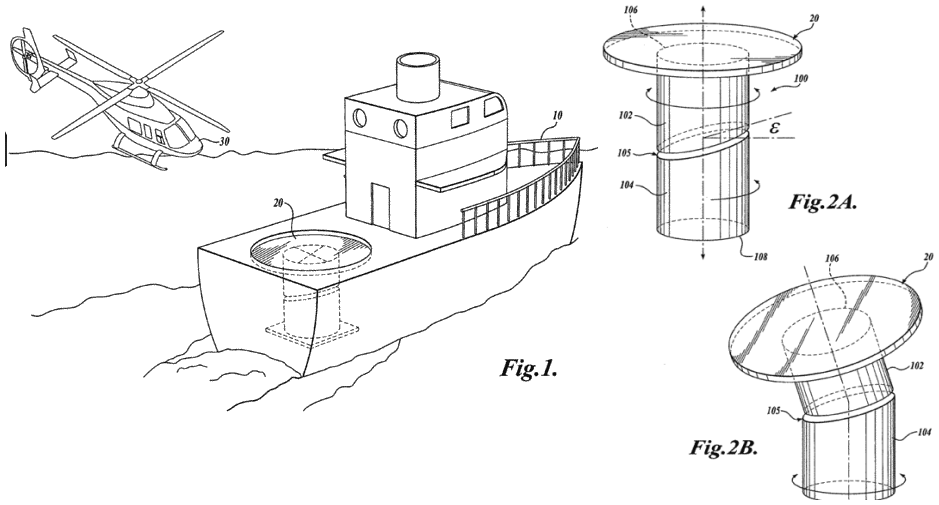

Figure 10: Dual rotating cylinder design for a landing platform from patent 7,299,762 [20]

This patent describes a system consisting of two rotating cylinders at an offset angle from each other, allowing for leveling with the environment. This landing surface is primarily designed to solve the problem of landing helicopters on aircraft carriers and is therefore designed to respond to low-amplitude/high-frequency deviations from level caused by waves. In contrast, ISLANDS is designed to respond to high-amplitude/low-frequency deviations from level caused by steep terrain. As with the SPAWAR system, this system does not have refueling/recharging capabilities, or the capability of being a standalone system.

2.1.2 Previous Work on Pneumatic Systems

For ISLANDS to achieve a level and safe landing surface it requires two separately actuated Degrees of Freedom (DOF). To implement this, ISLANDS uses different actuation methods. For the first DOF, a DC motor is used to rotate ISLANDS to align the major axis of the platform with the gradient; DC motor control has been studied extensively in the literature (see e.g. [21]). For the second DOF, a pneumatic piston is used to level the landing deck to the gradient (explanation as to why pneumatics are chosen will be presented in section 2.4).

The use of pneumatics for actuation in non-industrial applications has recently seen attention from the academic community. Pneumatics are often used due to their low cost, high power-to-weight ratio, and abundant supply of inexpensive components [22, 23, 24, 25, 26]. Additionally, pneumatic actuators have high compliance and are easily back-drivable; characteristics that are not shared by traditional gear boxes coupled with DC motors [27]. Back-drivability and compliance are desirable characteristic in the field of robotics [27] and to achieve compliance using traditional methods requires integration of force sensors and high speed position controllers, adding more cost to an already expensive system.

Figure 11 shows a general schematic of a pneumatic system capable of extending and retracting composed of a piston, two valves, and a source of compressed air. Pneumatic pistons operate by varying the pressure of air that enters the two chambers via the valves. The two chambers are separated by a sliding plunger to which a rod is attached that moves the desired load. When chamber 1 has a higher pressure than

chamber 2, the piston extends, when the situation is reversed it retracts. If the pressure in the two chambers is equal, the piston retains its position, and if the chambers are not pressurized, the piston can move freely (and is therefore back-drivable).

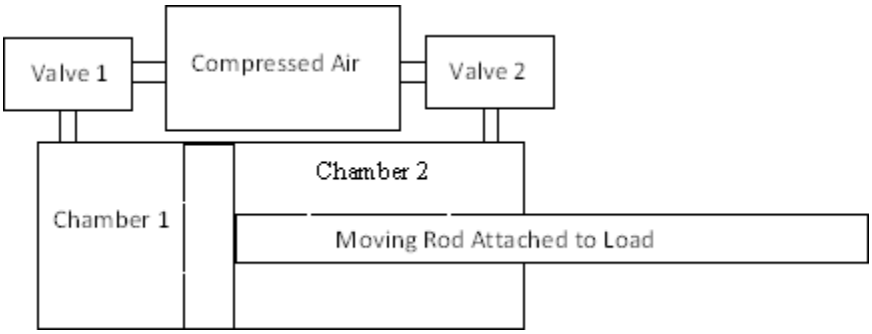

Figure 11: General schematic of a piston

For all pneumatic systems, the problem of controlling the piston's desired position and velocity is a function of controlling the pressure of air inside the two chambers of the piston. The fundamental equation governing the maximum force the piston can exert is a function of pressure and the surface area of the piston:

$$F = PA \tag{1}$$

where F is the force in Newtons, P is pressure in Pascals, and A is area of the chamber's cross section in m^2. The relationship between the chamber pressure and the piston position is modeled using the following equations [28]:

$$M\frac{d^2x}{dt^2} + B\frac{dx}{dt} = A(P_1 - P_2) \tag{2}$$

$$P_1Ax = m_1RT \tag{3}$$

$$P_2A(l - x) = m_2RT \tag{4}$$

where M is the load being moved by the rod, x is the position of the rod, B is the static coefficient of friction between the seal of the plunger and the inside walls of the piston, A is the area of the plunger, P_1 and P_2 are the pressures inside the chambers, m_1 and m_2 is

the mass of air in chapters, l is the total stroke length of the piston, R is the universal gas constant, and T is the temperature in degrees Kelvin. Since the control problem is one of change in pressure over time, differentiation with respect to time of Equations (3) and (4) leads to Equations (5) and (6), respectively:

$$\frac{dP_1}{dt} = \frac{1}{Ax}(-P_1 A\frac{dx}{dt} + RT\dot{m}_1) \tag{5}$$

$$\frac{dP_2}{dt} = \frac{1}{A(l-x)}(-P_2 A\frac{dx}{dt} + RT\dot{m}_2) \tag{6}$$

Equations (2)-(6) are general and are based on the assumptions of: constant temperature, ideal gas law relationship, and that static friction, B, is very small. The last assumption causes the most difficulties when modeling pneumatic systems. Static friction, as it turns out, plays a major role in pneumatic systems and is difficult to model. The static friction coefficient used in (2) is a lumped parameter including both static and dynamic friction. The dynamic component of the lumped friction parameter is non-linear and temperature dependent. This brings into question the constant temperature assumption. Air can be modeled as a compressible gas but only when it is under a certain Reynolds number [29]. The Reynolds number is a function of the fluids' velocity and density, which are dependent on temperature. Therefore, if temperature fluctuates substantially as the air undergoes compression, it may increase the Reynolds number enough such that the incompressibility assumption is no longer valid. Once the incompressibility assumption is violated, many complexities, including non-linearity, are added to the pneumatic modeling. For this reason, research in pneumatic systems control has taken two distinctive approaches. One group models and simulates pneumatic systems to determine

the appropriate values of gains needed in proposed controllers and is exemplified by Barth et al [30, 31, 32]. Others have taken the more direct approach of developing climbing robots [28, 33, 34], grinding gantries [35], space frames manipulators [27], and search and rescue robots [25] that use pneumatic systems where they experimentally determine the controller gains.

The controllers used in the pneumatic systems of [26, 27, 28, 33 ,34 ,35] control the valves, which regulate the air flow into the piston chambers and, according to Equations (2)-(6), control the position and velocity of the piston. Two types of valves are commonly used for this application: proportional servo valves, and solenoid on/off valves. Proportional servo valves operate similarly to servo motors where they are commanded to be either fully open, fully closed, or at any position in between. The different positions of the servo valves correlate to orifice size which determines the flow rate of air into the piston chambers. Servo valves were the first valves used [22] for controlling piston position as they are easily controlled. More recently, on/off solenoid valves are used due to the cost savings achieved, as servo valves cost $400, while solenoid valves can cost as little as $30 [24].

Low cost on/off solenoid valves are actuated by a pulse width modulation (PWM) signal from a microcontroller or another device capable of generating the signal. PWM signals are commonly used to control the velocity of DC motors where a carrier wave with a fixed frequency and a varying duty cycle controls the flow of electricity to a motor. The varying duty cycle control how long a transistor is open and allowing electricity to flow to the motor, as shown in Figure 12.

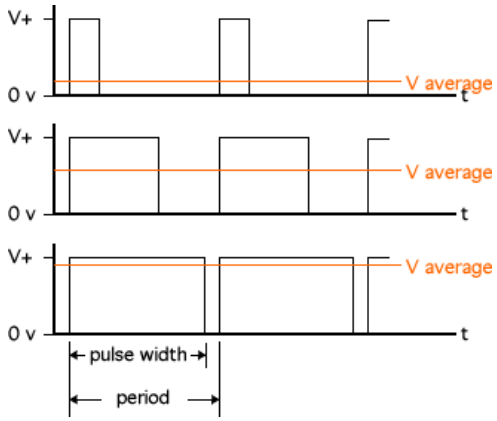

Figure 12: Different duty cycles on the same carries wave resulting in different net voltage to controlled device [36]

When the duty cycle is set to 100%, the motor gets all the available power because the switch is always open. A duty cycle of 50% means that the switch is open 50% of the time and the motor therefore gets 50% of the power and operates at 50% of its speed. Similarly, when using a solenoid valve, a PWM duty cycle of 75% means the valve is open 75% of the time and the flow rate is reduced to 75% of maximum. Thus, by using cheap on/off valves it is possible to control the pressure going into the chambers of the piston and, therefore, the position and velocity of the piston. One important difference between solenoid valve and transistor switches used for regulating electrical power is their switching times. Transistors switch almost instantly once a signal is applied, while solenoids have a significant time delay in switching states since the coil needs to energize before the switching can take place. This delay must be accounted for in the control law development.

Thus, the control problem is reduced to determining the appropriate duty cycle to send to the on/off solenoid valves to achieve the desired position of the piston. One of the first methods successfully used was proportional, integral and derivative (PID) control [26, 28, 35, 37]. This initial form of PID control is *fixed mode* PID since the gains are

permanently set. The problem encountered with this control method is that as the load varies, the PID gains become sub-optimal for the new mode of operation. For this reason, fuzzy and neuro-fuzzy PID controllers that update or learn the gains needed during operation are used [23, 28, 35, 38]. Other controllers include *sliding mode* controllers and non-linear controllers [30, 33]. Chillari et al. [26] compared the errors from a set point of PID, Fuzzy, and sliding mode controllers, with and without chamber pressure feedback using several different trajectories. The results show that for the simplest staircase based trajectory, a PID controller with no pressure feedback performed the worst but by only 15%. The staircase trajectory most closely resembles the operating regime of the pistons on ISLANDS and for this reason a PID controller is chosen, as it is easily implementable and produces desired results of the platform being within FAA regulations of level [39, 40] with a worst case error of 15% reported in [26].

2.2 ISLANDS System Overview and Requirements

ISLANDS has three major sub-systems on board, not including the power management system, which will be discussed in detail in Chapter 3. The first sub-system is associated with leveling ISLANDS to the environment. This sub-system includes two redundant linear actuators that are mounted in opposite directions. These actuators are responsible for leveling the landing deck to account for the gradient or slope of the background environment. An additional rotary actuator is used to rotate the entire landing platform on a turntable bearing through a gear train to align ISLANDS with the major

gradient of the environment. As this is the main structural support sub-system of ISLANDS, it is designed to handle a helicopter load of up to 150kg. 150kg was chosen because ISLANDS is designed to for use with Class I autonomous helicopters, which have fewer limitations of operations than Class II vehicles [41]. This leveling sub-system is also designed to accommodate gradients of up to 60%, which is equivalent to a 30^{o} tilt angle. This value was chosen because the most aggressive vehicles used by the military and that are commercially available, such as the Humvee, have a maximum climb gradient of 60% [42].

Once the landing surface of ISLANDS is level and the helicopter has landed, re-charging and data exchange processes can take place. In order to perform these tasks, the orientation of the helicopter with respect to ISLANDS must be known, and this is the responsibility of the second mechanical sub-system. To reposition the helicopter, four linear actuators with metal wipers move the helicopter to a pre-determined location on the landing deck. Next, two latching motors engage and connect to the helicopter skids. The contact point created by latching provides one possible means for recharging the helicopter.

All of these tasks are performed under the control of a microcontroller, the third major sub-system, which receives input through sensors integrated into the mechanical sub-systems. Level is measured by a tilt sensor, while the centering is done using proximity sensors for the wipers. In the future, the same microcontroller will also interact with the charge controllers for recharging the helicopter batteries. The microcontroller will also interact with the on board transmitter to relay the data from the ISLANDS node

to external systems. This microcontroller is to be housed in a weatherized container on-board ISLANDS, which was not designed and built for this work as it was deemed out of the scope of developing a working proof of concept prototype.

2.2.1 Leveling Subsystem

2.2.1.1 Leveling to Gradient Mechanism Overview

Figure 13 shows 3D oblique view of ISLANDS with a helicopter on the landing surface, with the long and short centering wipers in the 50% retracted position. In Figure 13 both the long and short centering blades are attached to the top deck substructure. The top deck substructure is rotated to level by a linear actuator. The top deck pivots on a pin shown more clearly in Figure 22, which is part of the centering mechanism, and will be discussed in Section 2.2.2. To reduce friction, the top deck pivot pin rides inside a bearing. The visible components on the underside of ISLANDS in Figure 13 include an air compressor to power the pneumatic linear actuators. The compressed air is stored in the air reservoir. The air coming out of the air reservoir is throttled through a 3-way solenoid valve actuated by a PWM signal from the microcontroller. The pneumatic linear actuator is controlled by pressure inside each of the cylinder halves and this pressure is varied by the valve. The solenoid valve and other electrical components on ISLANDS get their power from a battery.

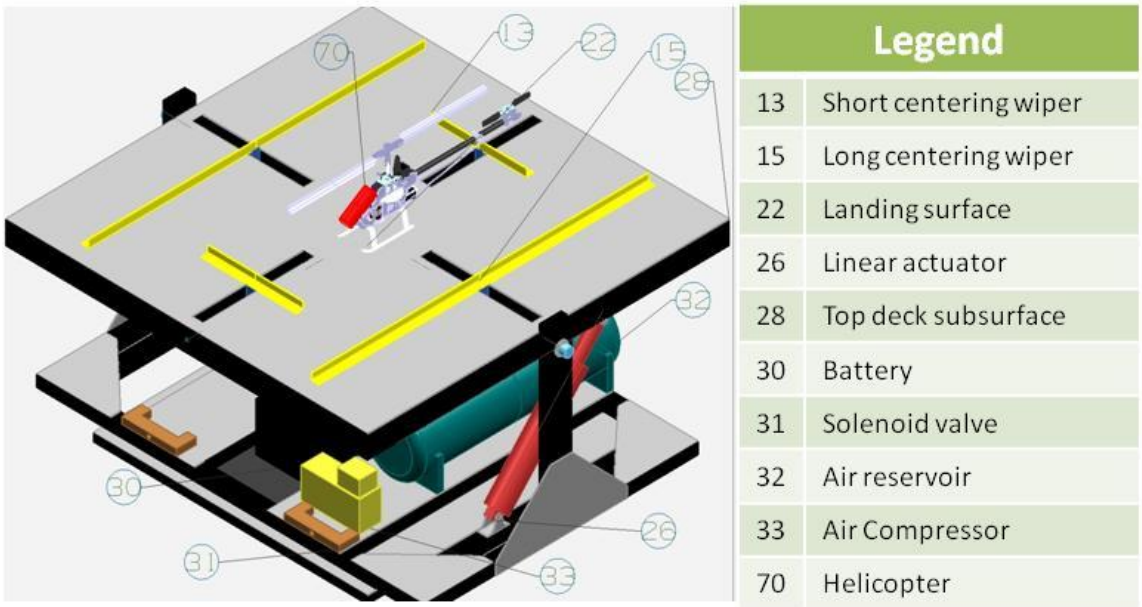

Legend	
13	Short centering wiper
15	Long centering wiper
22	Landing surface
26	Linear actuator
28	Top deck subsurface
30	Battery
31	Solenoid valve
32	Air reservoir
33	Air Compressor
70	Helicopter

Figure 13: Complete assembly of ISLANDS and assembly legend

2.2.1.2 Leveling to Gradient Design Analysis

To determine the force required by the pneumatic piston to level the landing deck to the major gradient axis, static and dynamic force analysis are described. The static analysis determines the force needed to hold the landing deck at a predefined position with the helicopter on the landing deck. Dynamic analysis determines the forces needed to move the landing deck to level before the helicopter arrives. The static analysis performed is based on the free body diagram of the landing deck shown in Figure 14.

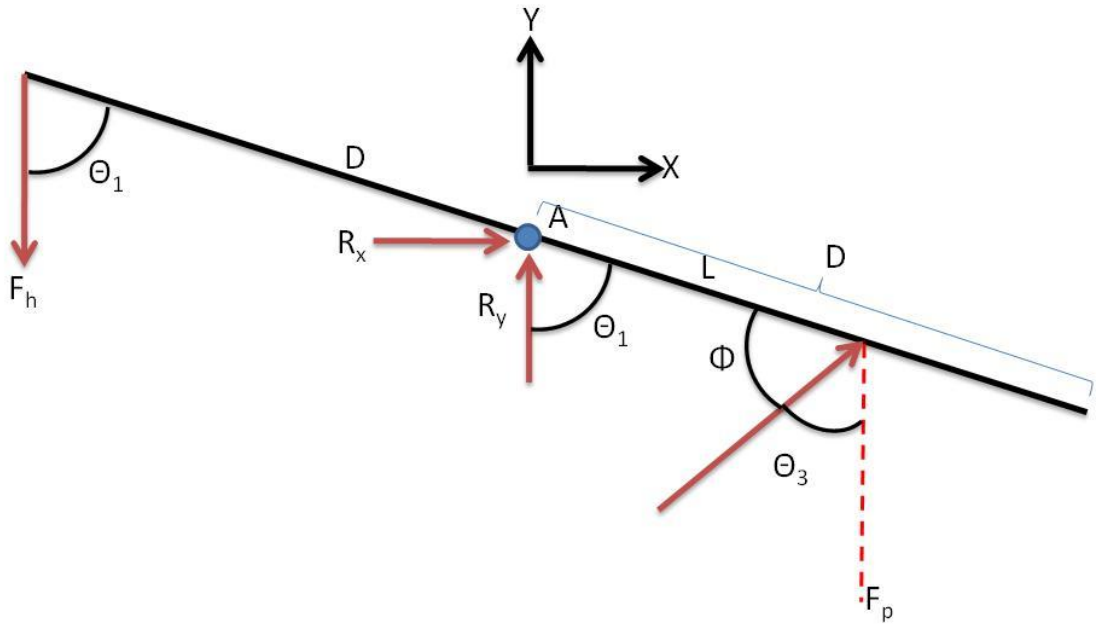

Figure 14: Free Body Diagram of landing deck

The free-body diagram in Figure 14 represents the worst case loading scenario on the landing deck. In this scenario F_h represents a point load encompassing the entire mass of the helicopter landing at the opposite side of where the piston force F_p is being applied. This scenario can never occur, therefore, by designing to this scenario the resulting ISLANDS design would withstand any real landing scenarios that do occur, where F_h would be a distributed load landing near the middle of the landing deck. For the static case, the sum of the forces in '*x*', '*y*' and the sum of the moments must equal zero, which is represented by

$$\sum F_x = R_x + F_p \sin\theta_3 = 0 \tag{7}$$

$$\sum F_y = R_y - F_h + F_p \cos\theta_3 = 0 \tag{8}$$

$$\sum M_A = L(F_p \sin\phi) - D(F_h \sin\theta_1) = 0\ , \tag{9}$$

and solving for F_p gives

$$F_p = \frac{\sin\theta_1}{\sin\phi}\frac{DF_h}{L} \quad . \tag{10}$$

In Equations (7) and (8) the variables R_x and R_y represent the reaction forces at the pin from the weight of the landing deck. These parameters are easily calculated but not relevant when solving for F_p.

The parameters in Equation (10) are a function of the landing deck geometry. A simplified end-on view of the landing deck is shown in Figure 15.

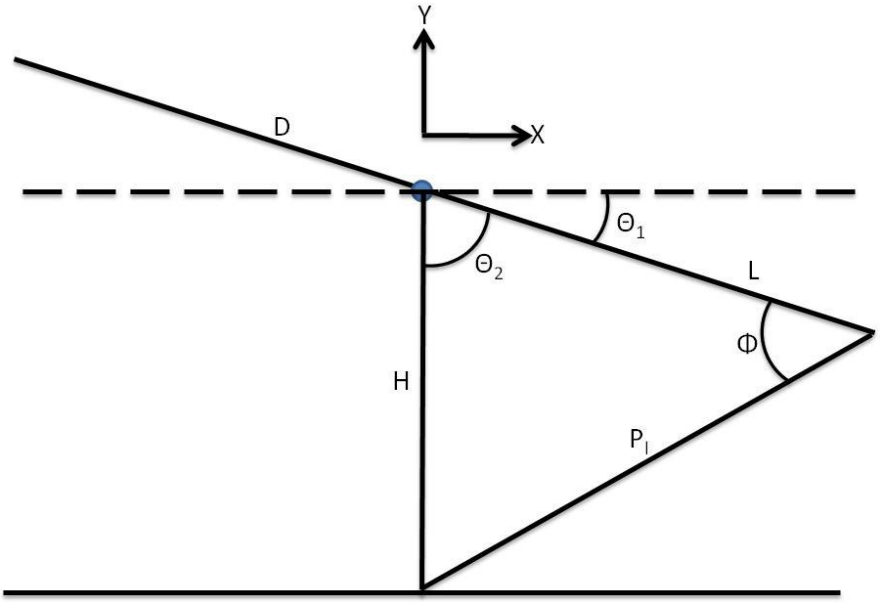

Figure 15: Simplified geometry of landing deck, with parameters associated with F_p from Equation (10)

D is the distance between the edge of the deck and pivot point *A*, which is always half the total length of the deck. Currently, the ISLANDS landing deck is square, where *2D* is the upper limit of a helicopters' main rotor diameter capable of safely landing on ISLANDS. *L* is the distance between the pivot point *A* and the attachment point of the piston and this can range from zero to *L*. The ratio of *D* over *L* represents the mechanical disadvantage that the piston must overcome, therefore, having *L* equal to *D* is ideal. As in this position, the mechanical disadvantage is one, and at all other positions the mechanical

disadvantage is greater than one. H is the distance between the bottom of the vertical support and that attachment point of pivot Point A. P_l is the piston length and Φ is the angle the piston makes with the top deck, both of these variables vary as a function of θ_1 which is the tilt angle of the top deck which in the calculation presented in this section ranges between +/- 30^o, which matches the design requirements.

As stated previously and seen in Equation (10), if D and L are equal, the mechanical disadvantage is equal to one and the force required by the piston is proportional to the force exerted by the helicopter multiplied by the ratio of $\sin(\theta_1)/\sin(\Phi)$ which is designated as the force factor. As the force factor is a function of the geometry, the goal in designing future versions of ISLANDS is to minimize the value of the force factor over the range of operation. Figure 16 shows the relationship between Φ and the tilt angle θ_1 and their effect on the force factor.

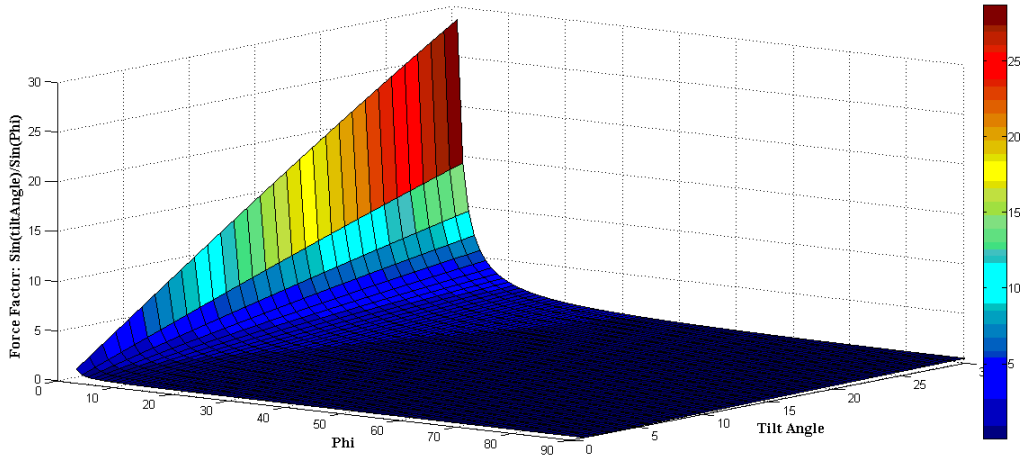

Figure 16: Force factor plot over the range of possible phi and tilt angle range of +/- 30 degrees

Figure 16 shows that the force factor is greatest at the maximum value of θ_1. This angle is application-driven, and therefore there is nothing to be done to the numerator of the force factor. The denominator of the force factor is a function of Φ, which can be controlled to

be within a certain range by choosing L and H appropriately. A physical constraint on H is that it must be greater than $D\cos(\min(\theta_1))$ to avoid having the edge of the platform hitting the ground. Figure 17 shows the force factor as a function of Φ, which shows that by keeping $\Phi > \sim 20^o$ during leveling the force factor remains under two.

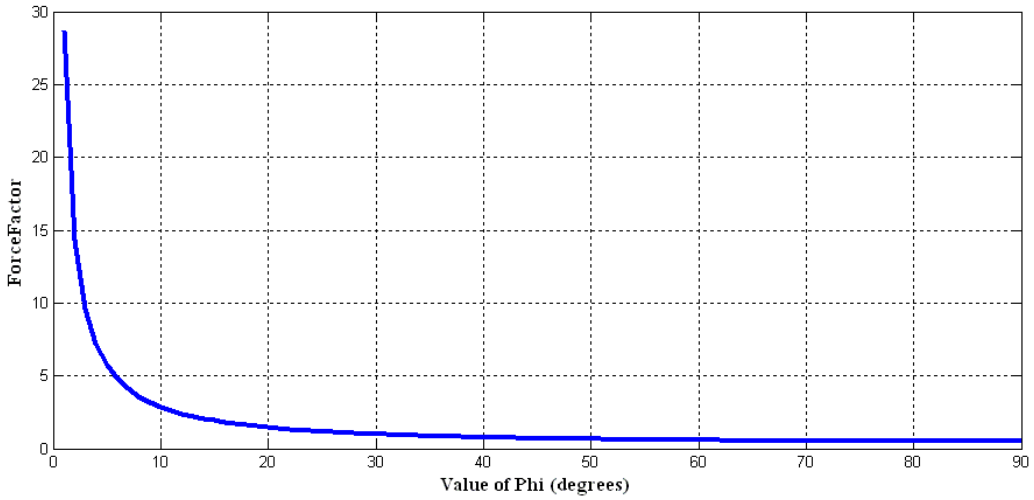

Figure 17: Force factor as a function of Φ given a tilt angle of 30 degrees

To determine the value of Φ, piston lengths are calculated over the +/-30^o range of θ_1 from the triangular geometry of the leveling mechanism in Figure 16 based on fixed values of L and H. Using Equation (11), which is derived from the law of cosines:

$$\phi(H,L) = \cos^{-1}\left(\frac{(L^2 + P_l^{\,2}) - H^2}{2LP_l}\right) \tag{11}$$

the value for Φ and therefore the force factor is calculated. Figure 18 shows how the force factor varies throughout leveling given various ratios of L/H ranging from 0.1 to 1.0. The force factor and the L/H ratio are directly proportional, therefore the smaller the L/H ratio is, the lower the force factor as shown in Figure 18.

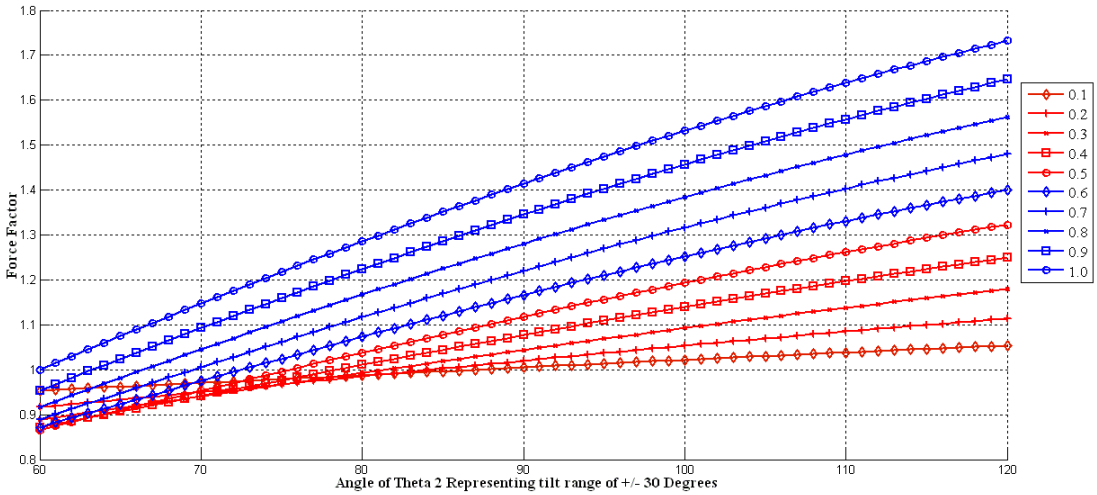

Figure 18: Force factors over the +/-30^{o} range of θ_1 r given different L/H ratios

Given a geometry minimizing the *L/H* ratio in combination with piston capable of the range required, it is possible to calculate the maximum static force needed by the piston using Equation (10)

The dynamic forces accelerate the landing deck from one position to another in preparation for helicopter landing. The pneumatic piston is sized according to which forces are greater, dynamic or static. The governing dynamics equation for the ISLANDS geometry is similar to Equation (9), with the exception that the acceleration components are added as shown in

$$\sum M_A = L(F_p \sin\phi) - D(F_h \sin\theta_1) = I\alpha \ . \tag{12}$$

In Equation (12), I is the moment of inertia of the rotating landing deck while α is the angular acceleration of the landing deck at the pin, the point labeled as *A* in Figure 14. In Equation (12), α is not known, therefore, it must be calculated from existing parameters used in the design. One parameter is the time for the landing deck to arrive at level from a non-level starting position. Assuming a worst case scenario that the piston must extend *l*

meters from P_o at 0 meters with an initial velocity of V_o *m/s* to a position *P l* meters away in *t* seconds, it is possible to determine the constant linear acceleration a_p from

$$P(t) = P_0 + V_0 t + \frac{1}{2} a_p t^2 \ . \tag{13}$$

The constant acceleration experienced at the point where the piston attaches to the landing deck must be equal to the angular acceleration α at the pin, which is needed in Equation (12). Angular acceleration on rigid rotating bodies is composed of tangential a_t and normal a_n acceleration components. At the point of attachment between the piston and landing deck the sum of a_t and a_n must equal the linear acceleration of the piston a_p. This is depicted in

$$a_{px} = \left|a_p\right| \cos\phi = a_n = \frac{V^2}{L} \tag{14}$$

$$a_{py} = \left|a_p\right| ain\phi = a_t = L\alpha \tag{15}$$

and Figure 19, where the piston acceleration is decomposed into its *x* and *y* components, which are aligned with normal and tangential angular accelerations, respectively, and *L* is the distance between the attachment point and the pivot point as shown in Figure 15.

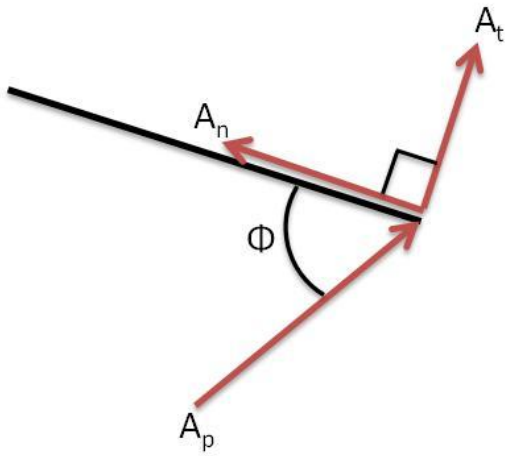

Figure 19: Acceleration diagram of landing deck at point of actuation

Solving for α from Equation (15), and plugging it into Equation (12), where the mass moment of inertia expression of a cube with uniform mass distribution *m* (kg) is used to represent the landing deck, produces

$$F_p = \frac{m(2D)^2 \alpha}{6L \sin \phi} \ . \tag{16}$$

In Equation (16) *D* represents the distance from the pivot to the edge of the landing deck, as shown in Figure 15, where the pivot point is always in the middle of the landing deck. Since the landing deck is square, the mass moment of inertia component is simplified and it is independent of the thickness of the landing deck.

Independent of size Equations (10) and (16) are the two governing equations determining the force required by the linear actuator of ISLANDS, assuming that the geometry adheres to that depicted in Figure 15. The parameters required by Equations (10) and (16) for the ISLANDS prototype are summarized in Table 1; calculated values are appended by a '-calculated' for clarity.

Parameter	Value
L	0.3 m or 12"
H	0.52m or 20.5"
D	0.61m or 48"
Top Deck Mass	50kg or 110lb
Tilt Range	+/- 30 deg
Piston Range -calculated	0.27m or 10.6"
Piston Acc -calculated	.06m/s^2 or 2.3"/s^2
Φ Range -calculated	38-84 degrees

Table 1: Summary of ISLANDS parameters for dynamic and static force calculations

The L to H ratio for the ISLANDS prototype is 0.58 which is not the lowest it could have been but was deemed reasonable given constraints imposed in the building process.

These constraints primarily focused on cost of construction, availability of materials and fabrication time. The modular structural material used in ISLANDS allows for quick assembly without the need for welding, but came at the cost of increased weight, as seen by the heavy top deck. The piston available for use for the construction of ISLANDS has a 12" (.30 m) throw, a major design constraint, which led to *L* being 12" or .3m, producing a mechanical disadvantage of two. Given these considerations and a helicopter system that weighs 20kg, the static force required over the range of landing deck operation is shown in Figure 20 with the additional curves representing helicopters weighing 50, 70 and 90kg, with Table 2 summarizing the results.

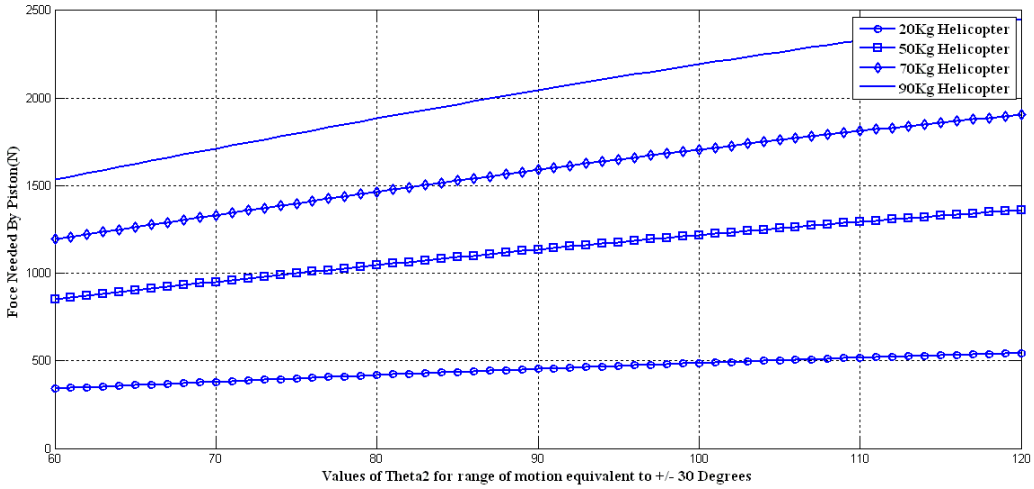

Figure 20: Static force need by piston over range of landing deck angles for various helicopter loads

Helicopter Weight (kg)	Maximum Static Force (N)
20	545
50	1360
70	1905
90	2449

Table 2: Summary of maximum static forces needed for various helicopter loads

These results are based on the assumption that as the platform size grows to accommodate larger helicopters, the *L/H* ratio stays the same at 0.58.

The results for the dynamic force calculations are summarized in Table 3. As constant acceleration was assumed in the dynamic force calculations the force is constant throughout the range of motion of the piston.

Side Dimension (m)	Deck Mass (kg)	L (m)	H (m)	Force (N)
0.6	50	0.3	0.5	200
1	60	0.5	0.8	240
1.5	80	0.7	1.3	320
2	110	1	1.7	440
3	150	1.5	2.6	600

Table 3: Summary of dynamic force calculations and ISLANDS dimensions

The dynamic calculations are independent of the helicopter mass as the leveling is done without a helicopter present. The geometry and mass of the landing deck are important in the dynamic force calculations, therefore also included in Table 3 for different deck sizes. The first entry in Table 3 is for the constructed ISLANDS prototype. The other entries are for larger ISLANDS system with the top deck mass estimated, a constant *L/H* ratio of 0.58 for consistency with Figure 20, and a constant linear acceleration of 0.6 m/s^2. As all the entries in Table 3 have the same constant accelerations. Table 4 summarizes the results of varying the linear acceleration on the prototype from 0.1 m/s^2 to 1 m/s^2, which produces the expected linear relationship.

Linear Acc (m/s^2)	Force (N)
0.1	33
0.2	66
0.3	99
0.4	133
0.5	166

0.6	199
0.7	233
0.8	266
0.9	299
1	333

Table 4: Force vs. Various Linear Accelerations

2.2.1.3 Rotation to Gradient Mechanism Overview

Figure 21 shows the components necessary to produce the rotation for alignment with the major gradient of the environment.

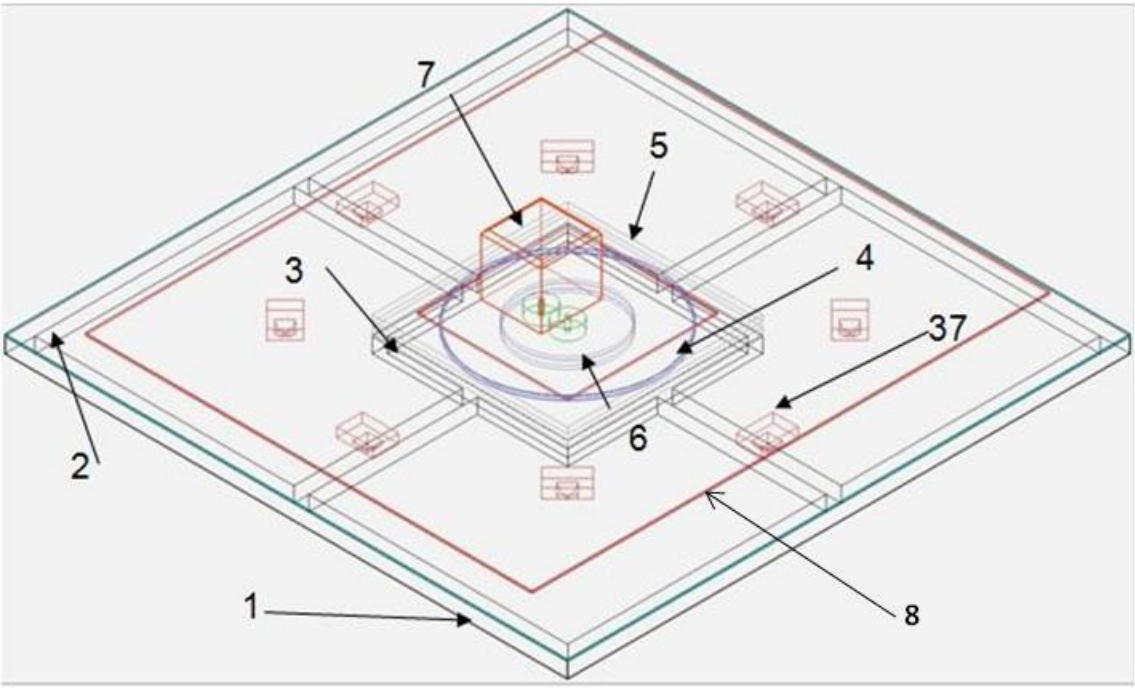

Legend			
1	Fixed base	6	Gears
2	Bottom metal sheet	7	Dc motor
3	Bottom turn table bracket	8	Top metal sheet
4	Turn table bearing	37	Transfer bearings
5	Top turn table bracket		

Figure 21: CAD drawing of ISLANDS base showing rotation mechanism and assembly legend

Rotation is achieved by an electric DC motor powered by the on-board batteries. The entire rotation assembly is a "sandwich" described in layers from the surface touching the ground up through the top of the substructure. The base that touches the ground is a rigid frame capable of being bolted onto other systems such as autonomous ground or sea surface vehicles. On top of the base a thin metal sheet is attached. At the center of the base there is a square to which the bottom half of the turntable bearing bracket is attached. The bottom turntable bearing bracket is a square plate the size of the center square in the base and half the thicknesses of the gears used. The turntable bearing is attached to the bottom half of the turntable bearing bracket. The top turntable bracket is attached to the top of the turntable bearing using the same construction as the bottom turntable bracket. The two rotating gears are located in the pocket formed by the two turntable brackets and the turntable bearing. One gear is fixed to the bottom turntable bracket. The other gear is attached to the motor rotating around the fixed gear. Another thin sheet is attached to the top of the turntable bracket which forms the bottom of the middle rotating sub-assembly. Six transfer bearings are attached to the bottom thin sheet in a circular array. These transfer bearings are used to support the weight of the rotating sub-assembly and avoid excessive wear on the turntable bearing. The motor is attached to the top of the thin plate of the rotating sub-assembly thereby completing the sandwich and allowing rotation of ISLANDS for alignment with the gradient of the environment.

2.2.1.4 Rotation to Gradient Design Analyses

To determine the size of the DC motor needed to rotate the landing deck, the total inertia of the mechanical components is calculated. This is done by fixing the motor at the bottom center of the deck as shown in Figure 21. The motor is positioned to align with the *z* axis of the rotating mass, which allows the utilization of the parallel axis theorem to sum all the inertia components of the individual parts making up the rotating mass. The centering motors on the top deck, for example, are modeled as cylinders of uniform mass, for which mass moment of inertia values are commonly available [43]. By knowing the total inertia of the rotating mass and picking the desired acceleration the torque specification τ of the motor is determined based on the relationship

$$\tau = I\alpha \tag{17}$$

For the ISLANDS prototype, a 100W motor with a 100:1 internal gear reduction producing 30 Newton Meters of torque was chosen.

2.2.2 Centering and Latching Mechanism

The landing deck of ISLANDS houses the electronics and actuators necessary for centering and latching of the helicopter for refueling/recharging and data exchange. The centering mechanism is designed to take into account the errors associated with the vision and attitude controller on board an autonomous helicopter. By having the helicopter land approximately in the right spot on ISLANDS, the centering mechanism then moves the helicopter to a pre-defined position. For these tasks, the top deck centering and latching

mechanisms are very important, and depicted in Figure 22, without the top deck support structure.

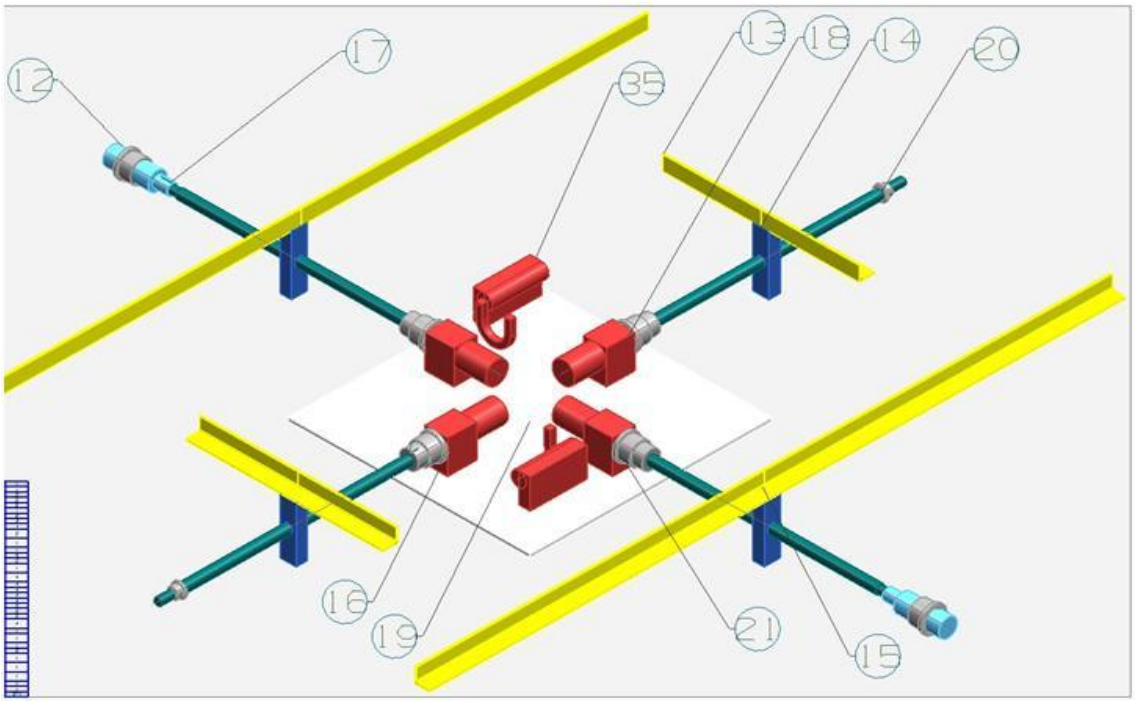

Legend			
12	Support deck pin	18	Coupler
13	Short centering wiper	19	Plate
14	Wiper attachment block	20	Bearing
15	Long centering wiper	21	Bearing
16	Centering motor	35	Latching mechanism
17	Acme thread rod		

Figure 22: Centering mechanism inside landing deck and assembly legend

The centering mechanism is composed of four centering motors mounted to a plate, which is mounted to the center of the top deck sub-structure. Each of the four motors connects to an acme thread rod via a coupler. The coupler is needed since the motor shaft diameter and acme diameters are different. Bearings are attached to each end of the acme

thread that goes through the top deck substructure. Two of the bearings on the long wiper ends are larger because they support the deck pin. A block is attached with a nut to each of the four acme rods, therefore when the motor turns and the block is restrained from rotating by the top deck sub-structure it ends up translating along the acme rod. The latching mechanism engages once centering is complete by rotating hooks that latch onto the skids of the helicopter.

The motors currently being used for centering the helicopter are 12V DC motors rotating at 263RPM with a stall torque of 2527oz-in or 181 kg-cm. Theses motors were chosen for their size and cost. The size of the motors is determined by using

$$T_{su} = \frac{Pd_p}{2}\left(\frac{u\pi d_p + L\cos\theta)}{\pi d_p \cos\theta - uL}\right) \tag{18}$$

$$T_{dsu} = \frac{Pd_p}{2}\left(\frac{u\pi d_p - L\cos\theta)}{\pi d_p \cos\theta + uL}\right) , \tag{19}$$

which represent the torque needed for pulling and pushing a load along the acme thread screw **[**43**]**. The difference between the two equations has to do with the angle of the thread θ when moving up or down the screw. One way the thread is inclined up and the other the thread is inclined down. In Equations (18) and (19) P represents the maximum allowable helicopter load of 150kg, d_p represents the pitch diameter of the acme thread, L represents the thread pitch of the acme thread, θ represents the acme thread angle, and μ represents the coefficient of friction. All the values in Equations (18) and (19) are provided in the acme thread data sheet, except for the coefficient of friction. For the purpose of this project the coefficient of friction was chosen aggressively at 0.25. This is done to accommodate both the friction between the nut and the acme thread, and the

friction between the helicopter skids and the landing deck. Figure 22 and Figure 23 show the CAD and prototype of the centering mechanism for ISLANDS, that when tested took 90 seconds to perform a complete centering operation.

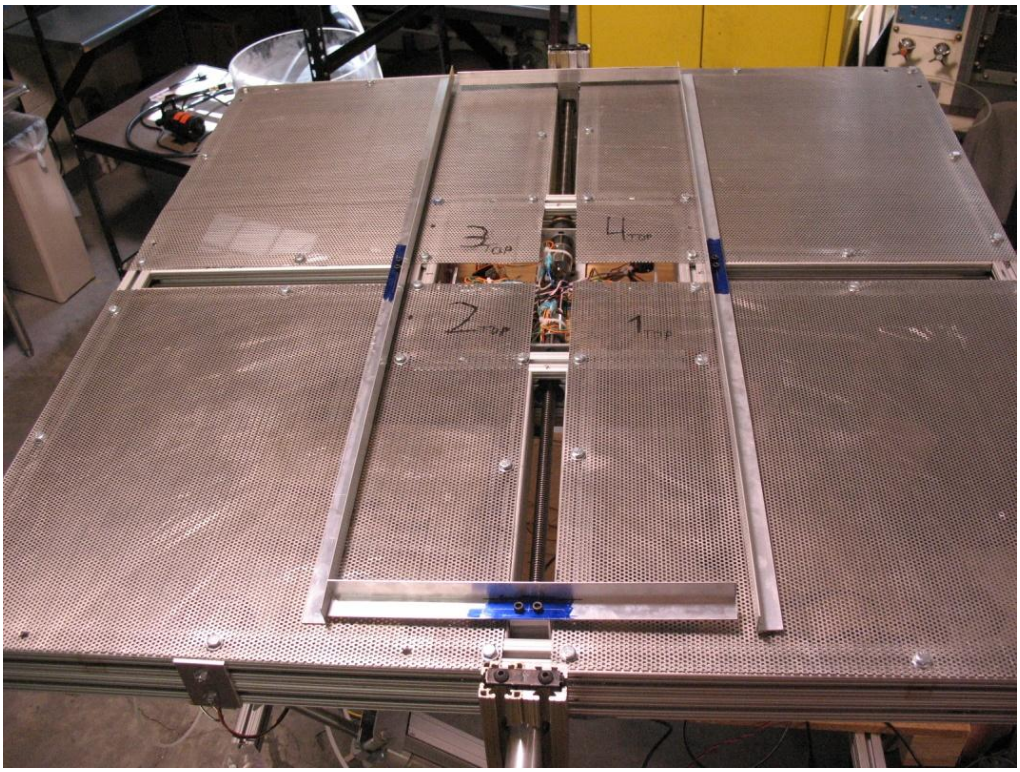

Figure 23: Assembled top deck of ISLANDS with centering wipers

2.2.3 Electronics

The entire ISLANDS system is controlled via an XMOS based microcontroller. XMOS is a technology that allows for real-time task scheduling. This is done by having a hardware based scheduler on board the XMOS servicing the 32 available threads on the XS1-G4 XMOS chip. In the current prototype of ISLANDS the tasks running include:

- Listening to the inclinometer sensor for leveling.
- Running the algorithm that generates appropriate PWM signals to the solenoid valves driving the pneumatic piston.

- Turning on and off the rotation motor
- Listening to proximity sensors of the centering mechanism
- Turning on and off the centering motors.
- Actuating the latching mechanism once the landing deck is level and the helicopter is aligned with the known ISLAND reference frame.

One drawback of XMOS, as with any microcontroller, is that the output/input ports can source/sink low current compared to the level needed by the components they are controlling. For this reason, every electrical component on ISLANDS is attached to the microcontroller via a daughter board capable of sinking/sourcing the higher current levels needed. The daughter board is controlled by low level signals from the XMOS to activate the high power needed by the device. For example, the solenoid valves used in this project draw 0.25 amps at 24V DC which is considerably more than the XMOS can provide. On the daughter board there is a motor driver integrated circuit chip controlled by a low level Transistor Transistor Logic (TTL) signal from the XMOS which can control the 0.25 amps and 24V DC needed by the valves. Similarly, automotive relays are in series with the same TTL integrated circuit component to control the centering motors, which draw 6 amps at 12V DC. ISLANDS has components that require both 12V and 24V DC voltage levels. To achieve this, two 12V lead acid deep cycle batteries are on-board ISLANDS and are wired in series to produce the 24V power bus needed, while one battery is wired as a dedicated 12V DC power bus. Further details of the electronics are presented in Chapter 3.

The XMOS board currently used is capable of controlling the additional tasks still to be added to ISLANDS associated with refueling/recharging and data exchange.

2.3 Pneumatics

One of the driving factors for choosing pneumatic actuation is the high force required to level the landing deck of ISLANDS, as shown by Equations 10 and 16. Other actuation methods were also considered and dismissed, such as electric and hydraulic linear actuators. Hydraulics were dismissed due to the need for hydraulic fluids and pumps. If a leak in the hydraulic system were to occur, total failure will eventually occur due to the loss of actuating fluid. However, controlling hydraulic systems is straight forward due to the inherently slow response times, and the incompressibility of the working fluid (usually a very heavy oil). Electric actuators where also considered and dismissed because their force to power consumption ratio is the lowest of the three, and electric linear actuators are not back drivable, while pneumatic actuators are easily back drivable.

2.3.1 Pneumatic System Overview

As ISLANDS uses a novel PWM-based signal for actuating on/off solenoid valves. The pneumatic actuation is achieved by using a 4-way 3-position pneumatic valve actuated by two 24V DC solenoids to control air flow into a 6.3 cm diameter bore 2-way piston with a 30cm throw. A 4-way 3-position valve is used because the default state of the valve is that both valves are closed and hence the piston holds its position. A linear transducer with .01% linearity is used for position feedback during testing. ISLANDS

uses an inclinometer for position feedback to eliminate the need for inverse kinematic calculation. The XMOS microcontroller produces the PWM signal based on the controller implemented, to signal the two on/off solenoid valves. The test bed used for initial testing is depicted in Figure 24.

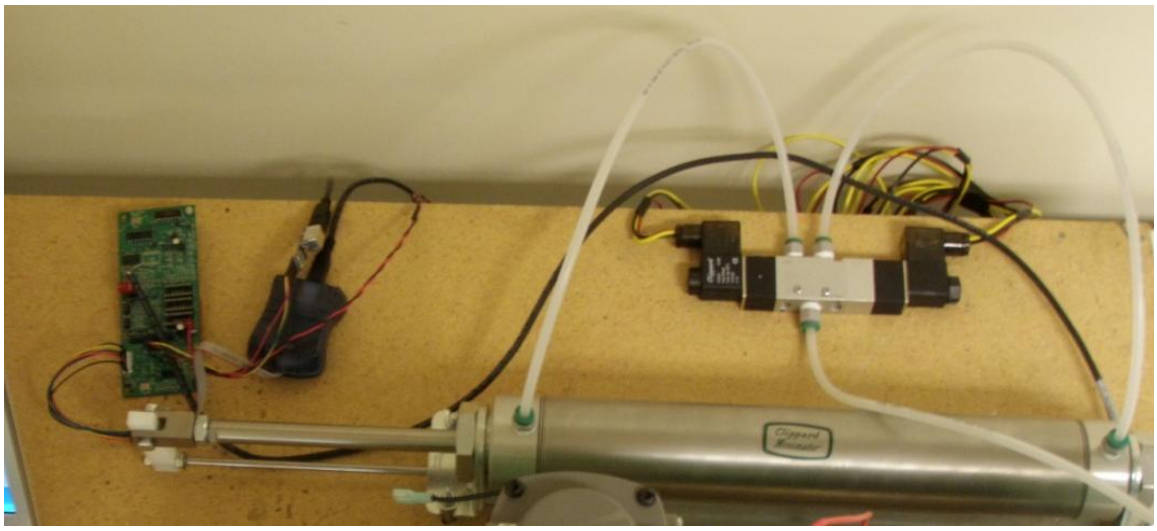

Figure 24: Test bed used for testing pneumatic system

2.3.2 Pneumatic System Experiments and Results

The first step in the controller design is to determine the delay time associated with the solenoid valves. It was determined experimentally that the delay time on the valve was 8ms. This was done by generating a 20Hz carrier wave, similar to those used in DC motor actuation, and slowly increasing the duty cycle from zero until the valve completely opened and closed. Once the minimum duty cycle determined, an experiment was set up to determine the piston behavior under varying duty cycles. In the experiment, the valves were pulsed continually at different duty cycles ranging from 25% to 95%, while the piston went from retracted to extended position and back. From this data the

piston velocity under different duty cycles was determined. The results of this experiment are presented in Figure 25.

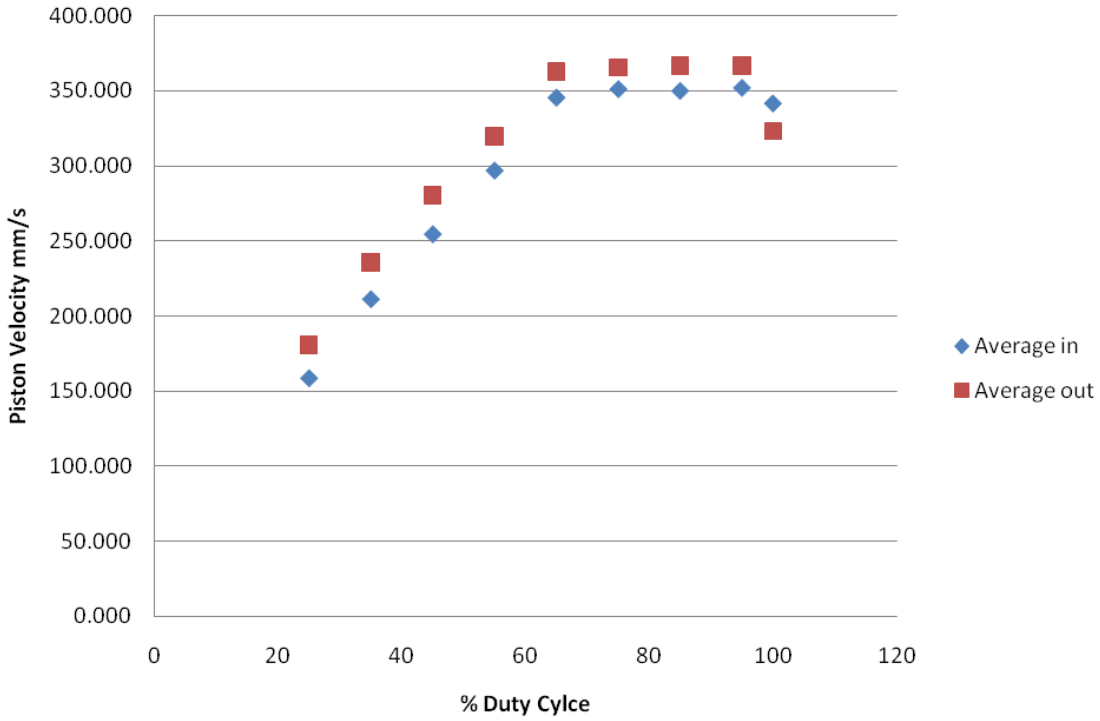

Figure 25: Results of varying duty cycles vs. piston velocity experiment given fixed air pressure of 65PSI

An interesting observation from this experiment is that at roughly 65% duty cycle, the piston velocity peaks at 345 mm/s for in and 362 mm/s for out. Based on these experiments, the upper and lower saturation limits of the controller are determined as being 16% and 65% duty cycles respectively.

Using the information gained from the two preliminary experiments, a proportional controller was implemented. The controller uses position error to generate the appropriate signal to the appropriate valve. This ensures that only one valve is working at time. To test the controller, a staircase trajectory was given to the controller with set points of 7.6, 15.2, 22.9 cm and a half second delay at each set point. Additionally a buffer of 1mm was given to the system which is within system

specification of level. Different combinations of proportional and differential gains were tested with the staircase trajectory. After the experiments, it was determined that, due to the slow response of the system, a differential gain is un-necessary. Figure 26 shows the results from five proportional gains tested when going from a set point of 7.6cm to 15.2cm. As can be seen, the higher the gain the faster the response but at a gain of 50 there is overshoot, hence a gain of 40 was selected. Using a proportional controller the piston is able to cover 7.6cm in 0.45 seconds which is within the time requirements of the system.

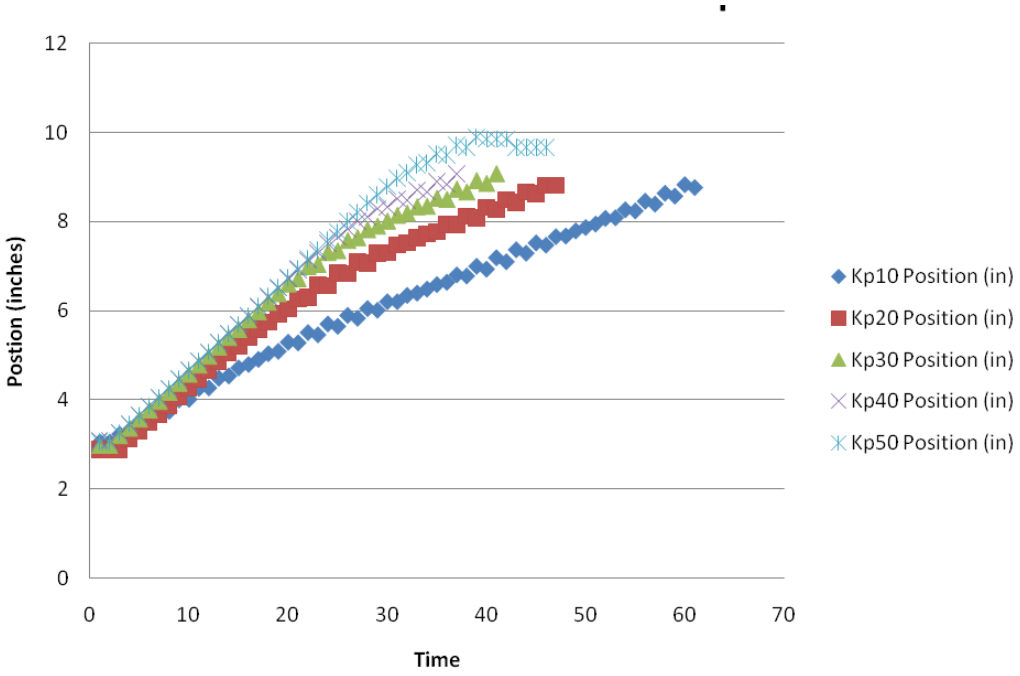

Figure 26: System response to moving from 7.6cm set point to 22.9cm set point

CHAPTER 3: ISLANDS POWER SYSTEM

For ISLANDS to increase the endurance of Class I autonomous helicopters it must be capable of operating in the field for prolonged periods of time. A major function of ISLANDS is to provide refueling/recharging services to helicopters; therefore, it must maintain reserves of electricity and fuel to meet the refueling/recharging demands of a multiday helicopter deployment. Additionally ISLANDS itself must maintain certain energy reserves to remain operational for the duration of the mission.

This chapter presents analysis of the different energy consumers and energy sources on-board ISLANDS to determine the amount of energy, battery or gas needed, in reserve for a mission of predefined length. The analyses performed are based on the types of helicopters ISLANDS is to service: electric, gas, or combination of both. The contribution of this chapter is a method for calculating the energy requirements of ISLANDS for missions of differing endurance and configuration.

The remainder of this chapter includes a literature review of relevant battery recharging/refueling systems showing how ISLANDS is different from existing systems since it primarily works "off the grid." A decomposition of all the energy consumers on-board ISLANDS and the equations governing those systems follow. Then, a section on the energy sources on-board ISLANDS and their governing equations follow. The chapter concludes with a section showing how derived equations from the previous two

sections are used in calculating the energy requirement of ISLANDS depending on the type of helicopters serviced.

Knowledge gained from this chapter along with the ISLANDS placement algorithm options to be presented in Chapter 4 will allow for a more accurate portrayal of the real-world deployment proposed in chapter 5.

3.1 Previous Work

As oil resources are predicted to be dwindling, more research has been focused on alternative fuel vehicles [44] operating as either gas/electric hybrids, e.g., Toyota Prius [45] or electric, e.g. Nissan Leaf [46]. The Nissan Leaf stores all its energy in on-board batteries, which must be recharged. Re-charging is not very novel, as rechargeable batteries have been around since 1960 [47] with ongoing development of recharging different battery chemistries. The additional loading of charging electric vehicles on the power grid and potential way of balancing this load is being research extensively [48]. Electric cars can only operate in areas that have access to the power grid or "on the grid," and in applications where long down time is acceptable. For example, the charging time for a Nissan Leaf is 7 hours [46].

A company called Better Place has proposed a solution to the long charging time of electric vehicles. Instead of charging stations, which are currently built into electric vehicle owners' homes, Better Place has developed battery replacement stations. A video of which is available at [49]. The owner of an electric vehicle drives into one of the bays at a Better Place replacement station, presses a button and a mechanical system

withdraws the depleted battery replacing it with a fully charged one, allowing the person to continue as if they just refueled their gas car. These Better Place replacement stations are currently being tested in small communities around the world. Better Place has not made public knowledge how they determine the number of batteries kept at a replacement center, and the energy consumption of each replacement station, which is one of the challenges this chapter tackles. Each Better Place replacement station can be seen as an ISLANDS station with an important difference being that ISLANDS stations are "off the grid." Each ISLANDS station must contain all the energy it needs for the mission duration, while Better Place stations are plugged into the power-grid providing them with an infinite source of energy.

Being "off the grid" and the types of vehicles serviced are two differences between ISLANDS and Better Place. Work on recharging an electric Vertical Take Off and Landing (VTOL) vehicle has been done by Dale et al. [50] in which a quad-rotor electric VTOL is kept flying for 24 hours with the use of a charging station. Their research focused on the charging mechanism for the quadrotor, which was plugged into a wall outlet providing unlimited source of energy. Similar to the battery replacement system for cars by Better Place, the work by Suzuki et al. [51, 52] proposes a system for battery replacement and recharging for the Lama V3/4 small size (230g, 8.1 oz) hobby helicopter that was used as an autonomous test-bed in [53]. Additionally, the work in [51] uses a Petri net model [54] for determining the amount of batteries stored on-board the replacement mechanism for a mission requiring h helicopters at a given time. As the primary function of the current prototype of ISLANDS is for refueling/recharging, this is

not relevant. Yet, the same Petri net model shows how many VTOLs/unit time can be in the air, which is important in the coverage problem of Chapter 4. Both the quadrotor recharging system and the Lama recharging/battery replacement systems assume an infinite source of energy, meaning "on the grid", and for this reason the "off the grid" analysis presented in this chapter for ISLANDS is necessary.

3.2 Energy Consumers

For the purpose of this section, it is assumed that the ISLANDS station has the capabilities of both refueling and recharging. This is important as some components for refueling are not used for recharging and similarly some components for recharging are not used in refueling. Table 5 lists the energy consuming components of ISLANDS needed for day-to-day operation of refueling, recharging or both. Not included in this section is the energy consumed by the helicopters serviced by ISLANDS, this will be addressed in 3.4.

Component	Needed for:
Centering Motors	Both
Latching Servo	Both
Air Compressor	Both
Solenoid Valves	Both
Rotation Motor	Both
Solar Charge Controller	Both
Microcontroller	Both
Fuel Pump	Gas
Battery Charger	Electric

Table 5: List of ISLANDS energy consuming components and the type of helicopter they support

3.2.1 Centering Motors

ISLANDS has 4 centering motors that must operate twice per helicopter refueling/recharging: once to move out to the edge of the landing deck before the helicopter lands and once to move the helicopter to the center after it has landed. Energy consumed by the centering motors E_c for r helicopter refueling/recharging cycles is governed by

$$E_c = 8r\frac{t(i_c v_c)}{e_c} \ . \tag{20}$$

In Equation (20) the constant *8* is the effective number of motors operating during each landing cycle, accounting for the retraction and centering stroke of each motor. The remainder of Equation (20) is the energy consumed by each motor according to [55], where i_c, v_c, and e_c are the current, voltage, and efficiency of the centering motors respectively, with t being the time each motor operates per cycle. Table 6 summarizes the variables in Equation (20), all of which are found in the motor data sheet or calculated based on the landing deck geometry.

Variable	Description (units)
E_c	energy consumed (Joules)
i_c	current (amps)
v_c	voltage (volts)
e_c	efficiency (%)
t	time (seconds/cycle)
r	refuels-recharges/day (unit-less)

Table 6: Summary of centering motors variables

3.2.2 Latching Servo

ISLANDS has two latching servos for each side of the helicopter skids. The servos actuate once the centering procedure is complete and the helicopter must stay in a fixed position for the duration of the refueling/recharging procedure. The servos are actuated to two predefined positions, unlatched when they do not consume energy, and latched when they do. Servos consume energy when moving from one position to another and when maintaining a position under load, such as when the helicopter moves against them. Energy consumed by the latching servos E_l for r cycles of helicopter refueling/recharging is governed by

$$E_l = 0.5r\frac{t(i_l v_l)}{e_l} \ . \tag{21}$$

Servo and DC motors operate similarly, for this reason Equation (21) and Equation (20) are similar. i_l, v_l, and e_l are the current, voltage, and efficiency of the latching servos respectively, with t being the time each latching servo operates.

The time the latching servo must be in the latched position is a function of the helicopter duration on the landing deck. While the helicopter is latched on the landing deck, we estimate that as a worst case scenario perturbations requiring the servos to engage the helicopter skids will occur for 25% of the refueling/recharging time. For this reason, a constant of *0.*5 is in Equation (21) accounting for perturbations and the number of servos. Table 7 summarizes the variables in Equation (21), all of which can be found from the servo data sheet or calculated based on refueling/recharging times discussed in Sections 3.2.7 and 3.2.8 respectively.

Variable	Description (units)
E_l	energy consumed (Joules)
I_l	current (amps)
V_l	voltage (volts)
e_l	efficiency (%)
t	time (seconds/latch)
r	refuels-recharges/day (unit-less)

Table 7: Summary of latching servo variables

3.2.2 Air Compressor

The air compressor on-board ISLANDS is used to provide the compressed air needed by the pneumatic piston, which levels the landing deck as discussed in Chapter 2. The air compressor initially fills the air tank from zero Pascals to a user predefined pressure p_{max} higher than that needed by the piston. The air compressor is then used to maintain the pressure in the reservoir between p_{max} and p_{min} due to air loss from the initial leveling, and air leaks associated with all pneumatic systems. p_{min} is the minimum pressure maintained in the air tank, and is also a user-defined parameter. The energy consumed by the air compressor E_{ac} is governed by

$$E_{ac} = \frac{p_{\max} v}{e_{ac}} + nv\left(\frac{p_{\max} - p_{\min}}{e_{ac}}\right) \ . \tag{22}$$

Equation (22) is similar to that found in Munsor et al. [29], which is the amount of energy needed to increase the pressure of a fixed volume tank to p_{max} neglecting compressor inefficiencies. In Equation (22) n is the number of times per day that the compressor must turn on to increase the pressure from p_{min} to p_{max}. For the ISLANDS prototype, n is determined experimentally to be four, and depending on pneumatic system configuration n will vary. The data sheet of a Viair Corp [56] air tank and compressor combination does not provide the compressor efficiency. The Viair data sheet, like others provides the

time it takes to fill a given air tank to a given pressure, along with the voltage rating, and current draw by the compressor at different air tank pressures. From this information it is possible to calculate the electrical energy consumed by the compressor. Comparing the calculated energy consumption to the ideal value calculated according to [29] provides the compressor efficiency. Performing this analysis for different compressor systems and averaging their efficiencies provides a general value for e_{ac} that is used throughout Chapter 3. Table 8 summarizes the variables needed in Equation (22).

Variable	Description (units)
E_{ac}	energy consumed (Joules)
p_{max}	maximum tank pressure (Pascal)
P_{min}	minimum tank pressure (Pascal)
v	volume of reservoir(m^3)
e_{ac}	compressor efficiency
n	tank refills/day (unit less)

Table 8: Summary of air compressor variables

3.2.3 Solenoid Valves

There are two solenoid valves on the current prototype of ISLANDS, which control the air flow into the pneumatic piston. The energy consumed by the solenoid valves E_s is governed by

$$E_s = 2(v_s i_s t) \ . \tag{23}$$

In Equation (23) v_s, and i_s are the current and voltage ratings of the chosen solenoid valves, and t is the duration for which the valves are activated. These variables are summarized in Table 9.

Variable	Description (units)
E_s	energy consumed (Joules)
v_s	solenoid (volts)
i_s	solenoid (amps)
t	time (seconds)

Table 9: Summary of solenoid valves variables

As stated in Chapter 2, only one of the valves is actuated at a time during extension or retraction. To provide a safety factor in Equation (23) it is assumed that both valves are actuated throughout the leveling operation. The duration of operation can be calculated from Equation (13) in Chapter 2, which is dependent on the linear acceleration chosen for the landing deck during leveling.

3.2.4 Rotation Motor

The energy consumed by the rotation motor is dependent on the power of the motor and the duration of operation during leveling. The rotation motor chosen for ISLANDS is capable of low rotational speed to avoid large accelerations and undue forces on the system. Knowing that at most the platform will perform one full revolution to align with the gradient, calculating energy E_r consumed by the motor is given by

$$E_r = P_r t \quad (24),$$

where the P_t is the power rating of the motor and t is the duration for making one revolution in seconds.

3.2.5 Solar Charge Controller

One of the energy sources on ISLANDS is the solar panel mounted on the underside of the landing deck, which is discussed further in Section 3.3. To most

effectively take advantage of the solar array, a charge controller is needed. Charge controllers are electrical devices that regulate the voltage and current coming from the solar cells to the batteries ensuring proper charging and preventing over charging. Figure 27 shows how the solar panels, charge controller, and batteries are to be connected.

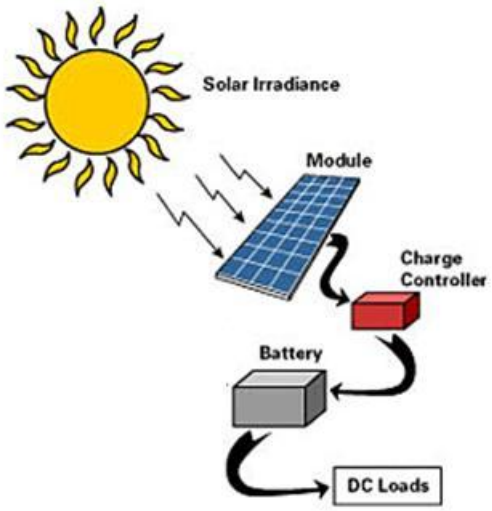

Figure 27: Typical application of solar charger **[**57]

Charge controllers can also compensate for different battery chemistries as different chemistries require different charge profiles [58].

Although the solar charger controllers are part of the energy source system, they consume energy when operating and idling at night. Typical charge controllers require 1 watt of power [59] and operate all day. Therefore the total energy consumed by the charge controller E_{cc} is equal to 86,400 joules per day, which is the number of seconds in a day.

3.2.6 Microcontroller

ISLANDS utilizes the XMOS XS1-G4B microcontroller. From the XMOS data sheet, when the XS1-G4B chip is utilizing all 32 threads it consumes 2.6 watts of power [60]. By knowing the power consumption of the XMOS chip, or of other microcontrollers possibly used in the future, and assuming 24 hour operation, the resulting total energy consumption E_{mc} can be determined. For the XMOS XS1-G4B the total is 224,640 joules per day.

3.2.7 Fuel Pump

The fuel pump energy consumption component E_{fp} is calculated according to

$$E_{fp} = tr\left(\frac{\rho g H \dot{Q}}{e_{fp}}\right) , \tag{25}$$

which is the general form of pump equations [29]. The ISLANDS geometry, helicopter, and fuel type affect the parameters in Equation (25). In Equation (25) ρ is the density of the fuel, which for helicopter fuel ranges from 745 kg/m^3 [61] for low grade diesel to 862 kg/m^3 for nitro methane. The distance the fuel must travel and the friction it has with the tubing is lumped in to *H,* which is the dynamic head that the pump must overcome. *H* will vary with the size of ISLANDS systems built, since the distance between the bottom deck where the fuel is stored and top deck changes with ISLANDS size. The fuel flow rate $\dot{Q}$ is a function of the pump chosen and is one of the two parameters needed to determine the pumping duration in *t,* the other being the volume of the fuel tank on-board the helicopter V_h. Again *r* is the number of helicopters refueling per day, and *g* is the

gravitational acceleration constant. These parameters and their units are summarized in Table 10.

Variable	Description (units)
E_{fp}	energy consumed (Joules)
t	time (seconds/fueling)
ρ	Fuel density (kg/m^3)
g	acceleration due to gravity (m/s^2)
H	dynamic Head (m)
$\dot{Q}$	flow Rate (m^3/s)
e_{fp}	efficiency (%)
r	refueling/day (unit-less)

Table 10: Summary of fuel pump variables

The fuel pump efficiency value used throughout this chapter was determined in a similar method to that described in Section 3.2.2 discussing the air compressor.

3.2.8 Helicopter Battery Charger

Battery chargers, like the charge controller described in Section 3.2.5, maintain proper charge conditions for batteries of different chemistries. For the lithium polymer batteries used in the Maxi Joker 2 [62] and various Rotomotion LLC [16] helicopters, proper battery charging is of utmost importance as improper charging could lead to battery explosion [63]. The energy consumed by the battery charger E_{hbc} is

$$E_{hbc} = r\left(\frac{3600 B_c B_v}{e_{hbc}} + P_{hbc} t\right) \tag{26}$$

where B_c and B_v are the helicopter battery capacity and voltage respectively, P_{hbc} is the battery charger power consumption, e_{hbc} is the efficiency of the battery charger and t is the time it takes to charge the helicopter battery, which is calculated according to

$$t = \frac{B_v B_c}{c_c c_v} \ . \tag{27}$$

In Equation (27) it is assumed that the helicopter battery is completely depleted when charging commences. Equation (26) combines the charger energy consumption with the energy that must be provided to recharge the helicopter battery. The parameters for both the charger and helicopter battery are summarized in Table 11.

Variable	Description (units)
E_{hbc}	energy consumed (Joules)
B_c	helicopter battery capacity(amp-hour)
B_v	helicopter battery voltage (volts)
C_i	charger current output (amps)
C_v	charger voltage output (volts)
e_{hbc}	efficiency (%)
P_{hbc}	power consumption (watts)
r	recharges/day (unit-less)

Table 11: Summary of helicopter battery charger variables

3.3 Energy Sources

All the consumer components from Table 5 are used by both gas and electric helicopters and use the onboard batteries as an energy source. These batteries are recharged by a solar array mounted on the underside of the clear top landing. When gas helicopters are used, the fuel reservoir will also be stored on-board. With a source of fuel on-board ISLANDS, the potential of using a generator as an additional source of energy will be discussed in section 3.3.3.

3.3.1 Batteries

The batteries on-board ISLANDS are the main source of energy for the entire system. As stated in Section 2.2.3, two 12V batteries are needed in the current ISLANDS prototype to provide both the 12V and 24V power levels needed by the components. Future iterations of ISLANDS will be designed to work with a single 12V battery by selecting a uniform voltage level for all components. Selecting the proper battery size will be discussed in further detail throughout Section 3.4. One of the assumptions made during the analysis in Section 3.4 is that the Depth of Discharge (DOD) of the batteries does not go below 50%. This means that the total energy depleted from the battery does not exceed 50% of the total available energy, and is taken into account in determining the effective energy E_b available from a fully charged battery on-board ISLANDS; this is calculated by

$$E_b = 0.5 v_b b_c 3600 \ . \tag{28}$$

The 50% level is a battery manufactures recommendation [64] to ensure battery longevity. In Equation (28) the energy available from the batteries in joules is calculated based on the parameters summarized in Table 12.

Variable	Description (units)
E_b	energy in batteries (Joules)
v_b	battery voltage (Volts)
b_c	battery capacity (amp-hours)

Table 12: Summary of battery variables

3.3.2 Solar Array

The solar array, charge controller and batteries work in conjunction to increase the duration that ISLANDS can stay in the field by using the sun's energy to replenish

energy consumed by the components discussed in Section 3.2. Solar arrays are specified by their power output in watts. Commercial Off The Shelf (COTS) solar arrays have a power output to area ratio S_{pa} of 13 watts/ft^2 (1.196 watts/m^2) [65]. By knowing the charge converter efficiency e_{cc}, the area of the solar array used A, and the duration of peak sun exposure in seconds it is possible to calculate the total energy gained from the sun each day E_{sa} according to

$$E_{sa} = S_{pa} A t e_{cc} \ . \tag{29}$$

Variable	Description (units)
E_{sa}	energy from sun (Joules)
S_{pa}	power/area (watts/ft^2)
A	area (ft^2)
t	sun exposure time (seconds/day)
e_{cc}	charge controller efficiency (%)

Table 13: Summary of solar array variables

In this work, five hours is used for the peak sun exposure time. This number is based on solar insolation maps such as the one in Figure 28, which describe by region the average number of hours per day solar panels can be expected to work at their peak production efficiency, e.g. 13 watts/ft^2. The map shown in Figure 28 is a yearly average map. Based on ISLANDS' deployment location, a more accurate value for peak sun exposure time can be found using monthly solar insolation maps.

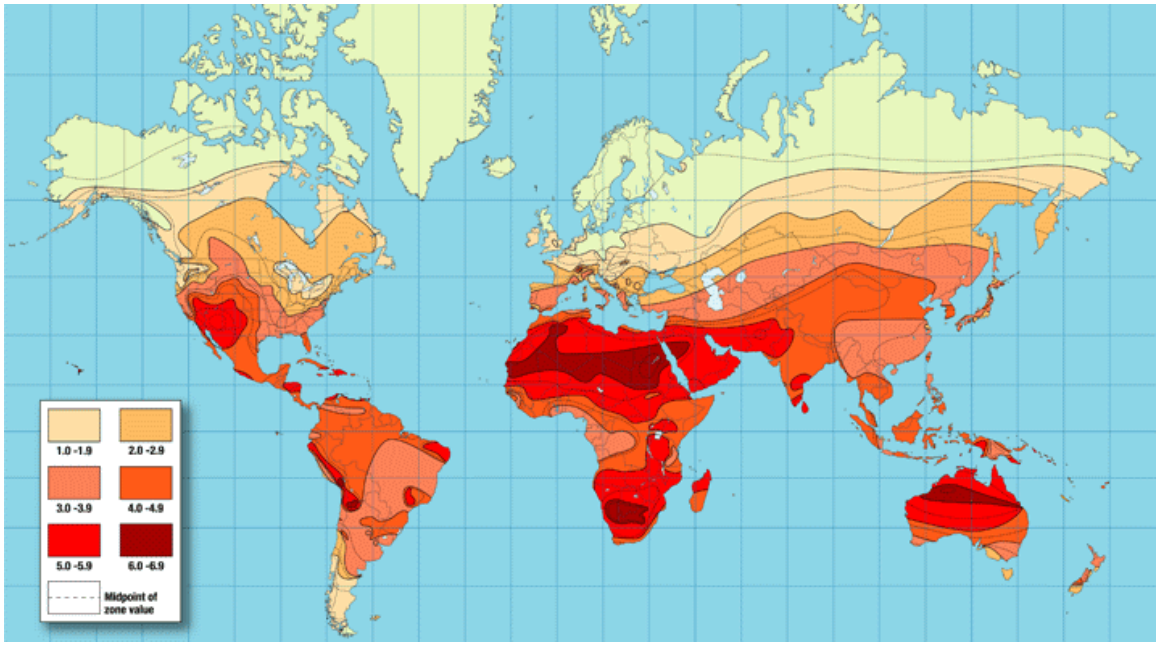

Figure 28: A world solar insolation map [66]

3.3.3 Fuel and Generator

When ISLANDS is servicing gas powered helicopters, fuel reserves will have to be kept on-board. Helicopters have gas engines that allow them to use the gas provided by ISLANDS, while for ISLANDS the fuel just takes up space. By integrating a generator into ISLANDS as shown in Figure 29 it is possible to convert some of the chemical energy in the fuel into electrical energy to potentially re-charge the helicopter batteries.

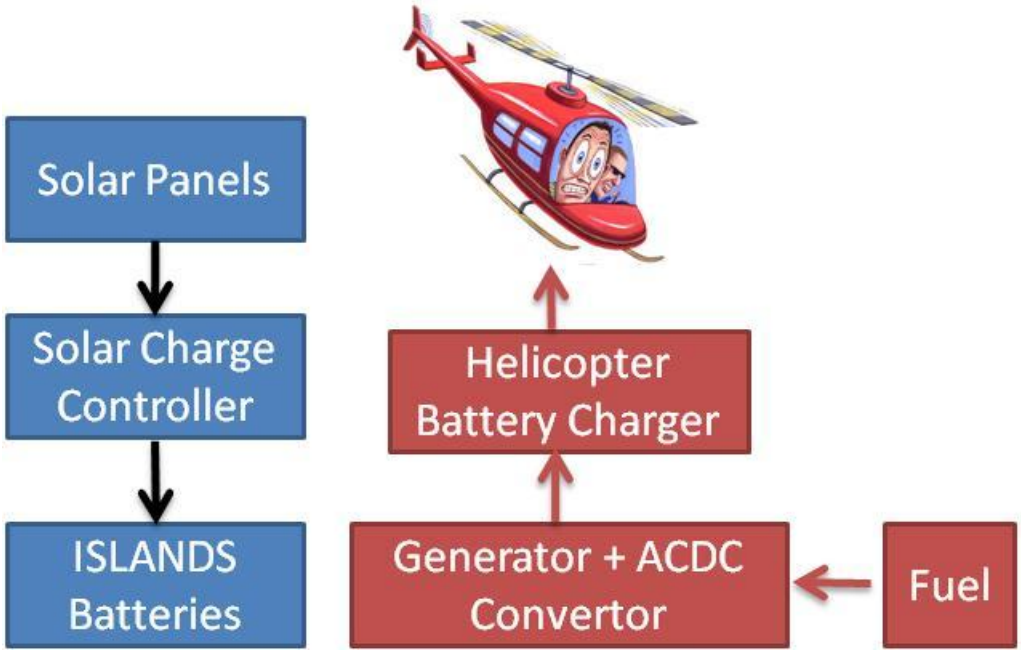

Figure 29: Proposed hybrid system to power ISLANDS

Calculating fuel reserves with the use of a generator is discussed in Section 3.4.3.

The energy reserves on board ISLANDS, as with other solar installations, are stored in deep cycle lead acid batteries. Lead acid batteries are used because they are inexpensive compared to other battery technologies such as the lithium polymer batteries used in electric helicopters. Lithium polymer batteries have an energy density of 720 kilo [61] joules/kg required by electric helicopters with strict payload limits. In solar installation, space and weight are not a constraint, which is why lead acid batteries with an energy density of 126 kilo joule/kg are used. ISLANDS does have space limitation. The 350-fold difference in energy density between lead acid batteries and gas (with an energy density of 45 mega joules/kilogram) makes using a generator as an additional source of energy for certain applications compelling. More detailed analysis of using a generator is presented in 3.4.3.

3.4 Analysis

In this section equations (20) – (26) for the energy consuming components and Equations (27) – (28) for the energy sources are used to calculate ISLANDS' "off the grid" battery and fuel requirements. As fuel and battery requirements are primarily determined by the type of helicopter serviced, four different ISLANDS deployment scenarios are presented. The description of each scenario begins with the assumptions made, and we attempt to stay as general as possible for future adaptability. Each scenario description concludes with general equations for determining the volume of fuel (liters) and the energy capacity of the batteries (amp-hours) needed in amps/hours as a function of ISLANDS deployment time (days) and/or number of helicopters serviced per day. The four ISLANDS deployment scenarios analyzed are:

1) Not servicing any helicopters
2) Servicing gas helicopters
3) Servicing electric helicopters
4) Servicing both gas and electric helicopters

When calculations are performed in the analyses of the different scenarios the variable values used are summarized in Table 14

Variable	Value	Description (units)
Centering Motors [67]		
i_c	6.2	current (amps)
v_c	12	voltage (volts)
e_c	71	efficiency (%)
t	90	time (seconds/cycle)
Latching Servos [68]		
I_l	1.5	current (amps)
V_l	12	voltage (volts)
e_l	76	efficiency (%)

Air Compressor		
p_{max}	6.8e5	maximum tank pressure (Pascal)*
P_{min}	2.7e5	minimum tank pressure (Pascal)**
v	8.8e-3	volume of reservoir(m^3)***
e_{ac}	40	compressor efficiency
n	4	tank refills/day (unit less)
Solenoid Valves [69]		
v_s	24	solenoid (volts)
i_s	0.25	solenoid (amps)
t	10	time (seconds)
Rotation Motor [70]		
P	100	power (watts)
t	10	time (seconds/revolution)
Solar Charge Controller [59]		
P	1	power (watts)
t	8.6e4	time (seconds/day)
e_{cc}	95	charge controller efficiency (%)
XMOS Microcontroller		
P	2.6	power (watts)
t	8.6e4	time (seconds/day)
Fuel Pump		
t	240	time (seconds/fueling)
ρ	862	Fuel density (kg/m^3)
g	9.8	acceleration due to gravity (m/s^2)
H	2	dynamic Head (m)
$\dot{Q}$	4.3e-6	flow Rate (m^3/s)****
e_{fp}	25	efficiency (%)
Helicopter Battery Charger [71]		
B_c	40	helicopter battery capacity (amp-hour)
B_v	44.4	helicopter battery voltage (volts)
C_i	20	charger current output (amps)
C_v	24	charger voltage output (volts)
P_{hbc}	1	power consumption (watts)
e_{hbc}	95	efficiency (%)
ISLANDS Batteries		
v_b	12	battery voltage (Volts)
b_c	33	Battery capacity (amp-hour)
Solar Array [65]		
S_{pa}	13	power/area ($watts/ft^2$)
A	16	area (ft^2)
t	1.8e4	sun exposure time (seconds/day)

*Equivalent to 100 PSI
**Equivalent to 40 PSI
*** Equivalent to 2 Gallons
****Equivalent to 250ml/min
Table 14: Summary of all variables and values used in Section 3.4

3.4.1 Not Servicing any Helicopters

Assuming that ISLANDS has just been deployed, has performed the necessary leveling procedure, and is idle (not servicing helicopters), what are the systems' energy needs for an *n* day deployment? The total energy consumed in an *n* day deployment is

$$E_t(n) = n(E_{ac} + E_r + E_{cc} + E_{mc} + E_s) \ . \tag{30}$$

In Equation (30) the energy consumption of the fuel pump, helicopter battery charger, centering motors, and latching mechanisms are neglected as those are only used during helicopter servicing. Using the values from Table 14 and Equation (30) the total energy consumed in one day is 340 kilo joules, which compared to the 3.6 mega joules available daily from the solar cells is <10%. Figure 30 shows the percentage of daily energy consumed by each of the electrical components. Predicatively, those components that must run continuously, such as the XMOS microcontroller and the charge controller, consume the most energy.

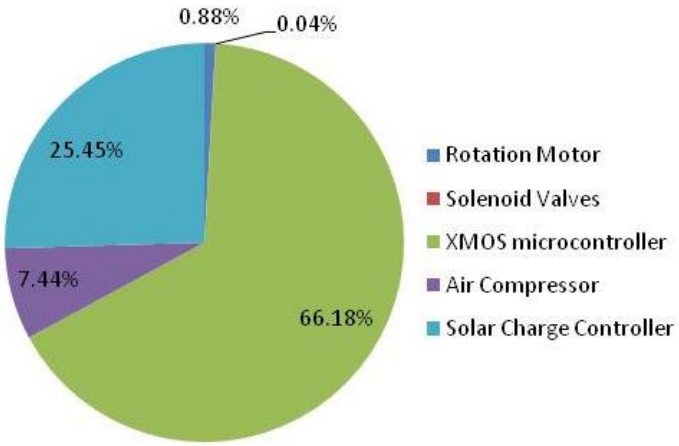

Figure 30: Pie chart of daily idle energy consumption

Using Equation (28) from Section 3.3.1 and the results from Equation (30), the minimum battery capacity for *n* days of operation with no sun is

$$B_c(n) = \frac{E_t(n)}{0.5 v_b 3600} \ . \tag{31}$$

According to Equation (31) each day requires a 12V battery with a minimum capacity of 15.8 amp-hour given the 340 kilo joules/day previously calculated. When counting on the sun for battery charging, the same size battery as calculated by Equation (31) will be sufficient for infinite sunny days of operation (limited to component failures). This is supported by

$$B_l = E_b - \frac{h}{24} E_t \rightarrow (1 \le h \le 12) \tag{32}$$

$$B_l = E_b - \frac{h}{24} E_t + \frac{h-12}{24} E_{sa} \rightarrow (13 \le h \le 24) \ , \tag{33}$$

which models the battery energy level B_l throughout a 24 hour day with 12 hours of darkness, Equation (32), and 12 hours of sun charging the batteries, Equation (33). For the system analyzed in this section, Figure 31 shows that after 12 hours of darkness it

takes one hour of light to completely recharge the batteries. Additionally, after 12 hours the battery energy level is still above the 50% DOD level, indicating a smaller battery could be used.

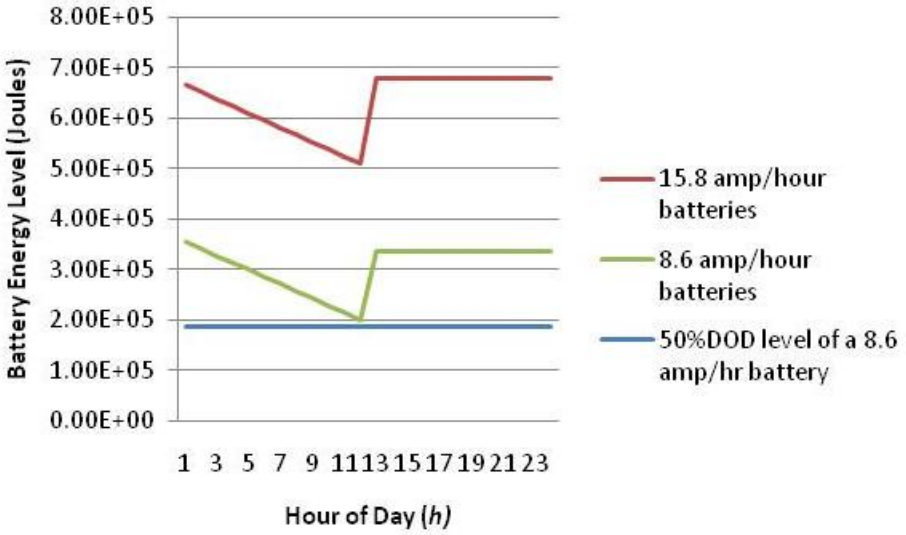

Figure 31: Energy level in batteries throughout a 24 hour day accounting for darkness

Therefore the minimum battery capacity needed is

$$B_c = \frac{(0.5E_t(1)) + \varepsilon}{0.5v_b 3600} \tag{34}$$

were ε is a small value ensuring that the battery capacity after 12 hours is above the 50% DOD needed for battery longevity. In Equation (34), when ε is zero after 12 hours the remaining charge in the batteries is exactly at 50% DOD level. The result of using Equation (34) with an ε of 15 kilowatts is a 12V with 8.6 amp-hour battery providing 370 kilo joules. An 8.6 amp-hour battery after 12 hours of darkness will be depleted to 200 kilo joules, which is above the 50% DOD for of the battery, as shown in Figure 31.

3.4.2 Servicing Gas Helicopters

The gas helicopter assumed in this section is a Rotomotion LLC SR30 shown in Figure 32, which has a two litter fuel capacity [15].

Figure 32: Rotomotion LLC SR30

The other specifications of the SR30 helicopter are not relevant in the analysis performed in this section. For this section, as with Section 3.4.1 and those to follow, 12 hours of darkness and 12 hours of light are assumed. The five hours of peak energy production from the solar array described in Section 3.3.2 is spread equally over the 12 hours of light.

The volume V_f of fuel needed on-board ISLANDS is a function of the deployment duration n in days, the number of refuelings per day r, the volume of the helicopter fuel tank V_h, and is limited by the space V_i available on-board ISLANDS for fuel.

$$(V_i \geq V_f) = nrV_h \tag{35}$$

In the current design of ISLANDS the fuel tanks will have to be placed opposite the air tank. Therefore, the mass of the fuel must be included in the total rotational inertia of Equation (17) from Section 2.2.1.4. In future designs, the on-board fuel tanks will be incorporated into the bottom fixed deck of ISLANDS, hence not affecting other design

elements (i.e., the rotation motor). The current ISLANDS prototype has space for a 15”(38cm)x12”(30cm)x24”(60cm) tank containing ~70 liters of fuel. Assuming that with additional funding the current ISLANDS prototype can be upgraded to handle the additional 60 kg of fuel; 70 liters will be used for the analyses performed in this section. Given either a mission requirement of deployment time, or a design requirement of fuel capacity availability, parameters in Equation (35) can be calculated.

The total energy consumed during a deployment servicing gas helicopters is the sum of energy consumed while idling and the energy consumed performing $R = nr$ refuels.

$$E_t(n) = n(E_{ac} + E_r + E_{cc} + E_{mc} + E_s) + R(E_c + E_l + E_p) \quad (36)$$

In Equation (36) the energy consumed while idling is the same as Equation (30) and is dependent on the length of the deployment. The energy consumed in performing the R refuels is independent of mission deployment time and can be accounted for as a one-time consumption when determining total energy consumption. In Figure 33 the one day energy consumption breakdown where $R=1$ is compared with the total energy consumption given R=35. The values are based on Equation (36) with the parameters from Table 14.

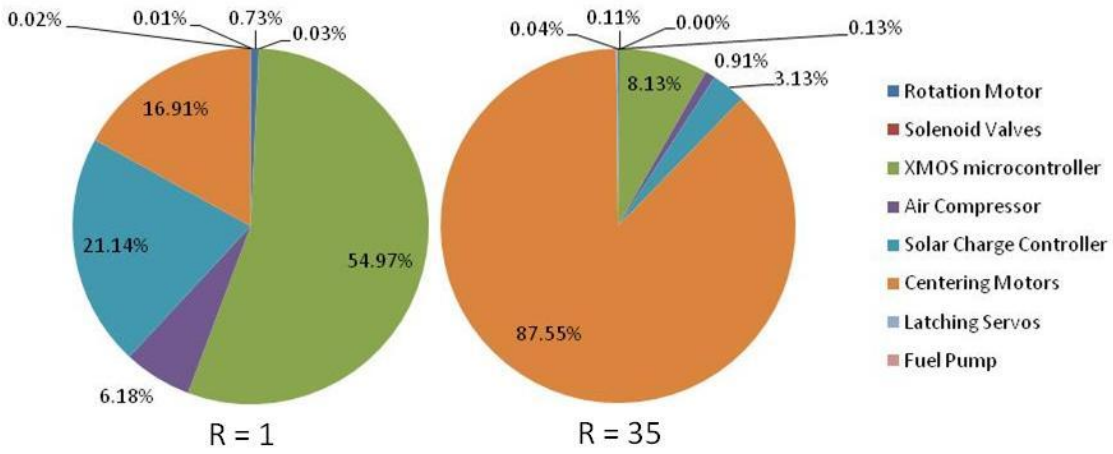

Figure 33: Energy consumption breakdown comparing 1 refuel to 35 refuels

As clearly seen from Figure 33, as the number of refuels increases, refueling components dominate the energy needs of ISLANDS, with the centering motors consuming the most energy and the small amount of energy consumed by the pump attributed to the low flow rate. The total energy consumed in one day given R=35 and $n=1$ according to Equation (36) is 2.76 mega joules, representing an 800% increase over an idle ISLANDS. Given the need for 2.76 mega joules for a one-day mission with 35 refuels, using Equation (31) yields the need for a 12V 128 amp-hour battery. This analysis is independent of energy produced by the solar array, and therefore is a worst-case energy consumption analysis for this scenario.

As in Section 3.4.1, the next step in the analysis looks at including ISLANDS' battery charging capability in determining battery size. In this section it is assumed that helicopter refueling occurs during the 12 hours of daylight because autonomous helicopters primarily use vision-based sensors for safe landing in predefined orientations [73], which require light. For this reason, ISLANDS' energy consumption during 12 hours of darkness is the same as a non-servicing station calculated for in Equation (30).

The net energy consumed by ISLANDS in a 24 hour period taking into account energy from the sun and the *r* refuels occurring during the 12 hours of sunlight is

$$E_{net} = E_{sa} - (E_{ac} + E_r + E_{cc} + E_{mc} + E_s) - r(E_c + E_l + E_p) \quad (37).$$

While E_{net} is positive and the recharging intervals stay constant, at the end of a 24 hours the battery will end fully charged, but if E_{net} is negative the battery will end the day with E_{net} joules less than the initial charge as shown in Figure 34.

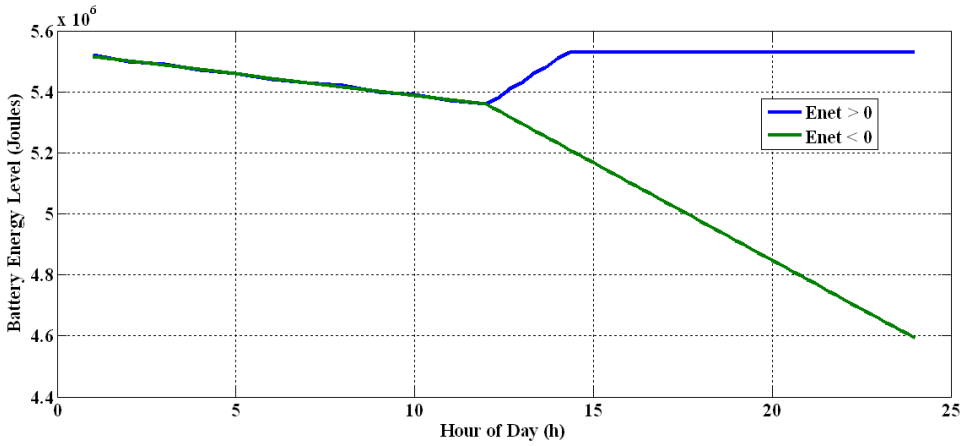

Figure 34: Battery level throughout the day with different E_{net}

From Equation (37) it is possible to find the maximum number of refuels in a day before ISLANDS starts operating at a deficit by setting E_{net} to zero. For the current scenario analyzed, the breakeven point is when *r* is 46, which is equivalent to one helicopter refueled every 15.6 minutes. 46 refuels are not possible in the current scenario as not enough gas is available for the helicopters to fly that much, and therefore ISLANDS will be running at an energy surplus.

If running ISLANDS at a deficit is desired, the battery capacity needed as a function of days deployed is

$$B_c(n) = \frac{n|E_{net}| + .5E_{idle}}{0.5v_b 3600} \ , \tag{38}$$

In Equation (38) E_{idle} is the energy consumed idling during the night. When E_{net} is positive the minimum battery capacity needed at the beginning of the deployment is independent of deployment time and is equal to

$$B_c = \frac{.5E_{idle} + E_{refuel}}{.5v_b 3600} \ . \tag{39}$$

Equation (39) takes into account the scenario where a refuel occurs first thing in the morning, before the batteries can recharge from the night's energy needs, driving the battery level below the 50% DOD. According to Equation (39) and the values used throughout this section, an 11 amp-hour battery is needed, which is eleven times smaller than the 128 amp-hour battery calculated for previously. According to the results from this section, ISLANDS' fuel capacity calculated according to Equation (35) limits deployment duration.

3.4.3 Servicing Electric Helicopters

Electric helicopters have shorter endurance compared to similar size gas helicopter due to the limited energy they can store in their lithium polymer batteries. The two liters of fuel on-board the SR30 helicopter referenced in Section 3.4.2 contain approximately 63.2 mega joules. A similarly sized electric helicopter with a 44.4 volt 40 amp-hour battery has 6.4 mega joules, 10% that of the gas helicopter. In comparing different size helicopters, main rotor diameter is used as a reference. Helicopter power requirements for hover at sea level are a function of the main rotor diameter and gross

payload [5]. The equations governing power during flight are out of the scope of this dissertation, but for helicopter hovering requires the most power [5].

The SR30 gas helicopter used in Section 3.4.2 has a main rotor diameter of 198 cm (78”) and the equivalent electric power helicopter used in this section is the SR100 from Rotomotion LLC, with a main rotor diameter of 201 cm (79”) shown in Figure 32 [16]. The SR100 carries a 44.4 V 40 amp-hour battery storing 6.39 mega joules for a mission endurance of 20 minutes with a maximum payload of 16kg.

Figure 35: Rotomotion LLC SR100 electric helicopter [16]

No other commercial electric platforms in this class size were found other than the laboratory-made autonomous prototypes based on the Maxi-Joker 2 [73, 74, 75] and shown in Figure 36.

Figure 36: Maxi Joker 2 electric helicopter [73]

The Maxi-Joker 2 autonomous platform carries a 37 V 10 amp hour battery storing 1.33 mega joules for a mission endurance of 17 minutes and a maximum payload of 10 kg. Smaller helicopter platforms were found but were not deemed suitable due to their limited payload and even more limited endurance.

The short endurance of electric helicopters means that they must spend a significant amount of time recharging. Upon landing, an electric helicopter will require

$$E_h = \frac{3600 B_c B_v}{e_{hbc}} \tag{40}$$

joules taking into account the 95% efficiency of high-end lithium polymer charger, such as the Thunder Power RC TP820 CD [71], and it will take

$$t = \frac{B_c B_d}{C_v C} \tag{41}$$

hours to completely charge the battery. For the SR100 helicopter 6.73 mega joules are required, which is 96 times more than the 70 kilo joules needed for one 2 liter refueling of the SR30. Assuming that the battery charger is charging at 20 amps C_i and 24 volts C_v

it will take 3.7 hours to charge the SR100 battery. With helicopters landing only occurring during daylight the maximum number of recharges in a day is equal to

$$\max(r) = \lceil 12/t \rceil + 2 \ , \tag{42}$$

which accounts for a helicopter landing right at the beginning and end of the day. With the SR100 this is equivalent to six recharges and 40.38 mega joules required on-board ISLANDS. The total battery capacity needed based on Equation (31) is 1870 amp-hour stored in 12 volt batteries weighing 320 kg. In the current analysis, Equation (31) neglects the energy needs of the centering motors and other continually running components. This is because based on Section 3.3.2 the energy from the solar photo-voltaic panels is sufficient for running those components.

Given the 1870 amp-hour battery capacity calculated, after six recharges on the first day of deployment the battery energy level will fall near the 50% DOD, at which point two days with no services are required to recharge the battery enough for one additional service and 12 days to completely recharge ISLANDS' batteries. The volume and weight of the additional batteries needed for *r* recharges by ISLANDS, which grows linearly with the number of days of deployment makes using only lead acid batteries impractical. For this reason, a gas powered generator as shown in Figure 29 is proposed to provide the energy needed for *R* recharges from on-board fuel instead of on-board lead acid batteries.

As shown in Section 3.4.2 a sufficiently small battery coupled with solar charging is sufficient for centering and refueling helicopters. In this section it has been shown that battery charging requires an amount of lead acid batteries that is impractical due to their

accumulated weight. The system proposed in Figure 29 will use the results from Sections 3.3.1 and 3.3.2 to determine the amount of liquid fuel needed for R recharges, when using a generator coupled to an AC-DC convertor to provide power to the helicopter battery charger.

The conversion between chemical energy in gas to electrical energy using a generator has an efficiency of e_g percent. Additional efficiency losses are experienced when converting between AC and DC power e_{acdc} required by the battery charger, which has an efficiency of e_{hbc}. Therefore, the overall efficiency of converting chemical energy to electrical energy e_{gtoe} is

$$e_{gtoe} = e_g e_{acdc} e_{hbc} , \tag{43}$$

which is 14% using a Honda EU1000i generator[76], with a ETA-USA ACDC [77] converter, and the Thunder Power RC TP820 CD helicopter battery charger. Compared to charging the helicopter batteries directly from the lead acid batteries, which are only dependent on the helicopter battery charger efficiency, using fuel for battery charging is 6.5 times worse on efficiency basis. The significant difference in efficiencies between using gas and batteries for charging the helicopter batteries is overcome by the 350 fold increase in energy density between gas and lead acid batteries. Accounting for the inefficiency of gas to electricity conversion the new effective energy density of gas is 50 times that of lead acid batteries.

In comparing the volume and weight saved by using gas over batteries for charging the weight and space required by the generator and ACDC converter is considered. Every unit mass of lead acid batteries are directly proportionate to electrical

energy storage, which is not true when using gas. Therefore if the amount of lead acid batteries needed is less than the gross weight of the generator and ACDC converter, the use of batteries is more beneficial from a weight and space perspective. This scenario would occur when battery energy densities increase, otherwise a generator system becomes more effective. The generator and ACDC convertor described mass is 15.1 kg which is equivalent to a 12V lead acid battery with a capacity of 44 amp-hours, which is not enough for one recharge cycle of the SR100 batteries. The general formula for the volume of gas per day needed by the generator to perform *r* refuels is

$$v_g(n) = n\frac{rE_h}{e_{gtoe}D_g\rho_g} \ . \tag{44}$$

In Equation (44) E_h is the energy needed per battery recharge based on Equation (40). The energy density of gas being 45 mega joules/kg is used for D_g and ρ_g is the density of gas at 0.702 kg/liter. Based on six refuels per day and Equation (44) the electric generator will require 9.1 liters of fuel, which including the weight of the generator and ACDC converter is a weight saving of 92%.

3.4.4 Servicing Gas and Electric Helicopters

When servicing both gas and electric helicopters the on-board battery needs will be determined according to the results of section 3.4.2, while the fuel consumption will be the sum of Equation (44) and Equation (35). The fuel pump energy needs are neglected in this section because as shown in Section 3.4.2 they are relatively low. A valve controlled by the XMOS microcontroller will ensure that refueling of the generator tank only occur when ISLANDS is servicing electric helicopters.

CHAPTER 4: DETERMINING ISLANDS PLACEMENT IN THE FIELD

Conventional unmanned helicopters are deployed and recovered for "eye in the sky" applications from the same human-operated station because of the need for refueling/recharging. ISLANDS' ability to provide a safe landing platform with the resources needed for refueling/recharging, as discussed in Chapters 2 and 3, eliminates the need for a return trip to a home base. This chapter presents three methods for determining ISLANDS placement in the field with corresponding helicopter flight paths, which take advantage of ISLANDS capabilities. These methods allow autonomous helicopters to operate over areas larger than previously possible for longer periods with less human interaction.

The three solutions presented are extensions or modifications of existing solutions to unmanned systems coverage problems that are adapted to the ISLANDS placement problem. A problem statement is presented in Section 4.1. The first solution is a genetic algorithm that solves a hybrid *p*-median and Maximal Coverage Location Problem (MCLP) [78, 79]. The results obtained by the genetic algorithm, although correct, do not take into account the helicopter flight path between ISLANDS stations while the other two solutions do take this into account. Two different algorithms are used for generating helicopter paths. One is based on solving a modified Traveling Salesman Problem (TSP),

and the other is based on a spanning tree following algorithm [80]. Furthermore, a single-loop versus a multiple-loop approach for ISLANDS placement are compared. The single loop approach calculates one continuous path for the entire arena. The multiple loops approach first decomposes the entire arena using polygon decomposing [81], and then defines independent loops for the smaller sub-areas. Both solutions work well in determining ISLANDS location in the helicopter arena, but either algorithm may be preferable, depending on mission requirements.

As all the solutions require discretization, Section 4.2 analyzes discretization as a function of the helicopters' sensor field of view. The subsequent sections present the proposed solutions and the existing work which they expand upon. The chapter concludes with a discussion of all the solutions with particular emphasis on the difference between the single and multiple loops method based solutions.

4.1 Problem Statement

The three solutions presented solve the problem of determining the placement of ISLANDS stations in the helicopter operating arena, which is larger than the maximum coverage possible by a single helicopter. In addition to placement, flight paths are calculated to achieve complete area coverage with minimal path overlap. In all of the solutions presented, it is assumed that the ISLANDS stations are pre-placed in the helicopter arena based on the coordinates calculated by the proposed solutions.

The use of autonomous helicopters with refueling/recharging stations has not been discussed in the literature. The area coverage problem for multiple ground robots has

been discussed in [82, 83], while the use of recharging stations in the form of a larger robots has been discussed in [84, 85]. Determining flight path for multiple aerial vehicles for specific tasks such as tracking of containment clouds was presented in [86], and forest fire monitoring in [87, 88, 89], both of which neglect the UAVs energy consumption. The results from this chapter fill the gap for the area of aerial systems with results that can translate to ground vehicles.

In area coverage problems for both ground and aerial vehicles, the first step is to discritize the arena based on the field of view of the sensor used on the helicopter or ground vehicle. All three solutions presented in this chapter are dependent on the discretization therefore determining the sub-region size based on sensor and vision algorithm requirements is analyzed in Section 4.2.

4.2 Discretization

Discretization is the process of breaking up a large area into smaller, more manageable sub-regions. For the purpose of this chapter and the "eye in the sky" applications tackled by autonomous helicopters, the smaller sub regions are sized to the field of view of the on-board sensor. Discretization based on the size of a sensor's field of view is common in both ground and aerial robotics coverage problems [80]. An example of discretization is shown in Figure 37 where a topographic map of Yosemite National Park is sub-divided into 234 arbitrary-sized sensor field of view sub-regions.

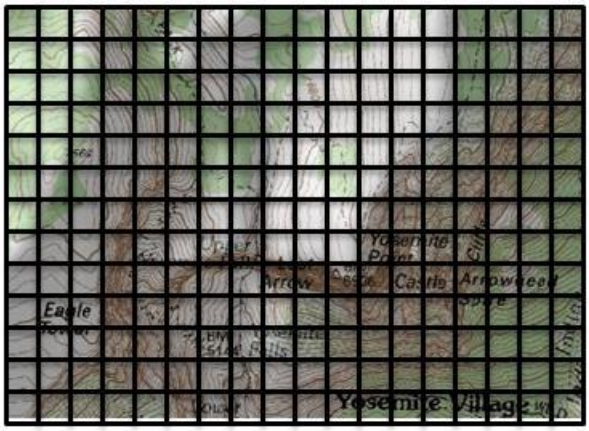

Figure 37: An arbitrary discretization of a part of Yosemite National Park

The center position of each sub-region is calculated yielding a list of local coordinate waypoints. These waypoints are translated from the local coordinate frame to the global latitude and longitude coordinate frame. Further detail on the translation between local and global coordinate frames is presented at the end of this section. Given that autonomous helicopters can successfully navigate between global coordinate waypoints, as shown in [90], and the helicopter visits all the waypoints in the region, the helicopter sensor successfully covers 100% of the region.

The maximum area a helicopter can cover is a function of its endurance, velocity and the sensor field of view. Helicopter applications requiring area coverage primarily use optical sensors, such as video or infrared cameras. For this reason the analyses presented in this section assumes that an optical sensor is on board the helicopter. The horizontal and vertical dimensions, which define the field of view for an optical sensor, are calculated according to

$$h = 2\tan(\frac{\alpha}{2})D \ , \tag{45}$$

which is derived from the geometric relationship of a simplified 2D camera shown in Figure 38.

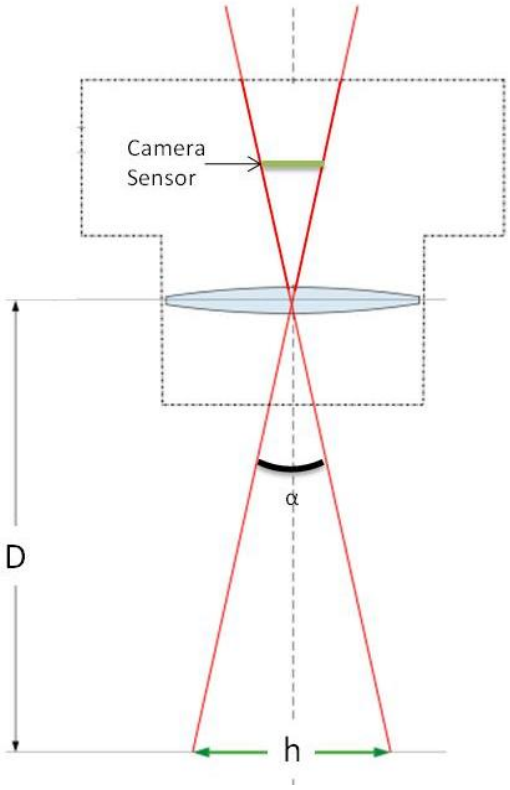

Figure 38: Simplified camera geometry with parameters used in Equation 45

In Equation 45, α is either the vertical or horizontal angle of view, which determines the aspect ratio of the image. Two assumptions are made on α. The first is that the vertical and horizontal angles of view are the same, meaning the image aspect ratio is unity and the camera sensor is square. The second is that α is fixed, which means the camera field of view is quadratically proportional to D, the distance of the down facing camera to the ground as seen in Figure 39. In this work the effect of diffraction on the resolution and sensor field of view is neglected. As diffraction must only be considered when the region examined is smaller than halve the light wave length.

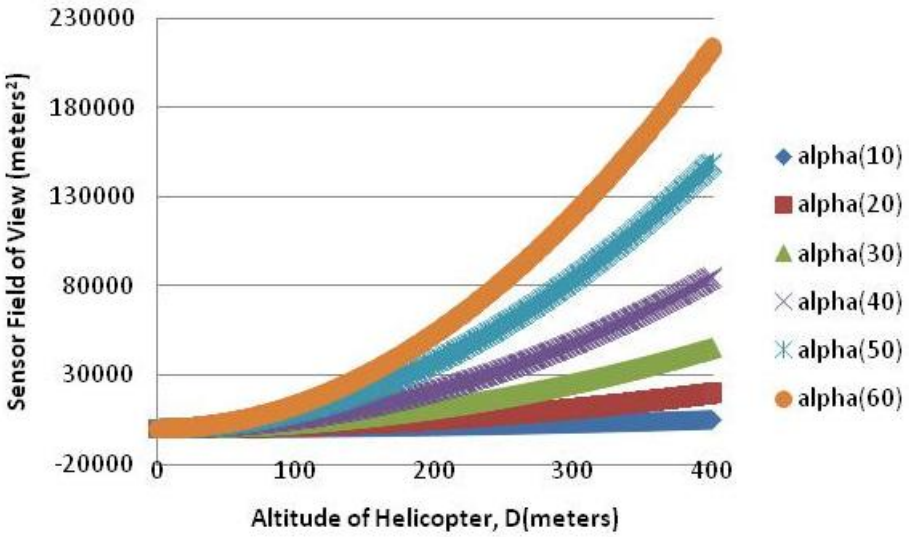

Figure 39: Sensor field of view as a function D given various α

According to Figure 39, depending on α, it is possible to have the helicopter hover high enough that the sensor field of view will equal the entire region of interest, and therefore eliminate the need for discretization. Due to spatial resolution requirements by vision algorithms [91], a maximum sensor field of view can be calculated given a fixed α.

Spatial resolution refers to the size of the smallest possible object that can be detected in the image captured by the sensor. In digital photography, spatial resolution is the physical size of a single pixel as shown in Figure 40.

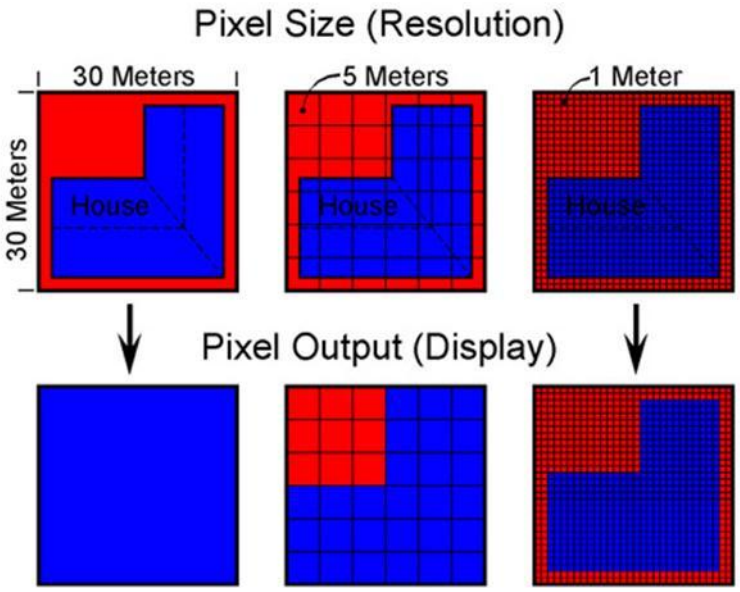

Figure 40: Comparing different spatial resolutions and their display output to the vision algorithms [92]

In this work spatial resolution is described as a ratio of pixels per unit distance. Spatial resolution is particularly important in image processing where a minimum number of pixels are needed to detect objects in the image. Many applications for autonomous helicopters listed in Chapter 1 require object detection. Different object detection algorithms require different spatial resolution depending on the object to be detected [91]. By knowing the digital camera sensor size in pixels, p ($\sqrt{megaPixels}$, assuming square sensor), and the spatial resolution, S_r, needed by the vision algorithm, it is possible to solve for h from Equation 45 using

$$h = \frac{p}{S_r} \text{ .} \tag{46}$$

By calculating h from Equation 46 it is possible to calculate the maximum altitude, D, of the helicopter given a fixed α. Figure 41 shows how spatial resolution affects both helicopter altitude and the sensor field of view given a fixed angle α of 40^o.

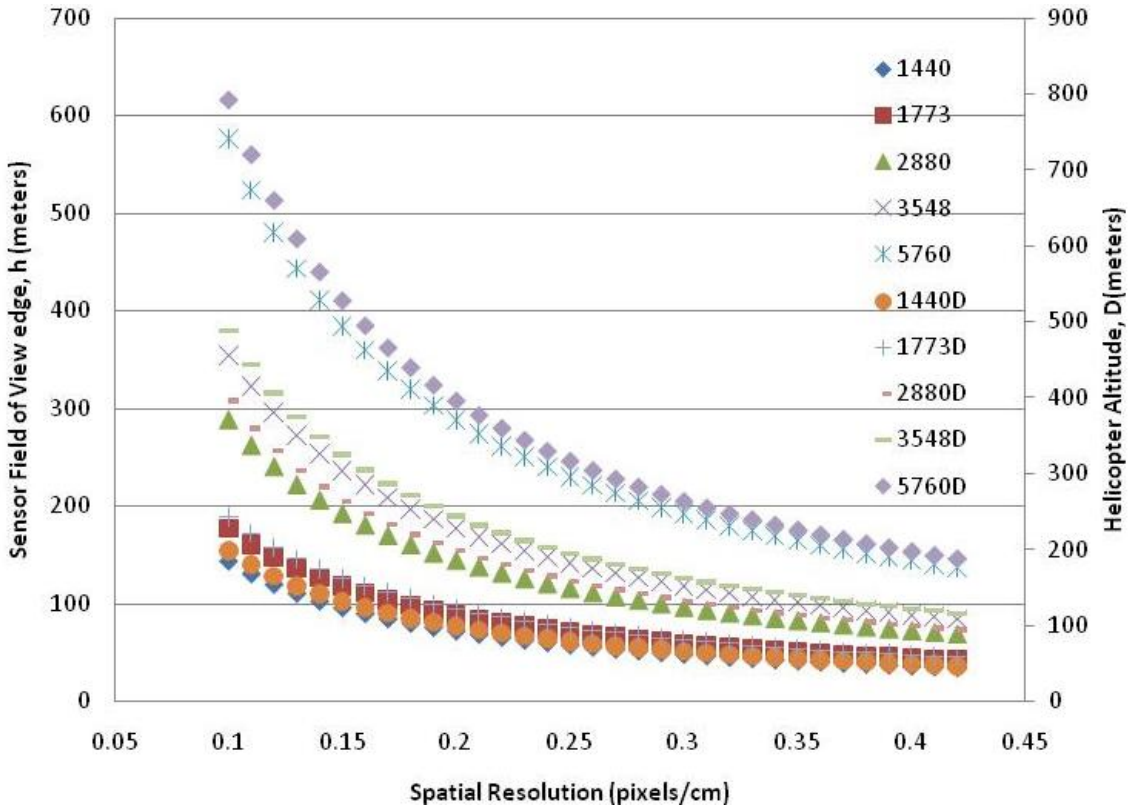

Figure 41: Maximum sensor field of view dimension, *h* and helicopter altitude *D* as a function of special resolution given different High Definition video formats resolutions (pixels), with a fixed angle α of 40°

As seen in Figure 41 spatial resolution decreases as the helicopter altitude increases. Spatial resolution requirements are fixed depending on the object detection algorithm used. In a scenario where the helicopter must fly at higher altitudes because of obstacles in the arena that cannot be circumnavigated, a drop in spatial resolution occurs. Compensating for a drop in spatial resolution is done by zooming, which is physically accomplished in a camera by decreasing the angle α. Decreasing alpha has the effect of decreasing the field of view of the sensor, which increases the spatial resolution as seen in Figure 41. By knowing the spatial resolution needed by the vision algorithm and using Equations (45) and (46) it is possible to determine the sensor field of view and therefore the discretization sub-area size required.

Once discretization is complete, the local center coordinate of each sub-area is calculated based on the sensor field of view. Those local coordinates are then translated to global latitude and longitude coordinates to be used by the helicopter's Global Positioning System (GPS). Translation is done by knowing the global coordinates of one point in the region and knowing the helicopters' GPS sensor resolution. In conjunction with the data from the helicopters' Inertial Measurement Unit (IMU) it is possible to translate the local coordinate to global coordinates using

$$lat_{new} = lat_{ref} + (GPS_{res}(b\sin(\theta_{imu})) \quad (47)$$

$$lon_{new} = lon_{ref} + (GPS_{res}(b\cos(\theta_{imu})) \ , \quad (48)$$

which are based on geometry from Figure 42.

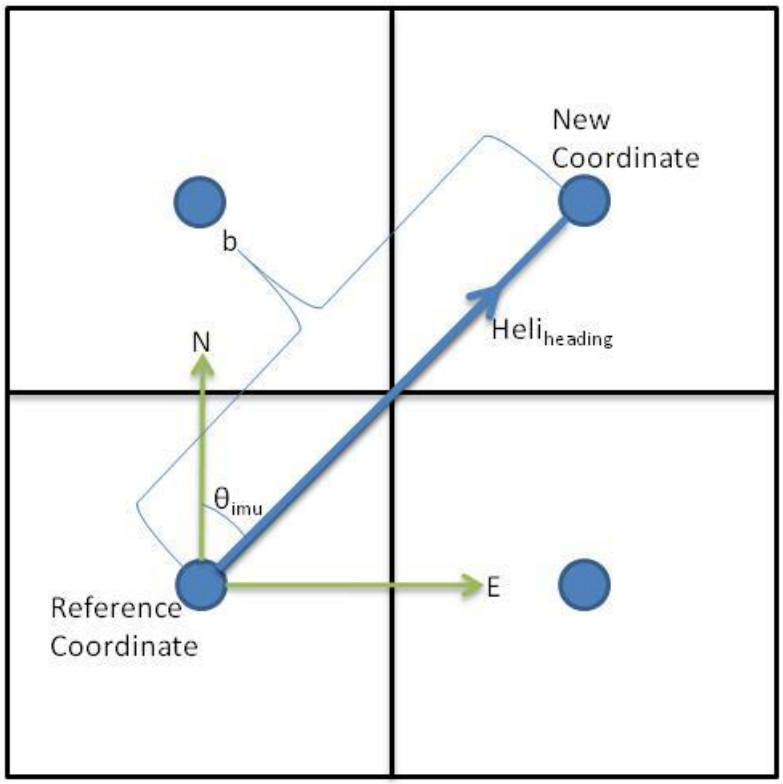

Figure 42: A discretized area showing the helicopter heading, IMU angle, reference point and the new point that the latitude and longitude are calculated for

In Equations (47) and (48), *b* is the distance between the reference point with a known global coordinate and a point in the local coordinate frame. For all the local coordinate points translation is done using the same reference global coordinate to avoid compounding of GPS sensor errors.

4.3 Modified MCLP and *p*-Median Solved Using a Genetic Algorithm

The initial approach taken to the ISLANDS placement problem is modeled after a combination of two problem formulations extensively studied in the field of operational research: the Maximal Coverage Location Problem (MCLP), and the *p*-median problem. A genetic algorithm is used to solve the NP-hard ISLANDS placement problem. This initial formulation and solution did not include consideration for helicopter flight path, and the results attained made it apparent that helicopter flight path must be considered in the ISLANDS placement problem formulation.

4.3.1 Previous Work

The initial ISLANDS placement problem was modeled after the problem formulation of wireless sensor networks, which require the determination of antenna locations to achieve maximal coverage of a fixed number of demand nodes. One way the wireless sensor network community solves this problem is by using work from the field of resource allocation [93]. Resource allocation research has also been applied to the fields of public service center location, ambulance/fire truck allocation [94, 95], and distribution center locations [96], to name just a few. One of the original formulations for

these problems, presented in [79], is called the Maximal Covering Location Problem (MCLP). In the MCLP formulation there are a fixed number of demand nodes or locations that must be serviced and a fixed number of supply nodes, which can be placed at any demand node location. The supply nodes must be placed in such a way that the total cost of servicing the demand nodes is minimized, and no single path segment cost is greater than some pre-defined maximum. Additionally, every demand point is only serviced by one supply node. In the case of wireless sensor networks the distance constraint is the maximum transmission range of an antenna with the cost being the total transmission power needed by all the antennas.

The problem with the MCLP formulation is that it minimizes the total distance cost between the demand and supply nodes at the cost of excluding some demand nodes, therefore, the solution does not guarantee 100% coverage. This is more clearly shown in Figure 43 were the circled points are the supply nodes and the rest are demand nodes.

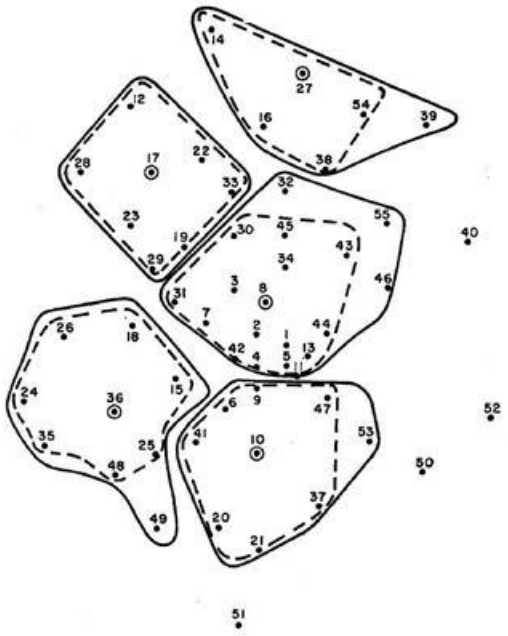

Figure 43: Example solution of MCLP formulation [79] where some nodes are not serviced

The nodes within the encircled regions are the demand nodes serviced by the supply node in the same region. The demand nodes not within any regions are sacrificed because servicing them requires more supply nodes or violation of the distance constraint. Due to the MCLP formulation, the solutions obtained do not guarantee 100% coverage, which, for the ISLANDS placement problem, is unacceptable since it means some sub-regions remain un-inspected by the helicopter.

Similarly, the *P*-median [78] formulation of the resource placement problem guarantees all demand points are serviced. The *p*-median problem is formulated very similarly to the MCLP with the exception that the maximum distance covered constraint is eliminated. The elimination of the distance constraint therefore guarantees 100% coverage of all the demand nodes. The elimination of the distance constraint could result in solutions where the helicopter flight distance is greater than its endurance. Therefore, the ISLANDS placement problem formulation is a combination of the *p*-median formulation with the addition of the distance constraint from the MCLP formulation and incrementally increasing the number of ISLANDS nodes available until a solution with 100% coverage results.

Both *p*-median and MCLP problems are considered NP-Hard problems [97]. This means that finding the optimal solution to the problem requires testing all the different combinations of supply node locations, which for problems with many supply and demand nodes is not computationally practical. For this reason, different heuristic methods have been proposed, such as Lagrangian relaxation where the constraints are eased [98, 99]. Another heuristic method commonly used is a genetic algorithm (GA)

[78], as it has been shown to successfully solve these kinds of problems within reasonable time [78, 97].

GAs are modeled after observations about evolution made by Charles Darwin. In a GA, the optimal solution is the one that has the best fitness. The fitness of a solution relates to how well it satisfies the objective function. GA algorithms operate on *chromosomes* that are made up of *genes*. These genes represent the possible solutions to the problem. An initial population of chromosome is created where all the genes are equally represented. Then, two chromosomes are randomly selected and combined to create a new chromosome. This chromosome's fitness is evaluated and compared to the existing chromosomes in the population. If this new chromosome's fitness is greater than any of those currently in the population the lowest fitness chromosome is replaced with the new chromosome. This goes on for *n* generations, at which point the algorithm terminates and the chromosome with the highest fitness is chosen as the solution.

4.3.2 Problem Formulation and Setup

In the ISLANDS placement formulation, the supply nodes are the ISLANDS stations and the demand nodes are the discretized sub-regions that must be surveyed. The cost function is the sum of all the flights the helicopters must perform to cover every sub-region. The distance constraint used is the product of the helicopter endurance and average velocity it maintains. Before starting the GA an $m \; X \; m$ matrix representing the distance between every sub-region center to all other sub-regions centers is calculated.

Two different methods are used for calculating the distance matrix needed by the GA. The first method is based on the Manhattan distances where diagonal movements are disallowed, and the distance between two sub-region centers is defined as

$$d_{12} = |x_1 - x_2| + |y_1 - y_2| . \tag{49}$$

The second method for defining the distance matrix is based on "zamboni/lawnmower"' distances. “Zamboni/lawnmower” distances maximize the number of sub-regions visited when going between two sub-regions. A zig-zag pattern between the two sub-regions appears as seen in Figure 44, where sub-figures (A)-(D) show the different possible patterns that can be taken between two points given 4 point connectivity. Figure 44 also shows how “Zamboni/lawnmower” distances are longer than Manhattan distances between the same two sub-regions.

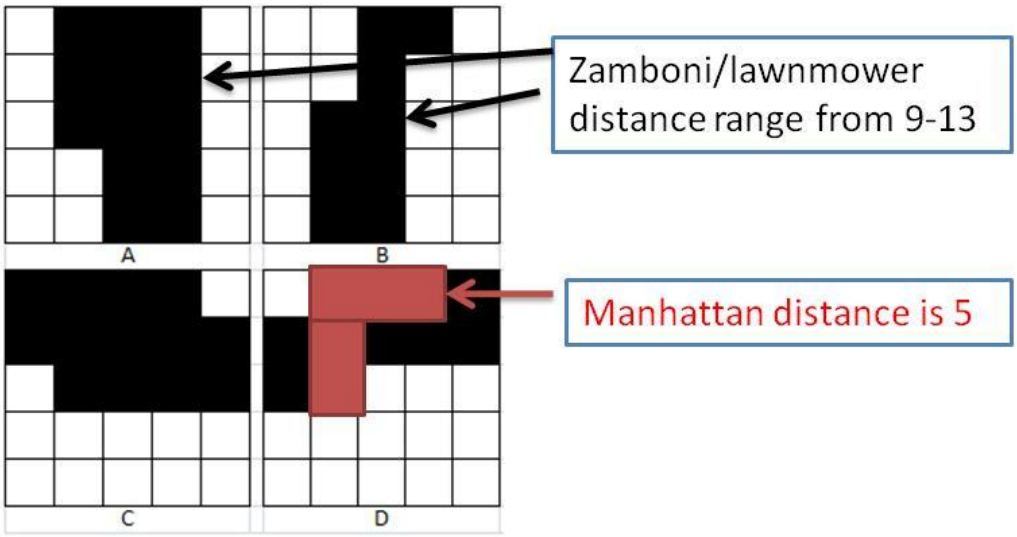

Figure 44: Different possible “zamboni/lawnmower” paths and their distance given two sub-regions compared to Manhattan distance

The solutions presented focuses on "zamboni/lawnmower" distances as this is the suggested path for area coverage for both ground and aerial robots [83, 89]. These distance calculations are performed first then loaded into the GA.

In addition to creating the *m X m* distance matrix, a population of chromosomes must be created before starting the GA. Each chromosome has *n* genes with each gene representing a possible location in the discretized area for an ISLANDS station. Initially each chromosome has one gene attempting to solve the problem with a single ISLANDS station. If no solution is calculated because the distance constraint is not satisfied, the GA is initialized again increasing the number of ISLANDS station available by one and re-generating the chromosome population with two genes each. This process continues until a solution is obtained that does not violate the helicopter endurance constraint. Determining the size and composition of the chromosome population is important as it affects both the runtime of the algorithm and the results. According to [78] the chromosome population size given *p* ISLANDS stations and *n* sub-regions that has equal representation of all the genes and is proportional to the solution size is

$$P(n, p) = \max\left(2, \left\lceil \frac{n}{100} \frac{\ln(S)}{d} \right\rceil\right) d \tag{50}$$

where

$$S = nCp \tag{51}$$

and

$$d = \lceil n / p \rceil \tag{52}$$

Equation (50) ensures that each gene is represented at least twice in the population. This is important to ensure that premature deletion of a possible solution in an early generation is avoided. Once the chromosome population is generated and the "zamboni/lawnmower" distance matrix is calculated, the GA iterates for $n\sqrt{p}$ generation [78].

4.3.3 Results

All tests were performed on a 10 *x* 10 grid (100 demand points). The first three experiments use Manhattan distances to evaluate the algorithm's accuracy. The first experiment used one ISLANDS station and no helicopter distance constraint. The expected answer of the ISLANDS station placed in the center of the grid was calculated (not shown). The second experiment used 5 ISLANDS stations, and no distance constraints. The result of this experiment is shown in Figure 45(A) and a star pattern of ISLANDS nodes is produced, which makes sense intuitively. The third experiment had a Manhattan distance constraint of five imposed. The algorithm was initialized with one ISLANDS station and increased the number of ISLANDS station by one until a feasible solution satisfying the distance constraint was found. With the need of four ISALNDS stations placed as shown in Figure 45(B).

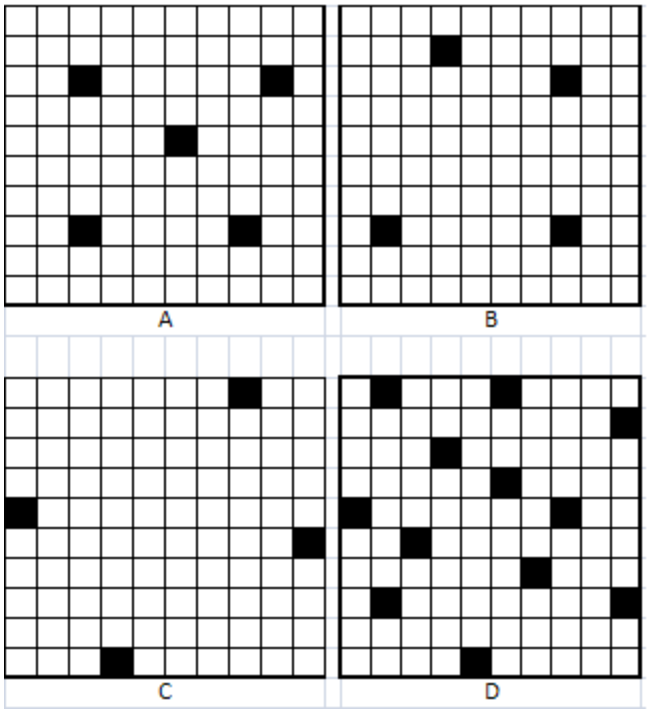

Figure 45: Results of GA implementation from different experiments both using Manhattan distances (A,B) and "zambon/lawnmower" distance (C,D)

The next two experiments used a "zamboni/lawnmower" distance calculation with a distance constraint of 10 and 5. For a distance constraint of 10, 4 ISLANDS stations are needed and are placed around the perimeter as shown in Figure 45(C). For the distance constraint of five, 12 ISLANDS stations were needed and were dispersed as seen in Figure 45(D). The distance constraint of five implies fuel reserves for the return flight back to the ISLANDS station. Figure 46 more clearly shows which sub-regions are associated with each ISLANDS stations. For example, the helicopter using the ISLANDS station located at the third column of the first row of Figure 46 will inspect all the sub-regions labeled with a three.

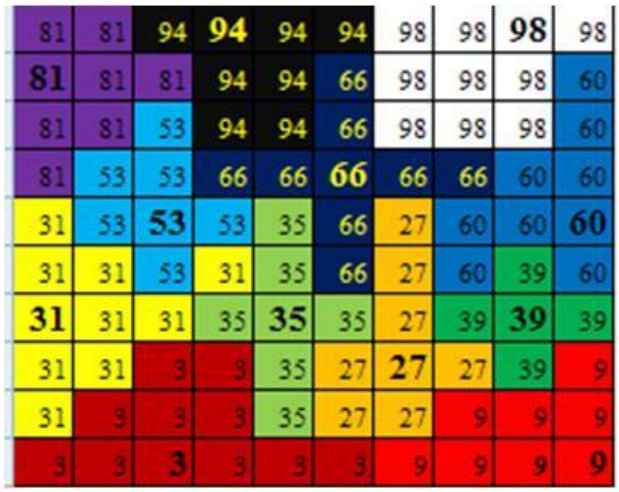

Figure 46: The sub-regions each helicopter/ISLANDS pair will survey based on a modified p-median/MCLP ISLANDS placement problem solved using GA

The same experiment with 12 ISLANDS stations and a "zamboni/lawnmower" distance constraint of 5 was run 300 times resulting in 300 different solutions and objective function costs ranging from 165-193 as summarized in Table 15.

Cost	*Frequency*	*Cost*	*Frequency*	*Cost*	*Frequency*
165	1	175	16	185	9
166	2	176	13	186	8
167	5	177	21	187	2
168	12	178	18	188	6
169	15	179	5	189	3
170	17	180	12	190	4
171	20	181	6	191	4
172	20	182	7	192	1
173	20	183	10	193	0
174	29	184	11		

Table 15: Summery of 300 runs with 12 ISLANDS stations and a "zamboni/lawnmower" distance constraint of 5

4.3.4 Discussion

Two interesting results appear in Table 15. The first is associated with the wide range in cost functions calculated at the end of the GA, and the second has to do with the frequency of the results that appear. The range in cost values calculated has to do with the fact that chromosomes are randomly selected during the process for mating and creation of new chromosomes. Therefore in every one of the 300 trials performed, the order of chromosomes selected is different and therefore the final solutions vary. Due to the nature of the problem, for a given solution there are multiple configurations and therefore increased frequency for certain results as seen in Figure 47. As it turned out no two solutions in the 300 trials were the same.

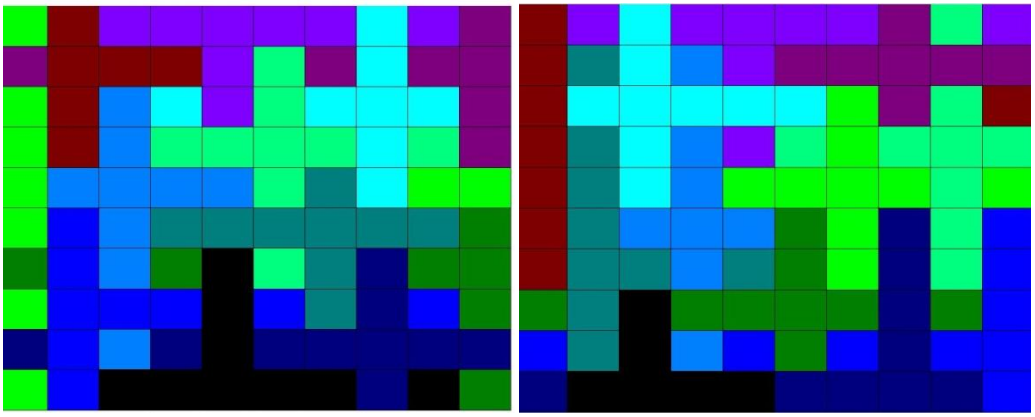

Figure 47: Results from two different runs with a cost of 167 and different layout of sub-region/ISLANDS station association

The overall results achieved by using a GA to solve a modified *p*-median/MCLP hybrid problem make sense for wireless sensor networks, for which these formulations are commonly used for but not for ISLANDS stations placement. The results shown in Figure 46 represent groupings of sub-regions which have the smallest one way distance between the ISLANDS station and the associated sub-regions the helicopter is to visit.

The current results imply that the helicopter will perform *w* round trips to visit all *w* sub-regions associated with a given ISLANDS station. During those *w* round trips the helicopter will end up visiting each of the sub-regions more than once because the problem formulation neglects the sub-regions visited on the way to a target sub-region and the sub-regions visited on the return trip back to the ISLANDS station.

These results show that the approach of only looking at the cost of getting to a sub-region that must be visited is not appropriate for the purpose of ISLANDS station placement. The path the helicopter takes between or around a single ISLANDS station must be considered when placing ISLANDS stations. Helicopter flight path such as the one in Figure 48 are desirable because the helicopter return flight and the sub-regions visited during the flight are considered.

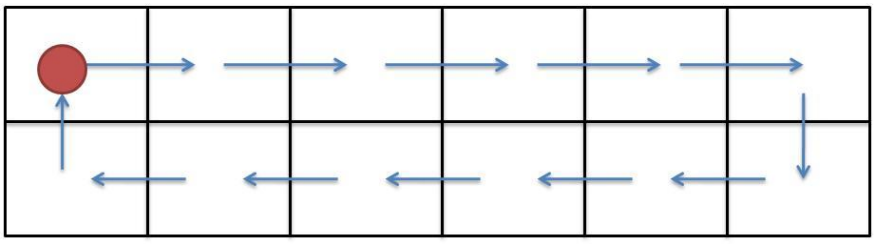

Figure 48: Desired helicopter flight path that require consideration during ISLANDS station placement

The results presented in this section, although correct, are not desirable for ISLANDS station placement. The results discovered in this section show that for coverage to be achieved, flight path and helicopter endurance are more important factors than the distance between sub-regions in determining ISLANDS placement. Leading to the placements methods discussed in the following section.

4.4 Loop Based Methods for ISLANDS Station Placement

As discussed in the previous section, to successfully place ISLANDS stations in the helicopter arena, the helicopter flight path and fuel constraints must be considered more heavily than the cost of traveling to individual sub-regions in the arena from a given ISLANDS station. Therefore paths in the form shown in Figure 48 are desirable even though the "zamboni/lawnmower' distance cost is high. Regardless of the loop generation method used or the number of loops used, determining the minimum number of ISLANDS stations is required. First the area a single helicopter can cover is calculated according to

$$A_{1h} = E_h V_h h \tag{53}$$

where E_h is the endurance of the helicopter on a single fuel tank in seconds, V_h is the average velocity maintained by the helicopter in meters/second, and h is the side dimension of the sensor field of view in meters from Equations (45) and (46) assuming an aspect ratio of one. Equation (53) assumes a flight path that does not self-intersect, meaning no sub-regions are visited twice except for the sub-region containing the ISLANDS station as shown in Figure 48. Some of the solutions presented will have some self intersection in the flight path, due to the loop generation algorithm used. By dividing the total arena area by A_h the minimum number of ISLANDS stations is calculated. The number of helicopters needed depends on the number of loops generated, and the frequency of visitation to each sub-region.

4.4.1 Previous work on Loop Generation

Two different methods for loop generation are presented in this chapter. Both methods ensure that every sub-region in the given area of the loop is visited. Each method starts by generating a graph that uses the sub-region centers as vertices and the different flight paths as edges. The difference between the two methods is the connectivity assumptions made between the vertices.

In the first method, every vertex is connected to its four orthogonal neighbors. The length of each edge in the graph is fixed at *h*, the side dimension of the sensor field of view. This type of graph guarantees that a Hamiltonian path within the graph exists. In graph theory, a path that visits every vertex exactly once is called a Hamiltonian path [100]. For calculating the Hamiltonian loop for the discretized arena a method proposed by [80] is used. In this work, a minimum spanning tree of a four-way orthogonally connected graph that is discritized at *2h* interval is first calculated as shown in Figure 49.

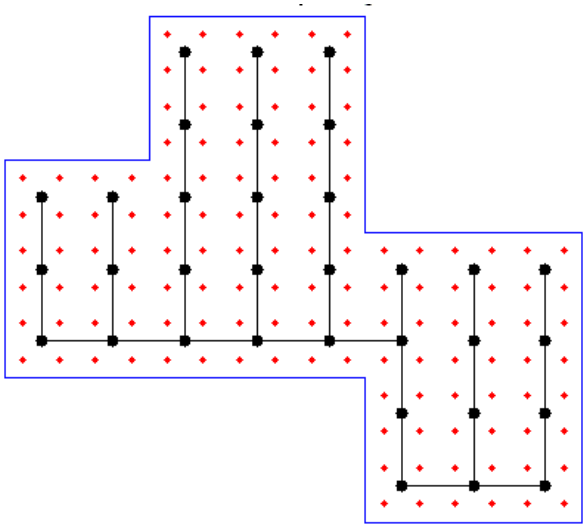

Figure 49: Spanning tree at *2h* discritization

The minimum spanning tree of a graph represents the minimum set of edges that connect all the vertices of a given graph [100]. Computing the spanning tree is done using

commonly available algorithms such as Kruskals[101] or Prim's[101]. Once the spanning tree is calculated, a wall following routine around the minimum spanning tree is performed moving from one vertex to another of the original graph. This method guarantees 100% coverage of the arena with no path overlap. 100% coverage is only guaranteed if during the *2h* discretization none of the sub-regions are deleted. In the proposed algorithm any sub-regions created during the *2h* discretization that are partially outside the arena perimeter are deleted resulting in less than 100% coverage, but this ensures the helicopters never goes outside the arena perimeter.

The second method starts with a fully connected graph [100], where every sub-region center is connected to all other sub-region centers. The distance between every sub-region and all other sub-regions is stored in an *m X m* matrix where *m* is the number of sub-regions. A nearest-neighbor algorithm [101] is then implemented to create a path that visits every vertex once. The nearest-neighbor algorithm is a greedy algorithm used to solve the Traveling Salesman Problem [102]. TSP is a commonly studied problem that requires the determination of the shortest path between a set of given cities. The cities in the ISLANDS placement problem are the sub-region centers. The results of the nearest neighbor algorithm to the NP-hard TSP are not optimal, but are suitable for the helicopter path generation because of the high density of sub-regions. Loop generation using the nearest neighbor algorithm works better for non-uniform areas than the Hamiltonian loop generation method. The drawback to this method is that the path generated can self intersect and go outside the perimeter.

Once the helicopter loops are generated, determining the number of ISLANDS stations and helicopters needed is dependent on the frequency of sub-region visitation required and the number of loops used to cover the area.

4.4.2 Single Loop Method

For this method, as the name implies, a single loop around the entire arena that visits every sub-region is calculated. Given that the arena is larger then what a single helicopter can cover according to Equation (53), by dividing the total loop length by the distance a single helicopter can travel yields the minimum number of ISLANDS stations needed in the arena. The ISLANDS stations are then placed every *d* meters along the loop, where *d* is the distance a helicopter can fly on a single fuel tank or battery charge. Effectively the helicopter flight path is flying from one ISLANDS station to the next along the single loop, a simplified example of which is shown in Figure 50.

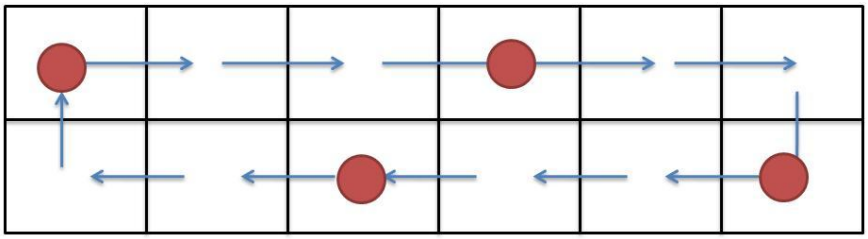

Figure 50: Simplified example of placing ISLANDS stations around the loop path calculated at predefined intervals of helicopter endurance.

In Figure 50 the circles represent ISLANDS stations with the arrows representing the helicopter flight path.

With the single loop method a single helicopter is sufficient to cover the entire area at a rate of once every

$$t_{loop} = It_r + \frac{l}{V_h} \tag{54}$$

unit time. Equation (54) is the total time a single helicopter requires to go around the loop including the time spent recharging It_r, and flying V_h/l. Increasing the frequency is possible by adding more helicopters into the loop. The maximum number of helicopters, H, in the loop without having helicopter waiting at ISLANDS stations is

$$\frac{H}{t_{loop}} \leq \frac{1}{t_r} \ . \tag{55}$$

4.4.3 Multiple Loops Method

The multiple loops method first decomposes the arena into sub areas that a single helicopter can cover in a single flight. This is done by using a polygon area decomposition algorithm from [81]. This algorithm has been successfully used in other surveying applications [89]. The polygon area decomposition algorithm can handle both concave and convex polygons and occlusions in polygons. The results of the algorithm from [81] are used in the following section as arbitrary maps to compare the different loop generation methods discussed in Section 4.4.1. Once the arena is decomposed into helicopter manageable sections and the loops are calculated, one ISLANDS station is placed per loop. The placement of the ISLANDS station along the loop is arbitrary allowing for flexibility due to terrain if needed.

Using the multiple loops method requires a minimum number of helicopters equal to the number of sub-areas calculated. The maximum number of helicopters and therefore the maximum frequency is also governed by Equation (55). The helicopter loop time is

calculated the same way as in Equation (54) with the number of ISLANDS stations available I equal to one.

4.4.4 Results

In this section, four arbitrary maps are used to compare the different methods of loop generation for both single and multiple loops approach for determining ISLANDS placement. The four maps include a simple map as in Figure 51 and three maps from [81] are shown in Figure 51. For maps B and C from Figure 51 a solution to the area decomposing problem from [81] is provided in Figure 52 where each sub-area is of equal size. For each sub-region in Figure 52, a loop based on nearest neighbor algorithm is then calculated.

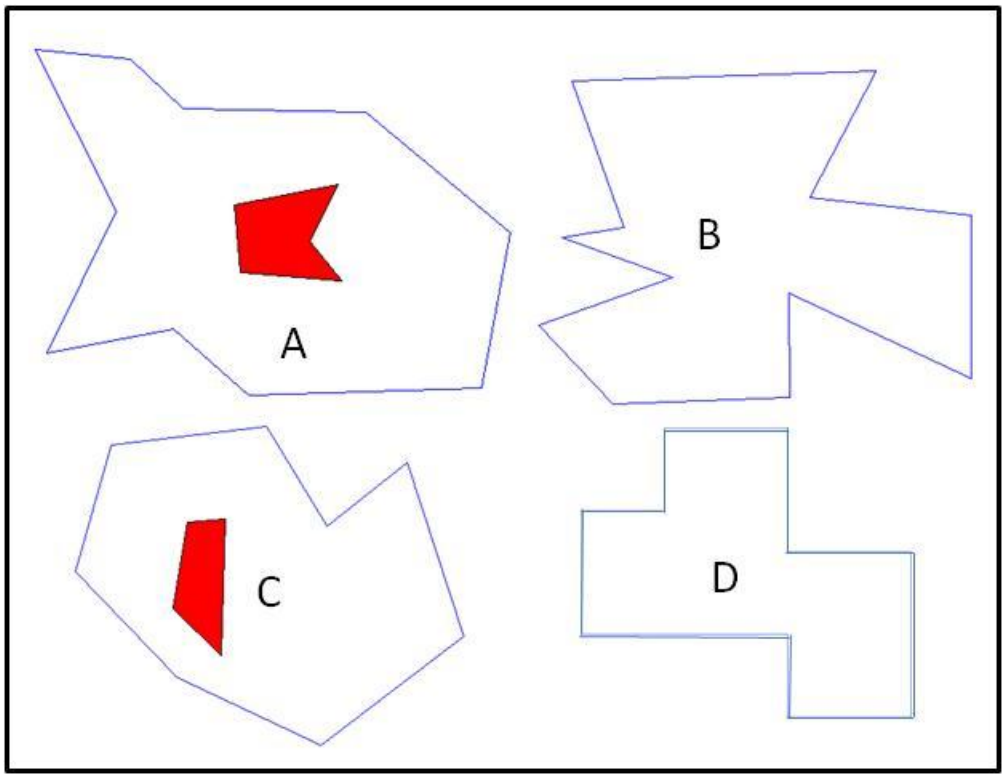

Figure 51 : Figure from polygon decomposition paper used to test different loop generation methods with the red polygon representing an occlusion

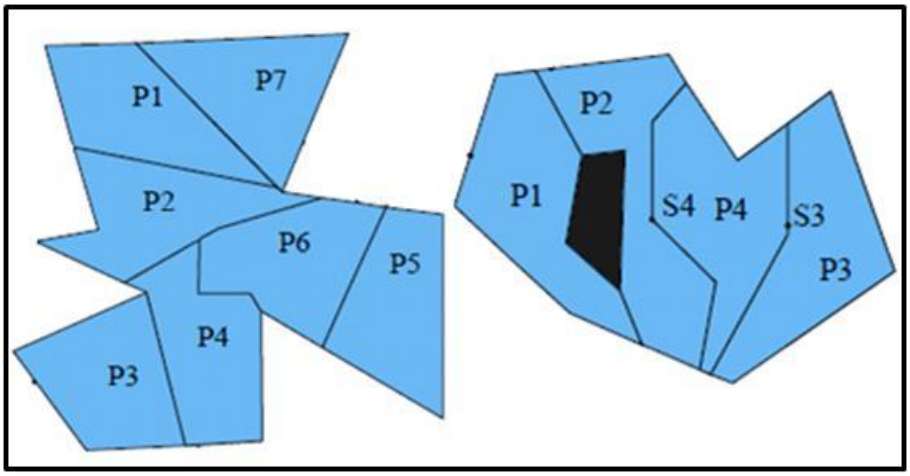

Figure 52: Results of polygon decompositions for maps B and C from Figure 51 [81]

Figure 53 and Figure 54 are the results of single loop paths for maps D and A from Figure 51 generated using both Hamiltonian and nearest neighbor algorithms. Results for map D used a sensor size of 10, while the results for map A used a sensor size of 8.

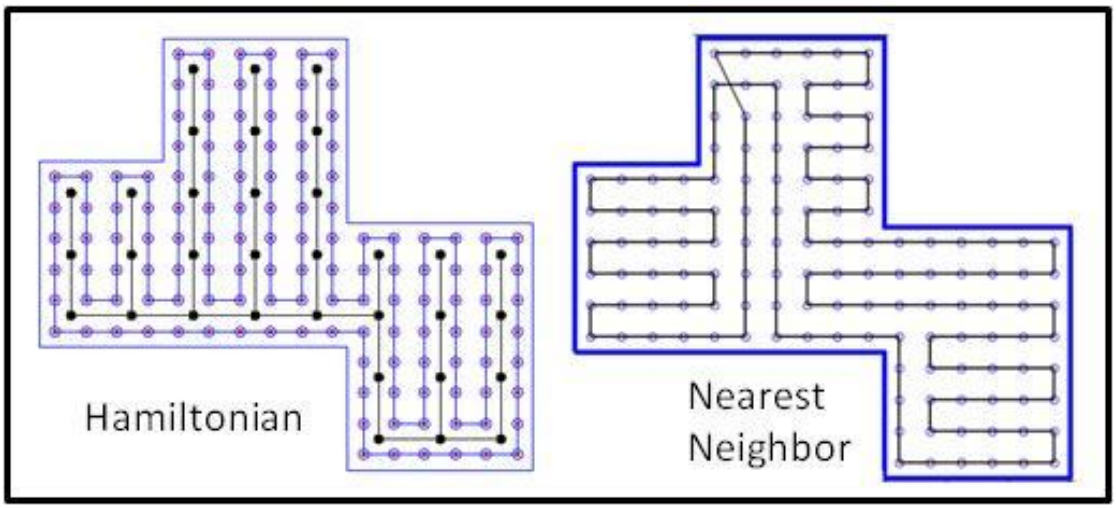

Figure 53: Hamiltonian and nearest neighbor single loop results for map D of Figure 51

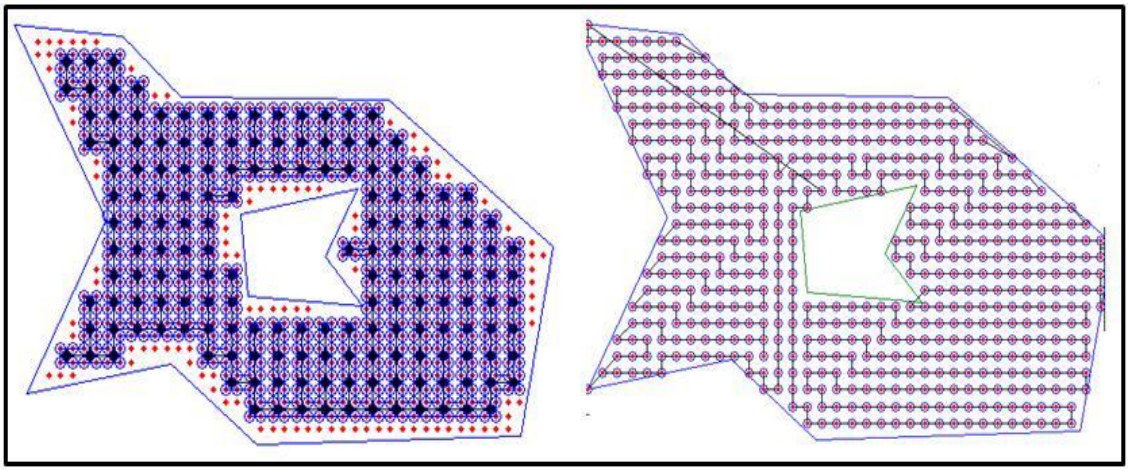

Figure 54: Hamiltonian and nearest neighbor single loop results for map A of Figure 51

Figure 55 is an example of the Hamiltonian algorithm not servicing sub-regions right along the perimeter of the map because they are deleted during the *2h* discretization, while the nearest neighbor algorithm results in a path that goes outside the area perimeter. The sensor size used for these maps is 10 units in length.

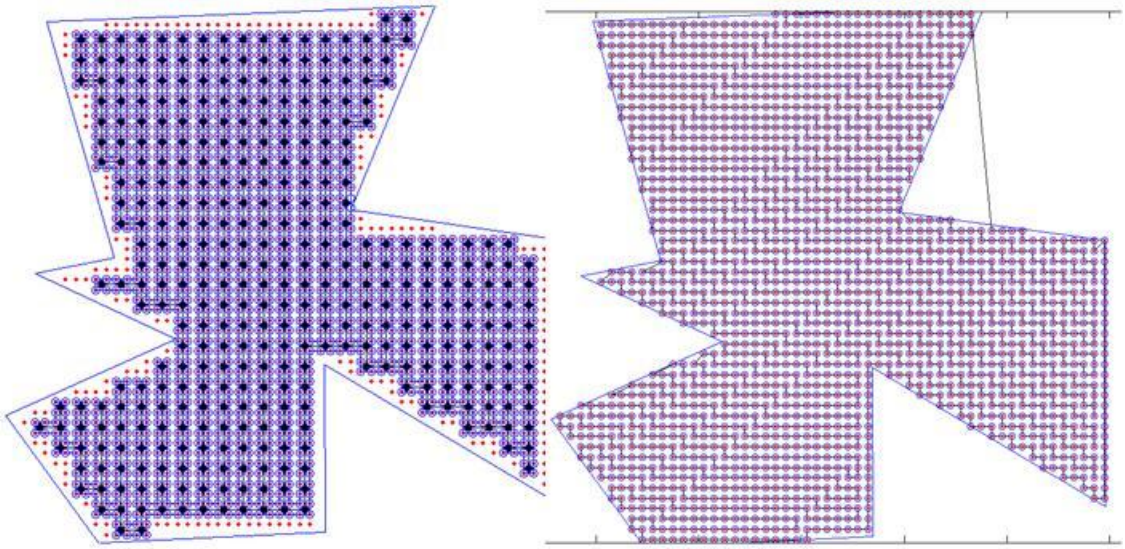

Figure 55: Map B from Figure 51 where perimeter sub-regions are deleted during Hamiltonian path generation and out of bounds loop created with nearest neighbor algorithm

Figure 56 is sub-area P2 from map C and highlights the need of considering sensor size when using Hamiltonian method for generating loops.

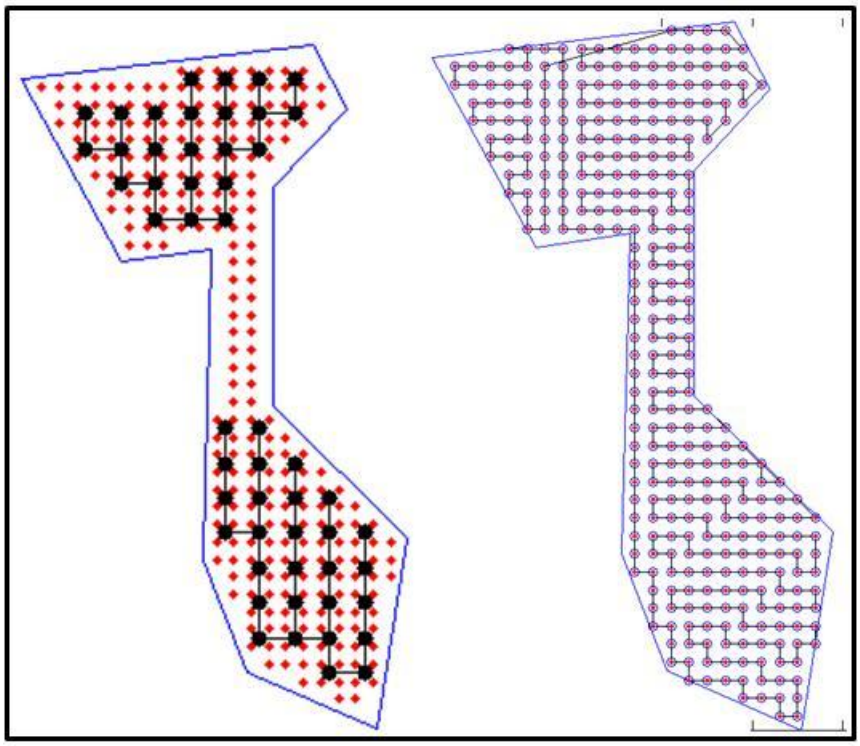

Figure 56: Narrowness of geometry produces no loop for Hamiltonian method but does for nearest neighbor method

As can been seen, due to the narrowness of the shape a complete spanning tree for the *2h* discretization of the region is not calculated. Therefore, a complete loop of the region cannot be calculated. Using the nearest neighbor algorithm requires a sensor size of four to achieve a loop that stays within the boundaries. As a general rule for a loop to be calculated when using the nearest neighbor algorithm the sensor size must be one half the size of the narrowest area in the map. For using the Hamiltonian method a sensor size one fourth the size of narrowest area is required.

Table 16 and Table 17 are summaries of all the experiments performed comparing the different methods of loop generation and the number of loops used based on area decomposition. The total area of each of the maps from Figure 51 was calculated using available tools. The effective area covered was calculated by multiplying the path length by the sensor size. Table 16 is the single loop area coverage results from all the maps analyzed in this section are shown, while Table 17 is the area coverage results of the loops associated with the decomposed areas calculated according to [81] of maps B and C.

			Path Length		Effective Area Covered		% of Total Area Covered	
	Total Area	Sensor Size	Hamiltonian	Nearest Neighbor	Hamiltonian	Nearest Neighbor	Hamiltonian	Nearest Neighbor
Map A	55085	8	5440	7195	43520	57560	79.01%	104.49%
Map B	182814	10	15280	18914	152800	189140	83.58%	103.46%
Map C	21174	4	4352	5664	17408	22656	82.21%	107.00%
Map D	3300	5	660	666	3300	3330	100.00%	100.91%

Table 16: Summary of single loop method comparing effective area covered to actual area of maps based on type of loop generating algorithm used.

			Path Length		Effective Area Covered		% of Total Area Covered	
	Total Area	Sensor Size	Hamiltonian	Nearest Neighbor	Hamiltonian	Nearest Neighbor	Hamiltonian	Nearest Neighbor
Map B	182814	10	15280	18914	152800	189140	83.58%	103.46%
P1	-	10	1720	2713	17200	27130	66.73%	105.17%
P2	-	10	1600	2875	16000	28750		
P3	-	10	1800	2672	18000	26720		
P4	-	10	1840	2764	18400	27640		
P5	-	10	1760	2802	17600	28020		
P6	-	10	1840	2731	18400	27310		
P7	-	10	1640	2670	16400	26700		
Map C	21174	4	4352	5664	17408	22656	82.21%	107.00%
P1	-	4	200	1459	800	5836	38.24%	105.85%
P2	-	4	N/A	1390	N/A	5560		
P3	-	4	880	1360	3520	5440		
P4	-	4	944	1394	3776	5576		

Table 17: Summary for multiple loops method for ISLANSD placement with area coverage comparison between the types of loop generation algorithm used

4.4.5 Discussion

From the results shown in Table 16 and Table 17 for the complex geometries of maps A,B and C using the nearest neighbor algorithm is effective in producing loops that guarantee a 100% coverage. The drawback of the nearest neighbor algorithm is that path overlaps occur and the paths generated can go out of the area perimeter as be seen by the greater than 100% total coverage and shown in Figure 54 and Figure 55. The Hamiltonian method for path generation produces poor results for complex geometries due to the need to remove sub-regions. This phenomenon is exacerbated when decomposing the area into sub-areas and using multiple loops as there is an increase in the number of sub-regions that must be deleted during the *2h* discretization process. The effect of allowing path overlap into adjoining areas during path generation for multiple loops is a possibility for future work. From map D, it is clear that for simple geometries the Hamiltonian method for loop generation produces the most effective path with no overlaps for simple geometries.

Deciding between single versus multiple loops for total area coverage is application dependent. For multiple loops, if a single ISLANDS station or a single helicopter fails only one part of the area loses coverage. When deciding to use the single loop method and a failure of a single ISLANDS station or helicopter occurs, eventual complete loss of coverage occurs. Total loss of coverage occurs because the helicopters start to back up at the failed ISLANDS stations, or at an ISLANDS stations occupied by a failed helicopter. Another major application difference between single and multiple loop method is the minimum frequency of sub-region observation required. Using the multiple loop method, higher minimum frequency of observation is attained then the single loop method. Additionally, with the single loop method fewer helicopters are needed as opposed to the multiple loop method which requires a number of helicopters equaling the number of loops. Therefore, depending on the risk level of the operation and the minimum frequency of sub-region observations that is necessary, a single loop or a multiple loop method is chosen.

CHAPTER 5: CASE STUDY IMPLEMENTING THE THREE-PRONGED APPROACH

In Chapters 2 through 4, solutions to the problems associated with using Class 1 <150kg autonomous helicopters for different "eye in the sky" applications are presented. The three-part solution presented in this dissertation solve the root problem of short endurance associated with Class 1 autonomous helicopters. Chapter 2 presents ISLANDS, which is an electro mechanical device that provides a safe landing surface for refueling/recharging. Chapter 3 presents a method for determining the energy resources required on-board ISLANDS depending on helicopter type, length of deployment, and number of refuel/recharges performed per day. Chapter 4 presents a method for calculating helicopter flight path in conjunction with ISLANDS location in the area to be surveyed. This chapter presents a case study implementing the results of Chapters 2 through 4 for an "eye in the sky" application over an area of Boulder, Colorado.

Section 5.1 explains the proposed case study and how the area selected is of interest for both urban and wilderness "eye in the sky" applications. Section 5.2 uses the analyses from Chapter 3 to determine the energy requirements needed to service a Rotomotion SR30 gas helicopter. Section 5.3 concludes the case study by analyzing the different methods of ISLANDS placements and helicopter flight path to achieve the requirements of the case study.

5.1 Case Study

5.1.1 The Area

The case study presented in this chapter uses a small Class I helicopter for wild fire monitoring, search and rescue applications, and traffic monitoring for the region of Boulder Colorado shown in Figure 57. The region selected in Figure 57 is specifically chosen to highlight the benefits gained by using inexpensive, Class I autonomous helicopters that operate for prolonged periods of time with the application of the current research presented. The 9,882,823 square meter (~9.8 square kilometer) region in Boulder, Colorado is composed of two distinct sub-regions, each benefitting from a different potential use of autonomous helicopters. The first sub-region is wilderness that is frequently visited by hikers and mountain bikers and would benefit from search and rescue helicopters. More importantly the wilderness near Boulder is susceptible to wild fires, which through the use of helicopters can be detected earlier preventing structural damage. The fire prone wilderness is close to the University of Colorado at Boulder campus and the adjoining residential neighborhoods. The second sub-region is Boulder's highly congested University and adjoining residential neighborhoods area in which traffic monitoring would be helpful to provide the residents with real time traffic updates. This unique geographical location makes for a suitable case study for this dissertation

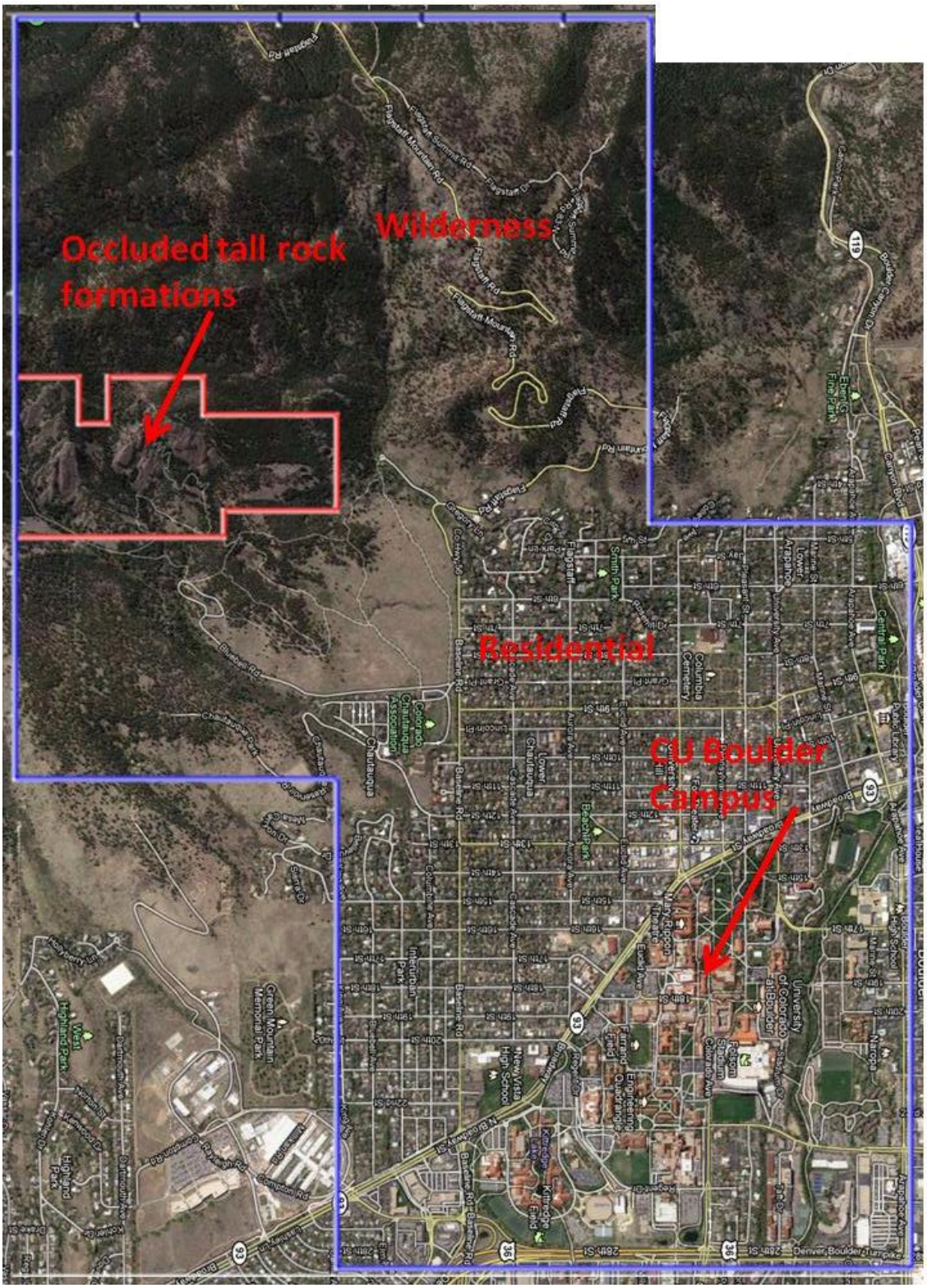

Figure 57: Map of Boulder Colorado and adjoining wilderness used in Chapter 5 case study

5.1.2 Case Study Requirements

The goal of this case study is to demonstrate how to use a commercially available Class I autonomous helicopter and commercially available optical sensor, to continually survey the region specified by Figure 57 in 10-day blocks of time without human intervention. As such, potential locations of ISLANDS refueling/recharging stations and the amount of onboard energy needed for 10-day deployment with a sub-region re-visitation frequency of once per hour must be identified. Also, way points for possible helicopter flight paths are calculated ensuring maximal area coverage.

5.1.3 Hardware and Assumptions

Using the SR30 gas helicopter requires an ISLANDS station with a landing deck that is 80" x 80" or 2 x 2 meters. The increase size in ISLANDS to accommodate the larger helicopter affects some of the energy consuming components of ISLANDS. The increased energy consumption's effect on determining the on-board battery needs of ISLANDS is discussed in Section 5.3.

The SR30 helicopter used for the case study has an average cursing velocity of 40 kilometers/hour, a fuel capacity of two liters, and an endurance of 1.5 hours. The camera on-board each helicopter is a down-facing high-definition digital video camera with a fixed field of view angle and a square sensor. The camera has a resolution of 2.07 mega pixels arranged in a 1440 x 1440 pixel array. The smallest feature the helicopter is required to detect is a human lying down (injured) during a search and rescue mission. From [103] the average person can be modeled as a rectangular block of 1.7 x 0.6 meters. In human detection vision algorithms, 900 pixels [91] are needed to successfully detect a

human. Given this information a minimal spatial resolution of 0.13 pixels per centimeter is needed. From this information and Figure 41 the camera minimum field of view is 120 x 120 meters at an altitude of 165 meters. To provide the vision algorithms more information a spatial resolution of 0.24 is used flying at 82 meters (270 feet) with a field of view of 60 x 60 meters. Eighty two meters is high enough to clear the tallest building in Boulder (which stands at ~45 meters (150 feet) [104]). Consistent with the bulk of this dissertation, it is assumed that the helicopter is only operating during the daytime, which lasts for 12 hours.

5.2 Placement and Helicopter Flight Paths

Before determining ISLANDS resource needs, the helicopter flight path and ISLANDS placement is determined to calculate the length of helicopter flights. Four possible solutions are shown and discussed in this section. The first two solutions are based on a single loop approach for the entire area calculated with both nearest neighbor and spanning tree following algorithms. The second two solutions are based on dividing the area into three sub-areas and then calculating the helicopter flight path using both loop generations methods.

The minimum number of ISLANDS station that is equivalent to the number of loops needed by the multiple loop method is first calculated. From Equation (53) in Chapter 4 the area a single SR30 helicopter can cover given a sensor field of view of 60 meters is 3.6 square kilometers. The total area in Figure 57 is ~9.9 square kilometers

dividing that by the area a single helicopter covers results in the need of three ISLANDS stations regardless of whether a single or multiple loop method is used.

The results for the single loop method using the nearest neighbor algorithm are shown in Figure 58 with the total path length of 169.017 km.

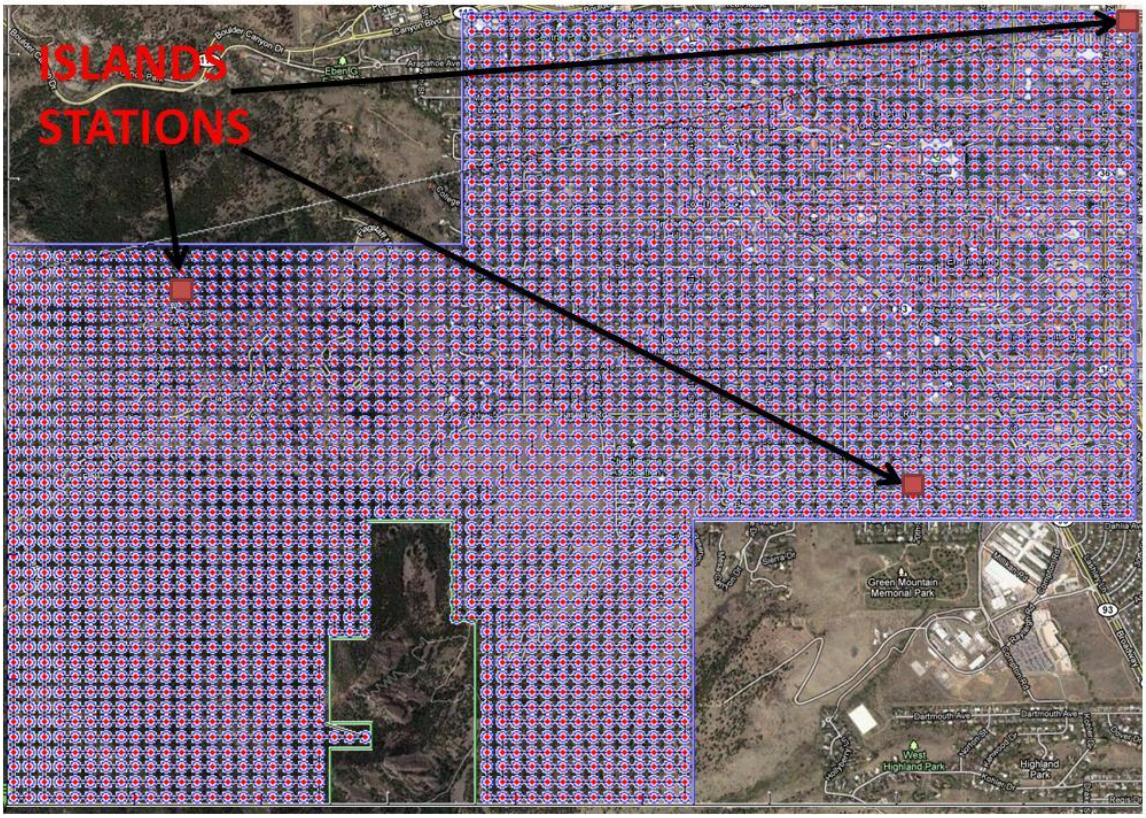

Figure 58: Helicopter path for single loop method calculated using nearest neighbor algorithm with locations of ISLANDS stations marked

As seen in Figure 58, the path generated goes out of bounds and crosses over itself as is seen in the results of Chapter 4. Therefore, when multiplying the calculated path length by the sensor field of view an area greater than that of

Figure 57 results. Even with the larger area covered by the path, three ISLANDS stations are still sufficient for complete coverage. Knowing that three ISLANDS stations are placed along the path each segment is 56.3 km taking 84 minutes to cover at an average velocity of 40 kilometers/hour.

The results for the single loop method using the spanning tree following algorithm are shown in Figure 59.

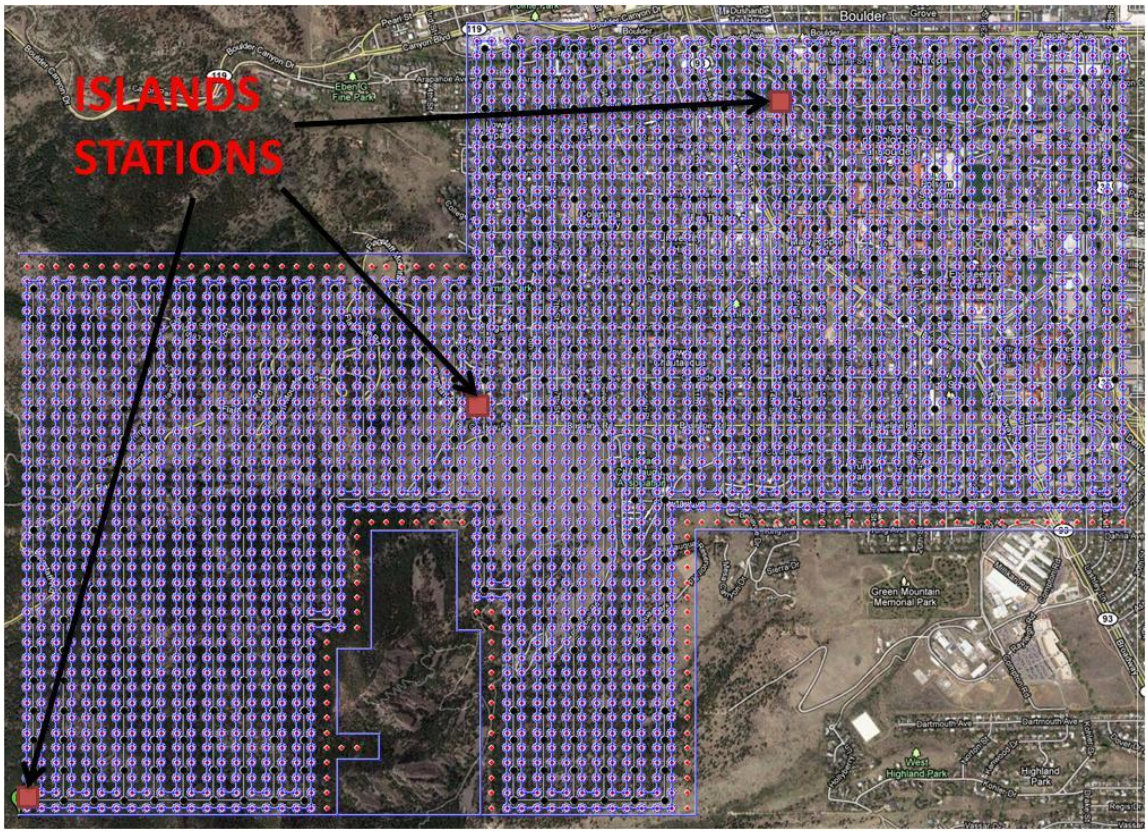

Figure 59: Helicopter path for single loop method calculated using spanning tree following algorithm with locations of ISLANDS stations marked

As expected with the spanning tree following algorithm, some of the sub-regions are not serviced creating a smaller area. The total flight path for the results in Figure 59 is 153.360 kilometers surveying 93% of the area. Placing one ISLANDS station every 51.12 kilometers along the loop, which will take 76 minutes to cover will ensure 93%

coverage of the proposed area. Alternatively the area boundaries can be adjusted to achieve 100% coverage of a larger area.

The three sub-areas created for the map in Figure 57 are shown in Figure 60 with the area of *A1*, *A2*, and *A3* being 3.23, 3.35, and 3.3 square kilometers respectively.

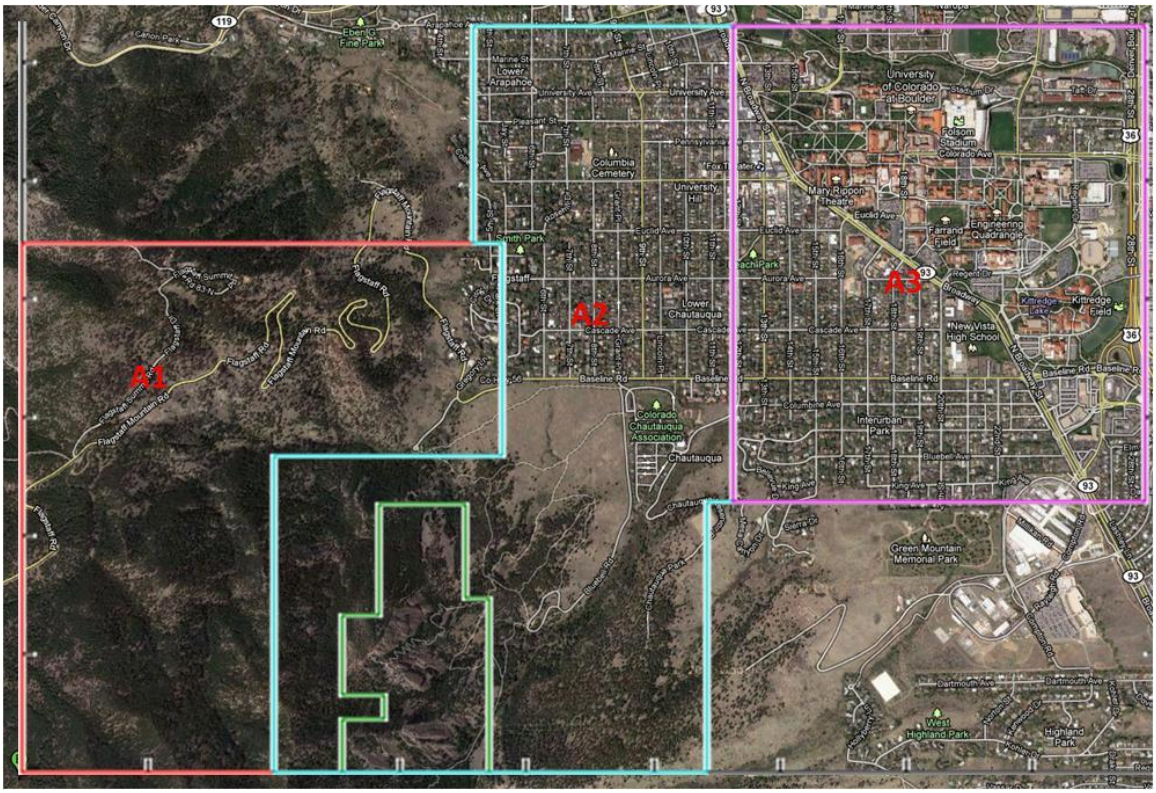

Figure 60: 3 sub-area of original map

Table 18 summarizes the results of the loop length and area covered by both the nearest neighbor and spanning tree following algorithm for the three sub-areas in Figure 60. For each of the three loops generated an ISLANDS station can be placed anywhere along the loop.

			Path Length		Effective Area Covered		% of Total Area Covered	
	Total Area	Sensor Size	Hamiltonian	Nearest Neighbor	Hamiltonian	Nearest Neighbor	Hamiltonian	Nearest Neighbor
Boulder Map	9,882,823	60	153360	169014	9201600	10140840	93.11%	102.61%
A1	3230000	60	44640	55344	2678400	3320640		
A2	3354551	60	44880	58250	2692800	3495000	84.66%	102.40%
A3	3298272	60	49920	55080	2995200	3304800		

Table 18: Summary of multiple loop method based on

5.3 ISLANDS Resource Needs

Given the ISLANDS placement calculated in the previous section, it is now possible to determine the amount of resources needed on board ISLANDS for a 10 day deployment with a sub-region re-visitation frequency of once every 60 minutes. For this section the data from the single loop method using nearest neighbor algorithm is used. To cover the entire loop, the SR30 will require 84 minutes of flight time and three refuels. Each refuel stop takes 4 minutes, 2 to re-fuel the helicopter and 2 to center the helicopter. Therefore, with one helicopter and three ISLANDS stations the sub-area re-visitation frequency according to Equation (54) is once every 96 minutes. By increasing the number of helicopters to three, the re-visitation frequency is increased to once every 32 minutes, which is acceptable for this case study. During the 12 hours of daylight, each helicopter is capable of performing 7.5 loops and with three helicopters each ISLANDS stations will be required to perform 23 refueling cycles. Given the need for a 10 day deployment this requires 460 liters of fuel at each ISLANDS station. Following Equation (39) from Chapter 3, the battery capacity required on each ISLANDS station is 14 amp-hours which will maintain the ISLANDS station at night and provide enough energy at dawn before batteries can re-charge. This value takes into account the larger deck size of ISLANDS that requires the centering motors to run longer and the increased height the fuel has to travel to the deck affecting the dynamic head of the fuel pump.

The case study presented in this chapter uses the knowledge gained throughout this dissertation to present a potential deployment of ISLANDS station and Class 1 helicopter for continuous surveillance of Boulder Colorado.

CHAPTER 6: CONCLUSION AND FUTURE WORK

6.1 Conclusion

This dissertation presented a three-pronged approach for a potential infrastructure implementation to increase endurance and usability of Class I helicopter for the purpose of "civilian eye in the sky" applications. The three-pronged approach starts with the development of ISLANDS, which is detailed in Chapter 2. Chapter 2 provides details of the mechanical design of ISLANDS, which is capable of adapting to uneven terrain to provide a safe landing surface. The dynamic and static force analysis performed in Chapter 2 is scalable to any future ISLANDS prototypes and the proposed centering mechanism allows for integration of a refueling/recharging system. With an electro-mechanical platform for refueling and recharging, the results of Chapter 3 determine the resource needs of ISLANDS for prolonged "off the grid" missions of ISLANDS. The analysis performed in Chapter 3 works for servicing of both gas and electric helicopters. Since servicing electric helicopters requires more electrical energy than can be feasibly stored in on-board batteries, a gas generator system is proposed that eliminates the need for large battery banks. With a refueling station capable of staying in the field for prolonged periods of time, Chapter 4 describes multiple ways for determining the location of ISLANDS station in the helicopter arena and flight paths for the helicopters. The methods proposed in Chapter 4 allow for user flexibility with the single versus

multiple loop approaches. The single loop approach allows for fewer helicopter systems while the multiple loop approach allows for longer mission in the event of an ISLANDS or helicopter failure. Chapter 5 concludes with a case study showing the implementation of the proposed infrastructure for using Class 1 helicopters. The large volume of fuel calculated in Chapter 5 for each ISLANDS station is due to the long mission endurance and the relatively high re-visitation frequency specified. With the deployment of ISLANDS in a city and wilderness environment that is easily accessible this large value of fuel is acceptable. Determining a way to refuel the ISLANDS stations themselves is possible future work. All the work presented in this dissertation is under the assumptions that the ISLANDS stations need to operate for predefined periods of autonomy, as human servicing of the helicopters and ISLANDS stations will be required. It is the author's hope that the work presented will provide additional motivation for others to develop cheaper helicopter platforms now that a method for prolonged missions is proposed.

6.2 Future Work

The increased autonomy gained by Class I helicopters with the use of the proposed three-pronged approach allows for many future avenues of research on: helicopter mission planning, improved path planning, and upgrades to the ISLANDS mechanical system.

Several upgrades to the ISLANDS prototype built are proposed. Starting with a refueling and recharging system that integrates with the chosen helicopter system. With development of a refueling system development of a fuel tank will also be required. For

use with electrical helicopters implementing the generator proposed in Chapter 3 for recharging is required. Comparing the efficiencies obtained with real systems with those calculated in Chapter 3 will help in furthering the autonomy of electric helicopters. A redesign of ISLANDS fixed base so it stores the fuel reserves, as opposed to the current design where fuel is part of the rotating sub-assembly as discussed in Chapter 3.

Improvements to the flight path selected can be made to incorporate real helicopter dynamics. Also with the multiple loop method, ways of moving helicopters between loops could be beneficial to increase the effective area coverage percentages.

From a helicopter systems point of view, work into nighttime accurate landing can be performed. This will increase the operating time of helicopters, which will then require more work into ISLANDS resource since ISLANDS cannot recharge its batteries at night. Finally research into communication and bandwidth requirements between the helicopters and the ISLANDS station and the ISLANDS station and a human operated base will be needed.

REFERENCES

1. E. Eckermann, *World history of the automobile*, Warrendale, PA: Society of Automotive Engineers, 2001.

2. L. Koskela, *An exploration towards a production theory and its application to construction*, VTT Publications 408, Espoo, Finland, 2000.

3. D. Vieyra, *Filler 'er up: An Architectural History of America's Gas Stations,* Macmillan, New York, 1979 .

4. J. Roskam, *Airplane Flight Dynamics and Automatic Control, Part I*, Roskam Aviation and Engineering Corp., Lawrence, KS, 1979.

5. J. G. Leishman, *Principles of Helicopter Aerodynamics*, Cambridge University Press, New York, NY, 2000.

6. K. Nonami, *Prospect and Recent Research & Development for Civil Use Autonomous Unmanned Aircraft as UAV and MAV*, Journal of System Design and Dynamics, Vol. 1, No. 2, 2000.

7. B. Yenne, *Attack of the Drones: A History of Unmanned Aerial Combat*, Osceola, Wisc.: Zenith Press, 2000.

8. Unknown. *Firbee UAV*. [cited 2011 August 1]; Available from: http://www.pbs.org/wgbh/nova/spiesfly/uavs_11.html.

9. Unknown. *Air force technology*. [cited, 2011 August 1]; Available from: http://www.airforce-technology.com/projects/predator-uav/.

10. Unknown. *Northrop Grumman*. [cited 2011 August 1]; Available from: http://www.as.northropgrumman.com/products/ghrq4a/index.html.

11. Unknown. *Conscious being*. [cited 2011 August 1]; Available from: http://www.consciousbeingalliance.com/2011/05/predator-drones-to-stop-genocide-in-darfur/.

12. Unknown. *Popular Mechanics Rise of the Drone Helicopter*. [cited 2011 August 1]; Available from: http://www.popularmechanics.com/technology/military/robots/the-rise-of-the-drone-helicopter#fbIndex1.

13. Unknown. *Northrop Grumman*. [cited 2011 August 1]; Available from: http://www.as.northropgrumman.com/products/mq8bfirescout_navy/index.html.

14. Unknown. *Rotomtion company*. [cited 2011 August 1]; Available from: http://rotomotion.com/images/SRE1_side.jpg.

15. Unknown. *Rotomtion company*. [cited 2011 August 1]; Available from: http://rotomotion.com/images/SR30-grass_sml.JPG.

16. Unknown. *Rotomtion company*. [cited 2011 August 1]; Available from: http://rotomotion.com/images/sr100_camrot_800w.jpg.

17. Unknown. *Rotomtion company*. [cited 2011 August 1]; Available from: http://rotomotion.com/images/sr200_800w.jpg.

18. K. D. Mullens, et al., *An automated uav Mission System*, in AUVSI Unmanned Systems in International Security 2003 (USIS 03), London, England, Sept. 2003.

19. Unknown. *RC airplane adviser*. [cited 2011 August 1]; Available from: http://www.rc-airplane-advisor.com/electric-ducted-fan.html.

20. C. F. A, *Stabilizing surface for flight deck or other uses*, U.S. Patent 7 299 762, Feb. 17, 2006.

21. P. Pillay, and R. Krishnan, *Modeling, simulation, and analysis of permanent-magnet motor drives. ii. the brushless dc motor drive*, Industry Applications, IEEE Transactions on, vol. 25, no. 2, pp. 274–279, Mar. 1989.

22. R. E. Rubio, et al., *Implementation of decoupled model-based controller in a 2-dof pneumatic platform used in low-cost driving simulators*, in Electronics, Robotics and Automotive Mechanics Conference, pp. 338 –343, Sept. 2009.

23. M. C. Shih and M. A. Ma, *Position control of a pneumatic cylinder using fuzzy pwm control method*, Mechatronics, vol. 8, no. 3, pp. 241 – 253, 1998.

24. R. van Varseveld and G. Bone, *Accurate position control of a pneumatic actuator using on/off solenoid valves*, Mechatronics, IEEE/ASME Transactions on, vol. 2, no. 3, pp. 195 –204, Sept. 1997.

25. G. Granosik and J. Borenstein, *Minimizing air consumption of pneumatic actuators in mobile robots*, in Robotics and Automation, 2004, vol. 4, pp. 3634 – 3639 Vol.4, 2004.

26. S. Chillari, S. Guccione, and G. Muscato, *An experimental comparison between several pneumatic position control methods*, in Decision and Control, 2001, vol. 2, Dec. 2001, pp. 1168 –1173, 2001.

27. S. Cubero and J. Billingsley, *Force, compliance and position control for a space frame manipulator*, in Mechatronics and Machine Vision in Practice, Proceedings, pp. 124 –129, 1997.

28. G. L. Rosa, et al., *A low-cost lightweight climbing robot for the inspection of vertical surfaces*, Mechatronics, vol. 12, no. 1, pp. 71 – 96, 2002.

29. Munsor, B., D. Young, and T. Okiishi, *Fundamentals of Fluid Mechanics*, John Wiler, New York 1990.

30. E. Barth, J. Zhang, and M. Goldfarb, *Sliding mode approach to pwmcontrolled pneumatic systems*, in American Control Conference, vol. 3, pp. 2362 – 2367 vol.3, May 2002.

31. E. Richer and Y. Hurmuzlu, *A high performance pneumatic force actuator system: Part ii—nonlinear controller design*, Journal of Dynamic Systems, Measurement, and Control, vol. 122, no. 3, pp. 426– 434, 2000.

32. E. Ricer, and Y. Hurmuzlu, *A high performance pneumatic force actuator system: Part i—nonlinear mathematical model*, Journal of Dynamic Systems, Measurement, and Control, vol. 122, no. 3, pp. 416–425, 2000.

33. H. Zhang, J. Zhang, and G. Zong, "Effective nonlinear control algorithms for a series of pneumatic climbing robots," in Robotics and Biomimetics, 2006. ROBIO '06. IEEE International Conference on, Dec. 2006, pp. 994 –999

34. H. Zhang, W. Wang, and J. Zhang, *High stiffness pneumatic actuating scheme and improved position control strategy realization of a pneumatic climbing robot*, in Robotics and Biomimetics, 2008. ROBIO 2008. IEEE International Conference on, Feb. 2009, pp. 1806 –1811

35. M. Samhouri, A. Raoufi, and B. Surgenor, *Control of a pneumatic gantry robot for grinding: a neuro-fuzzy approach to pid tuning*, in Control Applications, pp. 452-458, Aug. 2005.

36. Unknown. *Micro Mouse Information*. [cited 2011 August 1]; Available from: http://www.micromouseinfo.com/introduction/dcmotors.html.

37. K. Ahn and S. Yokota, *Intelligent switching control of pneumatic actuator using on/off solenoid valves*, Mechatronics, vol. 15, no. 6, pp. 683 – 702, 2005.

38. S. J. Huang and H. W. Shieh, *Motion control of a nonlinear pneumatic actuating table by using self-adaptation fuzzy controller*, in IEEE Conference on Industrial Technology, pp. 1-6, Feb. 2009.

39. Unknown. *Pilot outlook slope landing*. [cited 2011 August 1]; Available from: http://www.pilotoutlook.com/helicopter_flying/slope_landing.

40. Unknown. *FAA Advisory Circular*. [cited 2011 August 1]; Available from: http://www.airweb.faa.gov/Regulatory_and_Guidance_Library/rgAdvisoryCircular.nsf/0/412de833d6baa71286256f340060c072/$FILE/AC150-5390-2b_part1.pdf.

41. Weibel, R.E., Hansman, R.J., *Safety Considerations for Operation of Different Classes of UAVs in the NAS*, In: AIAA 4th Aviation Tehcnology, Integration and Operations Forum, AIAA 3rd Unmanned Unlimited Technical Conference, Workshop and Exhibit, 2004.

42. Unknown. *Military Analysis Network FAS*. [cited 2011 August 1]; Available from: http://www.fas.org/man/dod-101/sys/land/m998.htm.

43. R. Norton, *Machine Design, An Integrated Approach*, 2nd ed., Prentice Hall, Upper Saddle River, NJ, 2000.

44. Augustine L. K., Sandidge S. A., and Williams N.T., *Alternative Fuel Vehicles Which Shall Win the Race to Commercialization*, ISTM 6233, 2011.

45. Unknown. *Toyota*. [cited 2011 August 1]; Available from: http://www.toyota.com/prius-hybrid/.

46. Unknown. *Nissan*. [cited 2011 August 1]; Available from: http://www.nissanusa.com/leaf-electric-car/index#/leaf-electric-car/index.

47. M. Winter, J.O. Besenhard, *J.O. Besenhard (Ed.), Handbook of Battery Materials*, Wiley-VCH, Weinheim, Part III, ch. 5, 1999.

48. S.M. Amin and B.F. Wollenberg, *Toward a smart grid: power delivery for the 21st century*, IEEE Power and Energy Magazine 3 (5), pp. 34–41, 2005.

49. Unknown. *Better Place*. [cited 2011 August 1]; Available from: http://www.betterplace.com/.

50. D. Dale, J. P. How, *Automated ground maintenance and health management for autonomous unmanned aerial vehicles*, Thesis (M. Eng.), Massachusetts Institute of Technology, Department of Electrical Engineering and Computer Science, 2007.

51. K. Suzuki, P.F. Kemper, J.R. Morrison, *Automatic Battery Replacement System for UAVs Analysis and Design*, International Conference Unmanned Aerial Systems, 2011.

52. P. F. Kempter, K. Suzuki, J.R. Morrison, UAV *Consumable Replenishment: Design Concepts for Automated Service Stations*, Journal of Intelligent and Robotic Systems, Vol 61, pp. 369-397, 2010.

53. K. A. Swieringa et al., *Autonomous battery swapping system for small-scale helicopters*, In: IEEE International Conference on Robotics and Automation (ICRA), pp 3335-3340, 2010.

54. C. V. Ramamoorthy and S. H. Gary, *Performance evaluation of asynchronous concurrent systems using petri nets*, IEEE Transactions on Software Engineering SE-6:440-449, 1980.

55. G. Rizzoni, *Principles and applications of electrical engineering*, McGraw-Hill, Fourth Edition, 2003.

56. Unknown. *Viair Corporation*. [cited 2011 August 1]; Available from: http://www.viair.com/.

57. Unknown. *Green Enerjy blog*. [cited 2011 August 1]; Available from: http://www.green-enerjy.com/green/solar-energy/what-is-solar-energy-used-for.

58. S. Armstrong, M.E. Glavin, and W.G. Hurley, *Comparison of Battery Charging Algorithms for Stand Alone Photovoltaic Systems*, Power Electronics Specialists Conference, PESC pp. 1469-1475, 2008.

59. Unknown. *OutBack Power FLEXmax*. [cited 2011 August 1]; Available from, http://www.outbackpower.com/products/charge_controllers/flexmax/.

60. Unknown. *XMOS XS1-G4B datasheet*. [cited 2011 August 1]; Available from: https://www.xmos.com/download/public/XS1-G4-512BGA-Datasheet%281066D%29.pdf.

61. C. M Mi, M. Masrur, and D. W. Gao, *Hybrid Electric Vehicles*, Wiley Press, 2011.

62. Unknown. *Maxi Joker USA Distributer*. [cited 2011 August 1]; Available from: http://www.joker-usa.com/new.htm.

63. Y. Kobayashi, et al., *5 V Class All-Solid-State Composite Lithium Battery with Li[sub 3]PO[sub 4] Coated LiNi[sub 0.5]Mn[sub 1.5]O[sub 4]*, J. Electrochem. Soc. 150, 2003.

64. Unknown. *Concord Battery Datasheet*. [cited 2011 August 1]; Available from: http://www.solar-electric.com/sunxtpvagmse.html.

65. Unknown. *Kyocera Solar Module Datasheet*. [cited 2011 August 1]; Available from: http://www.solar-electric.com/kykd235wapos.html.

66. Unknown. *Solar Insolatin Map from altEu*. [cited 2011 August 1]; Available from: http://www.altestore.com/howto/Solar-Electric-Power/Reference-Materials/Solar-Insolation-Map-World/a43/.

67. Unknown. *Banebot RS390 12V Motor*. [cited 2011 August 1]; Available from: http://banebots.com/pc/MOTOR-BRUSH/M5-RS540-12.

68. Unknown. *Vex Robotics Servo*. [cited 2011 August 1]; Available from: http://www.vexrobotics.com/276-2162.html.

69. Unknown. *Parker 24V Solenoid Valves*. [cited 2011 August 1]; Available from: http://www.parker.com/portal/site/PARKER/menuitem.7100150cebe5bbc2d6806710237ad1ca?vgnextdiv=687821&vgnextfmt=default&vgnextcatid=2887383&vgnextcat=SOLENOID%20%20VALVES&vgnextoid=f5c9b5bbec622110VgnVCM10000032a71dacRCRD.

70. Unknown. *Oriental Motors 100W DC Motor.* [cited 2011 August 1]; Available from: http://www.orientalmotor.com/products/ac-dc-speed-motors/blh-series.html.

71. Unknown. *Thunder Power RC Lithium Polymer Charger*. [cited 2011 August 1]; Available from: http://thunderpowerrc.com/html/TP820CD.html.

72. Mahoor M.M., et al., *Vision-Based Landing of Light Weight Unmanned Helicopter on a Smart Landing Platform*, Journal of Intelligent and Robotic Systems, Vol 61, pp, 251-265, 2010.

73. R. D. Garcia and K. P. Valavanis, *The implementation of an autonomous helicopter testbed*, Journal of Intelligent Robotics Systems, 5, pp. 423–45, 2009.

74. G. Cai and B.M. Chen, *An overview on development of miniature unmanned rotorcraft systems*, Frontiers of Electrical and Electronic Engineering in China, Vol. 5, No. 1, pp. 1-14, 2010.

75. W. Pisano, D. Lawrence, and S. Palo, *Low-cost UAV Avionics for Autonomous Antenna Calibration*, Arlington, Virginia, pp. 26-29, September 2005.

76. Unknown. *Honda Recreational Generators*. [cited 2011 August 1]; Available from: http://www.hondapowerequipment.com/products/models.aspx?page=models&section=P2GG&category=play.

77. Unknown. ETA *USA AC/DC High Power Supplies.* [cited 2011 August 1]; Available from: http://www.eta-usa.com/110-5000.html.

78. O. Alp, E. Erkut, and Z. Drezner, *An efficient genetic algorithm for the p-median problem*, Annals of Operations Research, vol. 122, pp. 21–42, 2003.

79. R. Church and C. ReVelle, *The maximal covering location problem*, Papers in Regional Science, vol. 32, pp. 101–118, 1974.

80. Y. Gabriely and E. Rimon, *Spanning-tree based coverage of continuous areas by a mobile robot*,. Submitted to Annals of Mathematics and Artificial Intelligence, 2001.

81. S. Hert and V. J. Lumelsky, *Polygon area decomposition for multiple-robot workspace division*, International Journal of Computational Geometry and Applications, 8(4):437–466, 1999,

82. H. Choset, *Coverage for robotics - a survey of recent results*, Annals of Mathematics and Artificial Intelligence, vol. 31, pp. 113–126, 2001.

83. J. Lee, et al., *Complete coverage path planning for cleaning task using multiple robots*, In: Proceedings of the IEEE International Conference on Systems, Man and Cybernetics, pp. 3618–3622, 2009.

84. A. Drenner and N. Papanikolopoulos, *Docking station relocation for maximizing longevity of distributed robotic teams*, in Robotics and Automation, pp. 2436–2441, ICRA, 2006

85. C. Carlson et al,, *Modular mobile docking station design*, in Proceedings of the IEEE/RSJ International Conference on Intelligent Robot Systems, 2006.

86. B. A. White, et al., *Contaminant Cloud Boundary Monitoring Using Network of UAV Sensors*, IEEE Sensors Journal , 8 (10), S. 1681-1692, 2008.

87. D. W. Casbeer, et al., *Cooperative Forest Fire Surveillance Using a Team of Small Unmanned Air Vehicles*, International Journal of System Sciences, April 2005.

88. D. W. Casbeer, et al., *Forest Fire Monitoring Using Multiple Small UAVs*, Proceedings of the American Control Conference, 2005.

89. I. Mazza and A. Ollero, *Multiple uav cooperative searching operation using polygon area decomposition and efficient coverage algorithms*, 2004.

90. F. Bonin, A. Ortiz, and B. Oliver, *Visual Navigation for Mobile Robots: a Survey*, Journal of Intelligent and Robotic Systems. 53(3), 263-296 2008.

91. T. Zhao and R. Nevatia, *Car detection in low resolution aerial image*, In *Proc. IEEE Intl. Conf. Computer Vision*, 2001.

92. Unknown. *Satellite imaging corporation.* [cited 2011 August 1]; Available from: http://www.satimagingcorp.com/characterization-of-satellite-remote-sensing-systems.html.

93. M. L. Brandeau and S. S. Chiu, *An overview of representative problems in location research*, Manage. Sci., vol. 35, pp. 645–674, June 1989.

94. L. Brotcorne, G. Laporte, F. Semet, *Ambulance location and relocation models*, European Journal of Operational Research 147 (3), pp 451-46, 2003.

95. D. Eaton, et al., *Determining ambulance deployment in Santo Domingo, Dominican Republic*, Journal of the Operational Research Society 37 1986.

96. D.M. Crawford and S.B Hold Jr., *A Mathematical Optimization Technique for Location and Sizing Distribution Substations and Deriving Their Optimal Service area*, IEEE Transaction on PAS, pp. 230-235, March 1975.

97. J. H. Jaramillo, J. Bhadury, and R. Batta, *On the use of genetic algorithms to solve location problems*, Comput. Oper. Res., vol. 29, pp. 761–779, May 2002.

98. L. A. Lorena and M. A. Pereira, *A lagrangean/surrogate heuristic for the maximal covering location problem using hillsman's edition*, international Journal of Industrial Engineering, vol. 9, pp. 57–67, 2001.

99. R. D. Galvao, L. G. A Espejo, and B. A. Boey, *comparison of Lagrangean and surrogate relaxations for the maximal covering location problem*, European Journal of Operational Research, 2000.

100. J. A. Bondy and U. Murthy, *Graph Theory with Applications*, NewYork: Elsevier, 1976.

101. R. E Tarjan, *Data Structures and Network Algorithms*, SIAM, PA, 1983.

102. Kruskal, J. B, *On the shortest spanning subtree of a graph and the traveling salesman problem*, Problem. Am. Math. Sot. 7, 48-50, 1956.

103. Paolo de Leva, *Adjustments to Zatsiorsky-Seluyanov's segment inertia parameters*, Journal of Biomechanics, 29(9) pp. 1223–1230, 1996.

104. Unknown. *What is the tallest building in your town.* [cited 2011 August 1]; Available from: http://www.cockeyed.com/citizen/local/local_tall_buildings.shtml.